Impact Assessment of Vehicle Electrification on Regional Air Quality in China and Climate Impact Assessment of Electric Vehicles 2050

giz Deutsche Gesellschaft für Internationale Zusammenarbeit (GIZ) GmbH

On behalf of
Federal Ministry for the Environment, Nature Conservation and Nuclear Safety
of the Federal Republic of Germany

清華大學 Tsinghua University

The "Impact Assessment of Vehicle Electrification on Regional Air Quality in China and Climate Impact Assessment of Electric Vehicles 2050" is published under the framework of a Sino-German cooperation project on electro-mobility and climate protection. As part of the International Climate Initiative (IKI) of the Federal Ministry for the Environment, Nature Conservation, Building and Nuclear Safety (BMUB), the project has been implemented by the Deutsche Gesellschaft für Internationale Zusammenarbeit (GIZ) GmbH jointly with the China Automotive Technology and Research Center (CATARC).

Published by
Deutsche Gesellschaft für Internationale Zusammenarbeit (GIZ) GmbH

Registered offices
Bonn and Eschborn, Germany

Dag-Hammarskjöld-Weg 1-5
65760 Eschborn/Deutschland
T +49 61 96 79-0
F +49 61 96 79-11 15
E info@giz.de
I www.giz.de

Editing
Deutsche Gesellschaft für
Internationale Zusammenarbeit (GIZ) GmbH
Sunflower Tower 860
Maizidian Street 37, Chaoyang District
100125 Beijing, PR China
T +86 (0)10 8527 5589 ext. 403
F +86 (0)10 8527 5591

Sino-German Cooperation Project
on Electro-Mobility and Climate Protection
www.sustainabletransport.org

Project Director
Sandra Retzer

Authors
Ye Wu, Wenwei Ke, Boya Zhou, Xiaoyi He
Yu Zhou, Shuxiao Wang, Jiayu Xu, Jiming Hao

Design and Layout
Miao Yan
Ziad Elgendy

As at
October 2016

Impact Assessment of Vehicle Electrification on Regional Air Quality in China and Climate Impact Assessment of Electric Vehicles 2050

Disclaimer

Findings, interpretations and conclusions expressed in this document are based on information gathered by GIZ and its consultants, partners and contributors.

GIZ does not, however, guarantee the accuracy or completeness of information in this document, and cannot be held responsible for any errors, omissions or losses that emerge from its use.

Table of Contents

List of Figures

List of Tables

Glossary

A	
AER	All-Electric Range
B	
BC	Black Carbon
BCON	Boundary Conditions Processor
BEV	Battery Electric Vehicle
C	
CAFC	Corporate-Average Fuel Consumption
CATARC	China Automotive Technology & Research Center
CCTM	Chemical-Transport Model
CMAQ	Air Quality Model (U.S.EPA)
E	
EC	Element Carbon
EIA	Energy Information Agency
EMBEV	Emission Model and Inventory of Beijing Vehicle Fleet
EV	Electrical Vehicle
F	
FGD	Flue Gas Desulfurization
G	
GIZ	Deutsche Gesellschaft für Internationale Zusammenarbeit GmbH
H	
HDPV	Heavy-Duty Passenger Vehicles
HEV	Hybrid Electric Vehicles

I

ICCT	International Council on Clean Transportation
ICE	Internal Combustion Engine
iCET	Innovation Center for Energy and Transportation
ICEV	Internal Combustion Engine Vehicle
ICON	Initial Conditions Processor
IGCC	Integrated Gasification Combined Cycle
IEA	International Energy Agency
IVOC	Intermediate-Volatility Organic Compound

J

JJJ	Jing-Jin-Ji
JPROC	Photolysis Rate Preprocessor

L

LCA	Life-Cycle Assessment
LDV	Light-Duty Vehicles

M

MCIP	Meteorology-Chemistry Interface Processor
MDPV	Medium-Duty Passenger Vehicles
MEP	Ministry of Environmental Protection
MIIT	Ministry of Industry and Information Technology
Mtce	Million Ton-Coal Equivalent
MW	Megawatt
MY	Model Year

N

NEV	New Energy Vehicles

NO_x	Nitrogen Dioxide
NMVOC	Non-Methane Volatile Organic Compounds
NAAQS	National Ambient Air Quality Standards
O	
O_3	Ozone
OA	Organic Aerosol
OC	Organic Carbon
OH	Hydroxid
P	
PHEV	Plug-in Hybrid Electric Vehicle
$PM_{2.5}$	Particulate Matter of 10 micrometers
PM_{10}	Particulate Matter of 2.5 micrometers
POA	Primary Organic Aerosol
PRD	Pearl River Delta
S	
SCR	Selective Catalytic Reduction
SO_2	**Sulfur dioxide**
SOA	Secondary Organic Aerosol
SOC	State Of Charge
T	
TTW	Tank-To-Wheels
U	
U.S.EPA	U.S. Environmental Protection Agency
V	
VKT	Vehicle Kilometres Travelled

VOC	Volatile Organic Compound
W	
WRF	Weather Research and Forecasting
WTT	Well-To-Tank
WTW	Well-To-Wheels
Y	
YRD	Yangtze River Delta

Introduction

Hybrid electric vehicles (HEVs), plug-in hybrid electric vehicles (PHEVs) and battery electric vehicles (BEVs) have been globally developed in the past 10 years. The development of electric vehicles (EVs, including PHEVs and BEVs, hereinafter) could enhance fuel diversity and utilise renewable energy (e.g. renewable electricity), which is considered a promising, long-term solution to reduce high dependence on fossil fuels and alleviate climate change impacts from a global perspective. In addition, EV deployment is considered capable of improving urban air quality by reducing on-road emissions for traffic-populated areas.

Many countries have proposed fiscal policies, primarily including subsidies and tax exemptions, leading to a surge in global EV sales. Total global EV sales rose from 321,000 in 2014 to 550,000 in 2015, representing an annual increase of 72%. Among all major economies, China achieved one of the most impressive sales records in 2015 by overtaking the U.S. and becoming a global leader in the EV market. Annual EV sales in China accounted for more than 1 % of the total domestic vehicle sales in 2015. This trend in China's EV market is expected to continue, likely approaching the ambitious target of total EV sales of 5 million units by 2020 as proposed by authorities.

Policymakers are aware of the potential environmental benefits of EVs in lessening urban atmospheric pollution. Decade-long discussions regarding whether fleet electrification can deliver actual environmental benefits on a regional scale have been heated during recent years. Life cycle assessment (LCA) methods were applied to determine the well-to-wheels (WTW) reduction benefits of energy consumption and emissions of greenhouse gases and air pollutants through electro-mobility. During the initial phase of the project, the full life cycle energy consumption and emissions of CO_2 and major air pollutants for light-duty and heavy-duty vehicles at national and regional levels in China were estimated to the year 2030. This provides massive policy implications to policymakers in terms of EV promotion. Moreover, these results are in a complex pattern and vary considerably by the power generation mix and vehicle technology. Based on this, this report aims to delve deeper from two different perspectives: methodology and timeframe.

Two major problems are expected to be answered through this report:

(1) Whether fleet electrification can achieve actual air quality improving benefits in the two typical developed regions in China (Yangtze River Delta (YRD) and Jing-Jin-Ji (JJJ)) in the mid-term future (2030).

(2) Whether advanced electric vehicle technologies (PHEVs and BEVs) could realise advantages on saving energy and reducing CO_2 emissions over internal combustion engine vehicles (ICEVs) in the long-term future (2050).

Therefore, the major purposes of this project are to:

(1) Evaluate the impacts of fleet electrification scenarios on air quality in the Yangtze River Delta and the Jing-Jin-Ji regions through the application of a comprehensive air quality model, and propose recommendations on how electro-mobility in China can provide win-win strategies in both climate and environmental protection.

(2) Update and extend the energy consumption and emission databases of different vehicle propulsion technologies, design vehicle stock and composition, Vehicle Kilometres Travelled (VKT), and fleet electrification scenarios with a long-term perspective until 2050.

Through this project, a China-localised comprehensive database of WTW energy consumption and air pollutant emissions was developed and used to generate the detailed emission inventories as an input for air quality modeling in the mid-term future (2030), and to estimate the fuel cycle energy and environmental impacts of different light-duty vehicle technologies (i.e. ICEVs/EVs) in the long-term future (2050).

Part I: Air Quality Impact Assessment of Vehicle Electrification

In the first part of this report, the impacts on regional air quality from vehicle fleet electrification in China will be evaluated based on comprehensive emission inventories and a state-of-the-art air quality model. As illustrated in the report on the previous phase, promoting EVs could significantly reduce air pollutant emissions from the on-road transportation sector in urban areas relative to conventional ICEVs. However, in the meantime, it could result in marginal emissions in the well-to-tank (WTT) stages (e.g. electricity generation), especially for air pollutants mainly from power plants, such as Nitrogen Dioxide (NO_X) and Sulfur dioxide (SO_2,) both of which are important precursors for secondary $PM_{2.5}$. From the perspective of temporal variations, emission reductions from on-road transportation mainly occur during the daytime; while the marginal emissions from power plants associated with the charging of EVs mainly occur in the nighttime, considering that home charging is currently the most possible charging pattern.

Therefore, simply estimating the life cycle of air pollutant emissions of EVs and their conventional counterparts could not accurately reflect the differential environmental impacts of those vehicle technologies directly and explicitly, considering the complexity of temporal and spatial distribution of emission changes as well as the variations of meteorological conditions in terms of air quality impacts. Therefore, the air quality impacts of large-scale EV penetration in typical regions in China under various development scenarios for EVs are simulated in this study by combining detailed spatial and temporal emissions inventories with an advanced atmospheric chemical and transport model.

Chapter 1 presents the scope and research framework of this study; Chapter 2 presents the nationwide and regional emission inventories that are used as inputs for air quality modeling; Chapter 3 illustrates the basic information, mechanism enhancements, and simulation domains of the air quality modeling system adopted in this study; Chapter 4 presents the projected vehicle fleet electrification scenarios; Chapter 5 shows the major air quality simulation results of those EV scenarios and estimates the potential air quality improving benefits of EV scenarios.

Chapter 1 Scope and research framework

1.1 Scope

For the purposes of this study, 2030 has been selected as the model year representing the medium-term future. Future fleet electrification has been considered for light-duty vehicles (LDVs), medium-duty passenger vehicles (MDPVs), heavy-duty passenger vehicles (HDPVs), buses, and taxis. Trucks are currently not included in the EV market. Two regions have been selected to address the regional air quality impacts from vehicle fleet electrification in China - the Yangtze River Delta (YRD) region (i.e. geographically including Shanghai and major parts of Jiangsu and Zhejiang provinces) and the Jing-Jin-Ji (JJJ) region (i.e. geographically including Beijing, Tianjin, and Hebei province). Through air quality simulation, the concentrations of major air pollutants in the urban areas of major cities within the two regions are being used due to their higher population density and vehicle use intensity than those of rural areas. $PM_{2.5}$ is the air pollutant of prioritised concern, as the limit exceedance of ambient $PM_{2.5}$ concentration is currently the most significant air pollution issue in China. Other related criteria, including air pollutants such as NO_2, SO_2 and the chemical compositions of $PM_{2.5}$, are also included in this assessment. The air quality simulations take place in January and August to represent winter- and summertime, respectively.

1.2 Research framework

Figure 1-1 presents the logistics of methodology fundamentals, tools and major data inputs/outputs for life cycle analysis and air quality modeling work. The overall research framework consists of four parts:

1) Evaluate the fuel-cycle energy consumption and air pollutant emissions of different vehicle technologies by developing a database of energy use and pollutant emissions in both the well-to-tank (WTT) and tank-to-wheels (TTW) stages;
2) Calculate the emissions changes from the on-road transportation and power generation sectors associated with various vehicle electrification scenarios based on the well-developed database of vehicle emissions;
3) Combine the emissions from other sectors (i.e. industrial production, agricultural

activities, domestic fossil fuel and biofuel combustion, off-road transportation, and open burning, etc.) to obtain the overall emission inventories as input for air quality modeling;

4) Use the comprehensive atmospheric chemical and transport model to conduct the air quality simulations of those vehicle electrification scenarios in typical regions in China (i.e. the JJJ and YRD regions), based on dedicated emission inventories and corresponding meteorological fields.

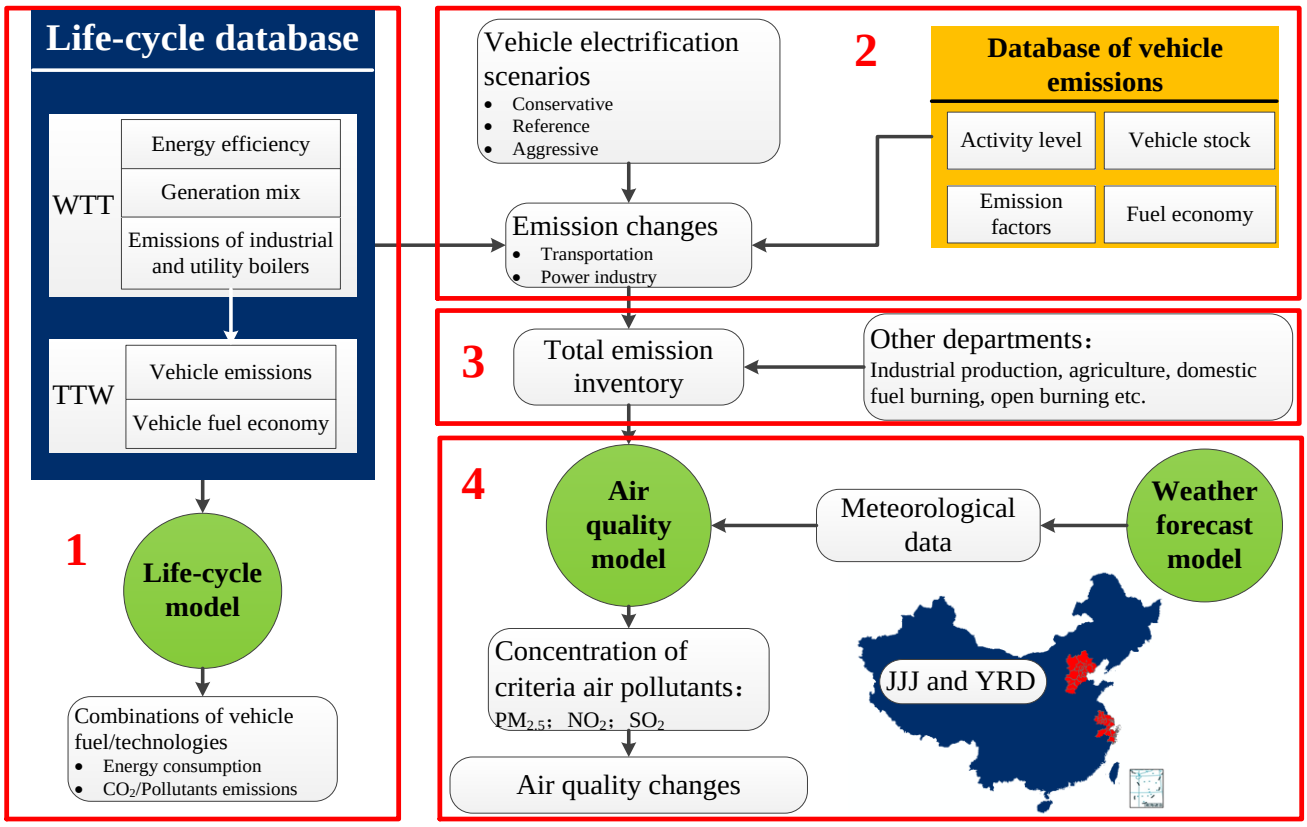

Figure 1-1 Logistics of methodology fundamentals, tools and major data inputs/outputs for life cycle analysis and air quality impact modeling for electric vehicles

Considerable work was done on the life cycle analysis of energy consumption and air pollutant emissions of EVs and conventional ICEVs in China at both the national and regional levels (e.g. JJJ, YRD, and the Pearl River Delta), which was shown in the report on the first phase of this project. A life cycle database of energy consumption and air pollutant emissions has already been well developed through our previous studies up to the year 2030. This provided the data required to conduct the air quality impacts assessment for EV penetration in China from a fuel-cycle perspective.

The air quality modeling has three steps. During the first step, the required baseline, multi-scale emission inventories (e.g. national and regional) were already well established by Tsinghua University. The major emission sectors include power plants, industrial production (e.g. iron and cement), residential heating, mobile sources, and uncontrolled open burning of biomass. Through previous research projects in cooperation with international and domestic institutes, much model validation and interpretation work was performed before applying this model to the evaluation of the environmental impacts of various energy policies and emission end-of-pipe control scenarios at both the national and regional levels in China.

The evaluation and validation of the air quality and meteorological models are not included in this report.

For the second step, various market penetration scenarios for EVs (including BEVs and PHEVs) with projected energy policies and emission end-of-pipe control scenarios in China in the future model year (MY) have been developed. This requires that the scenario process (life cycle emissions of EVs and ICEVs as well as the projected market penetration) as involved or developed in our previous studies feeds into the overall emissions inventory depending on the applied scenarios. In addition, the spatial and temporal boundaries have been set up to obtain the matching meteorological fields from the meteorological model – the Weather Research and Forecasting (WRF) model.

Finally, the Community Multiscale Air Quality (CMAQ) model is used to conduct a concentration simulation of major air pollutants (e.g. $PM_{2.5}$, NO_2 and SO_2) for those vehicle electrification scenarios compared to the baseline scenario (without EVs) in typical regions (i.e. YRD and JJJ) in China. Ozone is temporarily excluded from this study.

The calculation logistics for the emission changes from both the on-road transportation and power generation sectors are shown in **Figure 1-2**, which is also the second part of the overall research framework shown in **Figure 1-1**. First, the vehicle emission database developed by Tsinghua University is used to calculate the emission contribution rates of different vehicle categories to the total fleet emissions, which are then added to the vehicle electrification rates of corresponding vehicle categories to obtain the total reduction rates of air pollutant emissions from the on-road transportation sector. Secondly, combining projections of total vehicle stock and vehicle electrification scenarios, the EV

population (simplified as BEVs only) in MY 2030 can be calculated. The increased rates of emissions from power plants are assumed to be equal to the ratios of charging demands to the projected baseline electricity consumption (without EVs) in MY 2030. Moreover, the total charging demands (also known as the "marginal generation") are calculated based on the electricity consumption rates and activity data of various electric vehicle categories. This enables changes to the overall emission inventory to be calculated, combining the changes from on-road transportation and power generation sectors.

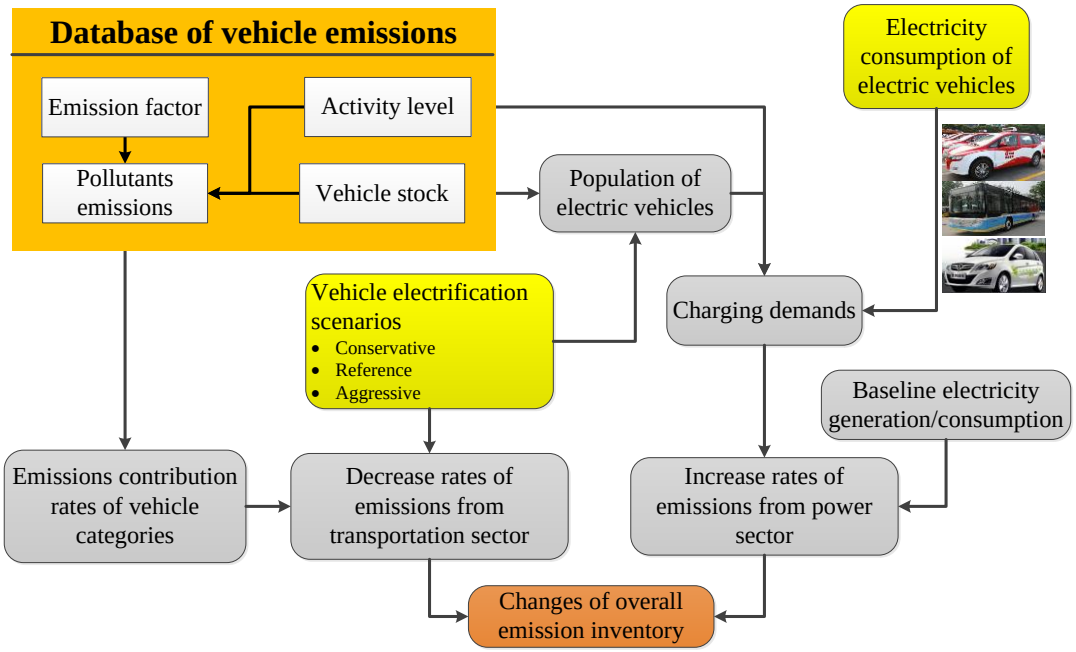

Figure 1-2 Logistics of calculation for the emission changes of electric vehicle penetration scenarios

From the fuel-cycle perspective, emissions from on-road transportation and power plants are probably the two most important sectors that relate to the penetration of EVs as replacements to conventional ICEVs. Additionally, emissions from the exploitation processes of raw materials (e.g. coal, natural gas, crude oil, and metals), transport and distribution processes of fuels, and production processes of vehicle batteries also contribute substantial proportions to the entire life cycle of emissions. However, due to a lack of localised China detailed and reliable data on the spatial and temporal distribution of emissions from those processes, this study only focuses on the emission changes of on-road transportation and power plants. Put simply, this evaluation assumes that emissions from other sectors remain unchanged with the penetration of EVs.

Chapter 2 Emission inventories

2.1 Nationwide emission inventory

The overall nationwide emission inventory in China has been developed and evaluated by Tsinghua University and is summarised and presented in this section. It includes emissions from major sectors such as thermal power plants, industrial processes, the cement industry, the iron industry, civil combustion of fossil fuels and biofuels, on-road and off-road transportation, and open burning of biomass, etc. As mentioned previously, on-road transportation and thermal power plants are the two sectors from which emissions are directly affected by vehicle fleet electrification. Specific emission inventories of the on-road transportation and thermal power generation (mostly coal-fired units) sectors are also briefly summarised in the following sections.

2.1.1 Overall emission inventories

The overall emission inventories (including SO_2, NO_X, $PM_{2.5}$, Black Carbon (BC), Organic Carbon (OC) and Non-Methane Volatile Organic Compounds (NMVOC)) classified by emission sectors of China in the baseline year 2010 and MY 2030 are summarised in **Figure 2-1**. As shown in **Figure 2-1**, SO_2 and NO_X emissions are mainly from industrial boilers and production processes; BC and OC emissions are mainly from fuel combustion (i.e. fossil fuels and biofuels); while industrial production (including the iron and cement industries) contributes a large proportion of primary $PM_{2.5}$ emissions. For NMVOC emissions, solvent use is the primary source. As for the sectors of particular interest in this study, the power generation sector contributed about 27% and 29% of total SO_2 and NO_X emissions, respectively, in 2010; while the on-road transportation sector contributed about 23%, 12%, and 20% to the total NO_X, BC, and NMVOC emissions, respectively.

The overall emission inventory in MY 2030 is estimated based on the emission inventory in MY 2010 and the projections for changes in terms of energy use and end-of-pipe controls in China. Generally, it was assumed that new and sustainable energy policies would come into force after 2010, which are meant to push forward the changes of production modes and lifestyles, adjustments to the energy structure and the improvement of energy consumption efficiencies. In addition, the policy

enforcements will be tougher. The energy consumption scenario refers to the major emission sectors, such as power generation, industrial production, domestic and commercial departments, transportation, and solvent use. For instance, the total energy consumption in China is expected to increase from the 4,159 million ton-coal equivalent (Mtce) in 2010 to 5,295 Mtce in 2030. The share of coal is expected to decrease from 68% in 2010 to 52% in 2030. The share of clean energy will definitely increase in the future. The proportion of natural gas, nuclear power, and other renewable energies will increase from 11% in 2010 to 25% in 2030. In addition, an assumption was made that the end-of-pipe emission control strategies will be continuously tightened.

The strategies assume new emission control measures will come into force in the future and control efforts will constantly be enhanced. For example, it is assumed that flue gas desulfurization (FGD) facilities will be 100% installed in coal-fired power plants in China by the end of 2015. Detailed information and assumptions for the projection of future energy use and end-of-pipe controls are not presented in this report.

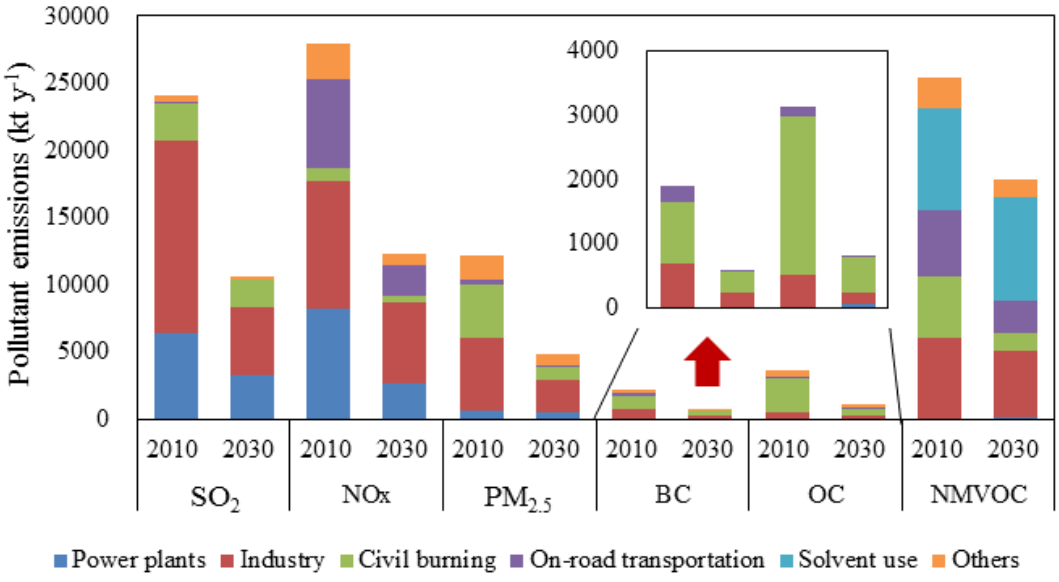

Figure 2-1 Estimated emissions of primary air pollutants by sector in China under *Scenario w/o EVs* and a comparison with the estimated emissions in 2010

Figure 2-2 presents the overall emission inventories distributed by regions (i.e. provinces) in China in 2010. Air pollutants emissions in China are highly concentrated in the eastern areas with their high level of economic development and density of population. In other words, the regions (i.e. YRD and JJJ) used

to evaluate the air quality impacts of vehicle electrification in this study are exactly the high-emission areas in China.

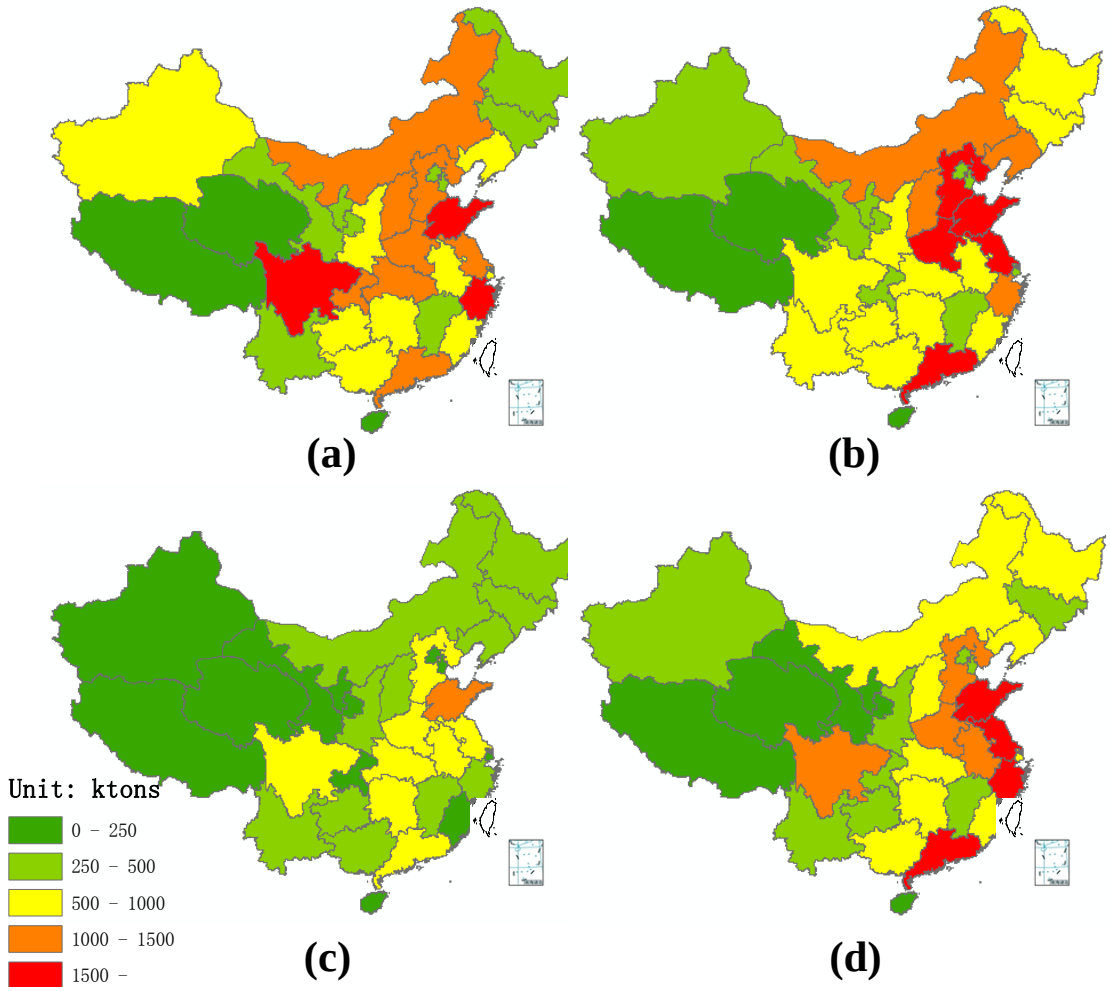

Figure 2-2 Overall emission inventory of China classified by regions in 2010
(a) SO_2; (b) NO_X; (c) $PM_{2.5}$; (d) NMVOC

2.1.2 On-road transportation sector

For on-road transportation, the emission factors were updated by using the Emission Model and Inventory of Beijing Vehicle Fleet (EMBEV)-China model, which was developed based on local laboratories and on-road measurement data of tailpipes and evaporative emissions and took into account numerous local corrections (e.g. fuel quality, weather conditions, driving conditions, vehicle size, high-emitters). As shown in **Figure 2-3**, different air pollutants have different emission patterns by vehicle category. Trucks are the dominant contributor of NO_X and primary $PM_{2.5}$ emissions from the on-road transportation sector, while HDPVs appear to be the secondary contributor. LDVs account for

a substantial percentage of the fleet NO_X and primary $PM_{2.5}$ emissions due to their huge population while being the principal contributor of NMVOC emissions from on-road transportation.

Based on the mid-term outlook for on-road vehicle emissions in China, a series of projections are developed when estimating the MY 2030 inventory. For example, the new fuel quality standards for automobile gasoline and diesel have recently been launched meaning that the China 6 emission standards will probably be implemented before 2020 in most areas in China. In addition, with the substantial scrappage of older vehicles, total on-road vehicle emissions in China could decrease by 53% for NMVOC, 66% for the NO_X and 88% for $PM_{2.5}$ from 2010 to 2030.

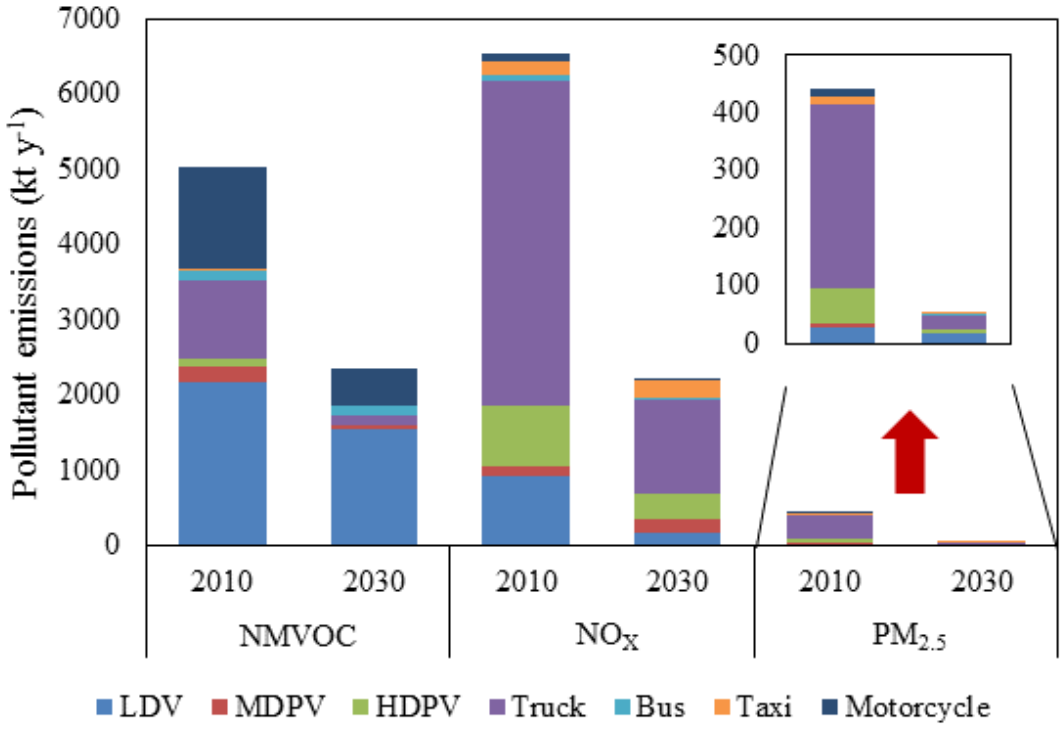

Figure 2-3 Estimated vehicle emissions of major air pollutants by vehicle category in China under *Scenario w/o EVs* and a comparison to the estimated emissions in 2010

2.1.3 Thermal power generation sector

The air pollutant emissions from the power generation sector in China mainly comes from coal-fired power plants due to their overwhelming share in the generation mix and relatively high emission rates. Researchers from Tsinghua University have investigated the major thermal power plants in China to obtain their locations (latitude and longitude), power generation capacities, fuel types, raw coal

consumption, installation of emission control devices, etc. Based on the key information, the air pollutants emissions can be calculated for each of those power plants. As shown in **Figure 2-4**, the coal-fired power plants are concentrated in the eastern areas of China, including the YRD and JJJ regions.

Figure 2-4 Distribution of power generation capacity of coal-fired power plants in China in 2010

2.2 Regional emission inventory

In addition to the national-level emission inventories mentioned above, this study also applied dedicated high-resolution regional-level emission inventories developed by Tsinghua University to improve the simulation performance of air quality modeling. In this section, the regional emission inventories of the YRD and JJJ regions are generally presented.

2.2.1 JJJ region

As shown in **Figures 2-5** and **2-6**, the regional overall emission and on-road vehicle fleet emission inventories for JJJ were developed for the baseline years of 2010 and MY 2030, respectively. As shown in **Figure 2-5**, SO_2 and NO_X emissions are mainly from industrial boilers and production processes; BC

and OC emissions are mainly from fuel combustion (i.e. fossil fuels and biofuels); while industrial production (including the iron and cement industries) contributes a large proportion of primary $PM_{2.5}$ and NMVOC emissions. Solvent use is also a substantial source for NMVOC emissions. As for the sectors of particular interest in this study, the power generation sector contributed about 25% and 26% of total SO_2 and NO_X emissions, respectively, in 2010 while the on-road transportation sector contributed about 30%, 14%, and 24% to the total NO_X, BC, and NMVOC emissions, respectively.

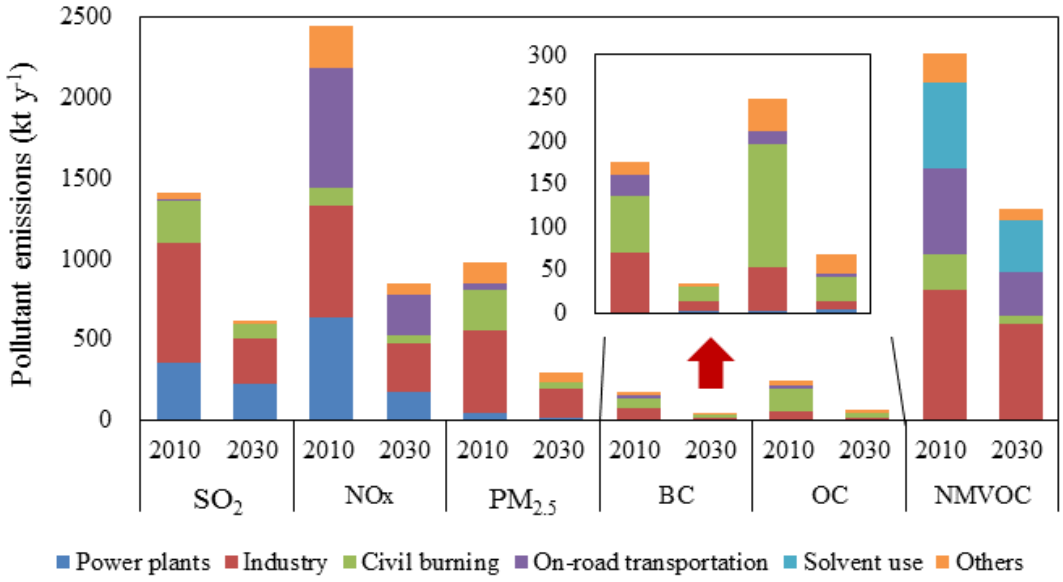

Figure 2-5 Estimated emissions of primary air pollutants by sector in the JJJ region under *Scenario w/o EVs* and a comparison to the estimated emissions in 2010

For on-road transportation, the same method and database as the nationwide emission inventory to generate the regional emission inventory for the JJJ region was used. As shown in **Figure 2-6**, different air pollutants have different emission patterns by vehicle category. Trucks are the principal contributor of NO_X and primary $PM_{2.5}$ emissions from the on-road transportation sector, while HDPVs appear to be the secondary contributor. LDPVs account for a substantial percentage of fleet NO_X emissions due to their huge population and are the principal contributor of NMVOC emissions from on-road transportation.

Based on the mid-term outlook for on-road vehicle emissions in the JJJ region, a series of projections were developed when estimating the MY 2030 inventory. Total on-road vehicle emissions in China are estimated to decrease by 53% for NMVOC, 66% for the NO_X and 88% for $PM_{2.5}$ from 2010

to 2030.

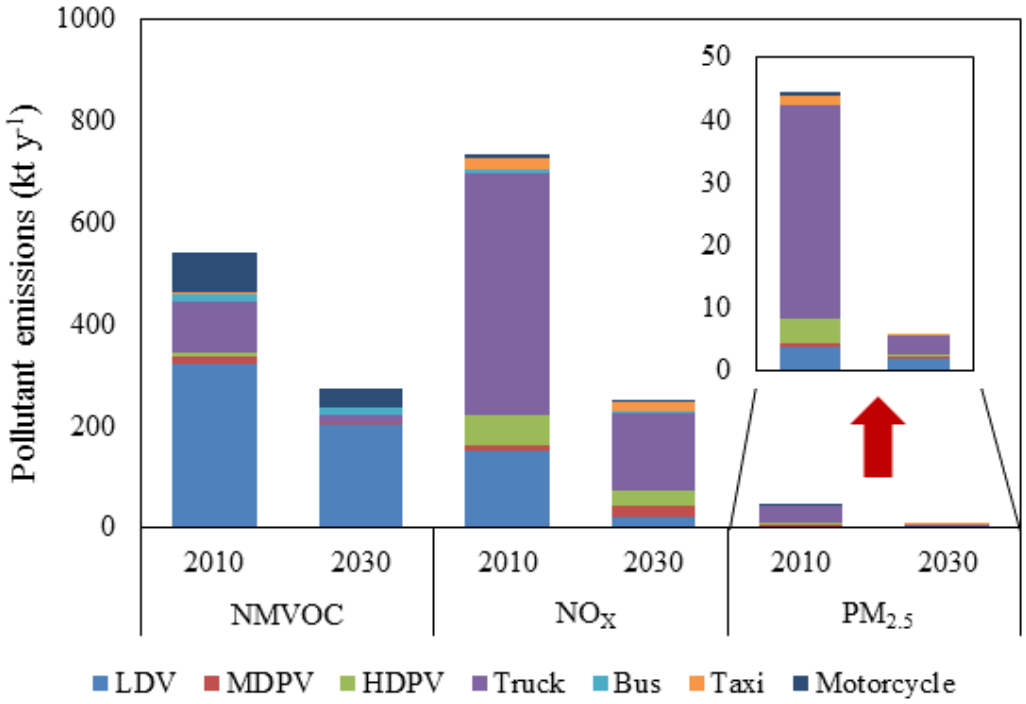

Figure 2-6 Estimated vehicle emissions of major air pollutants by vehicle category in the JJJ region under *Scenario w/o EVs* and a comparison to the estimated emissions in 2010

2.2.2 YRD region

As shown in **Figure 2-7**, the regional emission inventories of YRD are developed for the baseline years of 2010 and MY 2030, respectively. As a whole, the industrial sector is the principal emissions contributor and is responsible for 47%, 24%, 48%, 36%, 12%, and 33% of total SO_2, NO_X, $PM_{2.5}$, BC, OC, and NMVOC emissions, respectively. Civil burning of fossil fuels and biofuels is also an important source of BC and OC emissions, as is solvent use as a substantial source for NMVOC emissions. For the sectors of particular interest in this study, the power generation sector contributes about 48% and 38% of total SO_2 and NO_X emissions, respectively, in 2010. The on-road transportation sector contributes about 30%, 28%, and 21% to the total NO_X, BC, and NMVOC emissions, respectively.

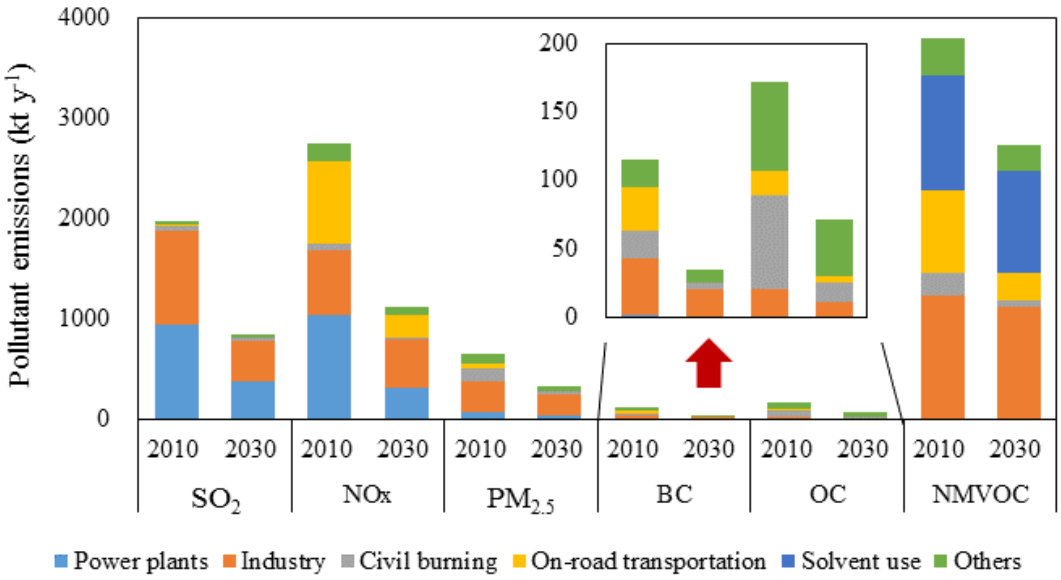

Figure 2-7 Estimated emissions of primary air pollutants by sector in the YRD region under *Scenario w/o EVs* and a comparison to the estimated emissions in 2010

For on-road transportation, to generate the regional emission inventory for the YRD region, the same method and database as the nationwide emission inventory utilises was used. As shown in **Figure 2-8**, air pollutants have similar emission patterns to those of the JJJ region. Trucks are the principal contributors of NO_X and primary $PM_{2.5}$ emissions from the on-road transportation sector, while HDPV appears to be the secondary contributor, and LDVs account for a substantial percentage of fleet NO_X emissions due to their huge population and are the principal contributor of NMVOC emissions from on-road transportation.

Based on the mid-term outlook for on-road vehicle emissions in the YRD region, a series of projections have been developed for estimating the MY 2030 inventory. Total on-road vehicle emissions in China are estimated to decrease by 66% for NMVOC, 73% for the NO_X and 90% for $PM_{2.5}$ from 2010 to 2030.

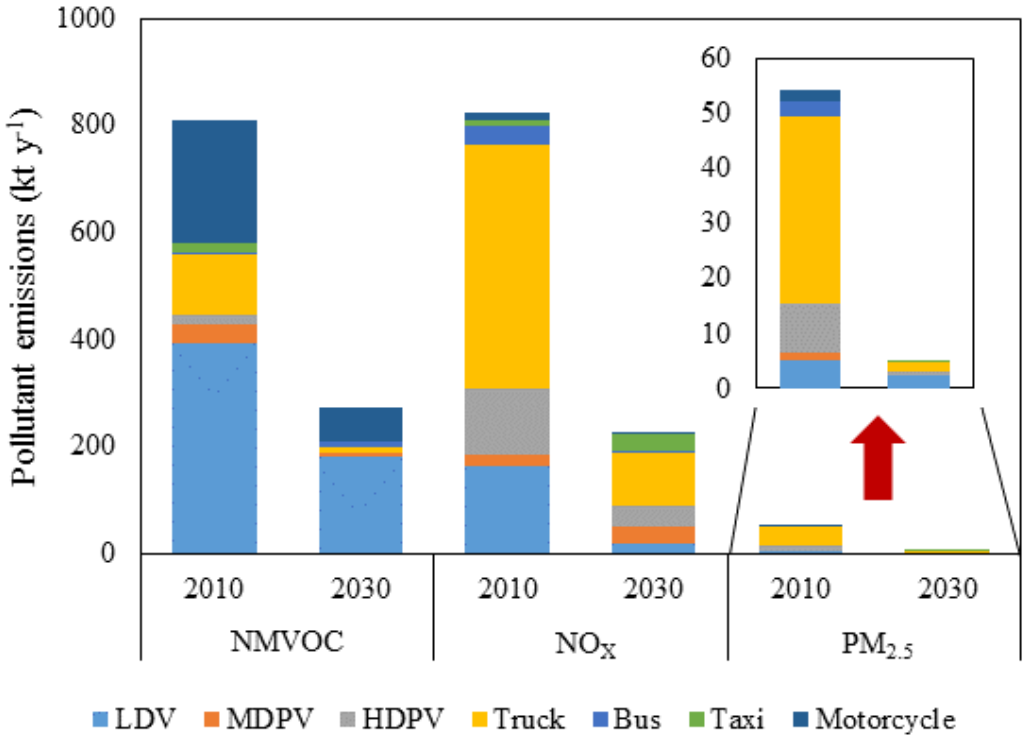

Figure 2-8 Estimated vehicle emissions of major air pollutants by vehicle category in the YRD region under *Scenario w/o EVs* and a comparison to the estimated emissions in 2010

2.3 Basic assumptions and key parameters

In this section, the basic consumption and key parameters adopted in this study for the calculation of the emission changes for on-road vehicles and the power generation sector associated with the replacement of EVs over conventional ICEVs are presented. The basic assumptions are:

1) EVs and ICEVs have identical annual VKT (Vehicle Kilometers Travelled);
2) Null time lapse between marginal electricity generation and EV charging;
3) Marginal generation from local and imported electricity for provinces in proportion;
4) No modification to the electricity consumption level of EVs for different provinces.

Based on these assumptions, emission changes from on-road vehicles and power plants for EV penetration scenarios were calculated. In addition, key parameters include the annual vehicle kilometers travelled and distance-based electricity consumption of different vehicle categories. **Figure 2-9** shows the national average VKTs and their standard deviations (from different provinces) by vehicle category. Taxis have the highest VKT and LDVs have the lowest.

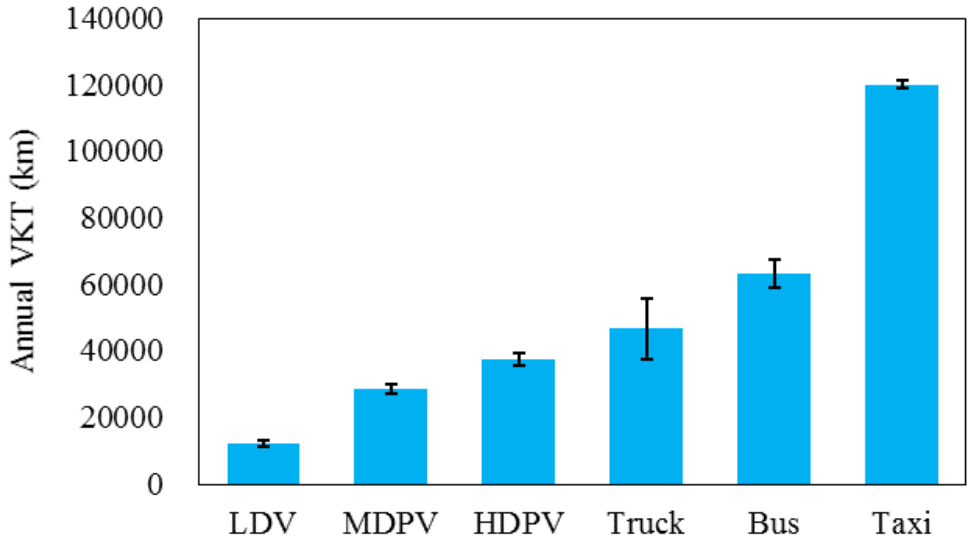

Figure 2-9 Annual average province-level VKT by vehicle category

Distance-based electricity consumption data of EVs have been obtained from real-world vehicle tests and literature review [1, 2]. The overall charging efficiency for EVs is estimated to be 90%, and the electricity transmission loss on the power grid is estimated to be 6% by 2030.

Chapter 3 Model description

3.1 Air quality modeling system

The CMAQ model is applied to simulate the air quality impacts of vehicle electrification with localised databases. CMAQ is a third-generation air quality model developed by the U.S. Environmental Protection Agency (U.S. EPA). Establishing the relationships between meteorology, chemical transformations, emissions of chemical species, and removal processes in the context of atmospheric pollutants, is the fundamental goal of this air quality model. Air pollutants emissions and meteorological data are its two primary inputs.

Modularity is one of the major features of this model, which maintains the flexibility to add new or select existing science modules to optimise model performance for specific applications. **Figure 3-1** presents the overall framework of the CMAQ model. The spatial lateral boundary conditions are estimated in CMAQ using the boundary conditions processor, (BCON). Similarly, a temporal boundary condition has been established with the initial conditions processor, (ICON), which estimates the chemical conditions in the first time step of a CMAQ model simulation. To model incoming solar radiation, which provides the energy source for photolysis reactions (JPROC), the program calculates clear-sky photolysis rates at various latitude bands and hours based on solar hour angles. Output from these three CMAQ programs is used with output files from the emissions and meteorological models and other CMAQ preprocessors to form the required input data for running the Chemical-Transport Model of CMAQ (CCTM), the core of this model system. The outputs of CCTM are gridded and temporally resolved information on air pollutants, such as gas- and aerosol-phase species mixing ratios, hourly wet and dry deposition values, visibility metrics, and integral-averaged concentrations, which also provide spatial and temporal boundary conditions for finer grids in nested simulation.

As shown in **Figure 3-1**, the meteorological model used in this study is the Weather Research and Forecasting (WRF) model. It is a next-generation mesoscale numerical weather prediction system designed for both atmospheric research and operational forecasting needs, serving a wide range of meteorological applications with scales from tens of meters to thousands of kilometers.

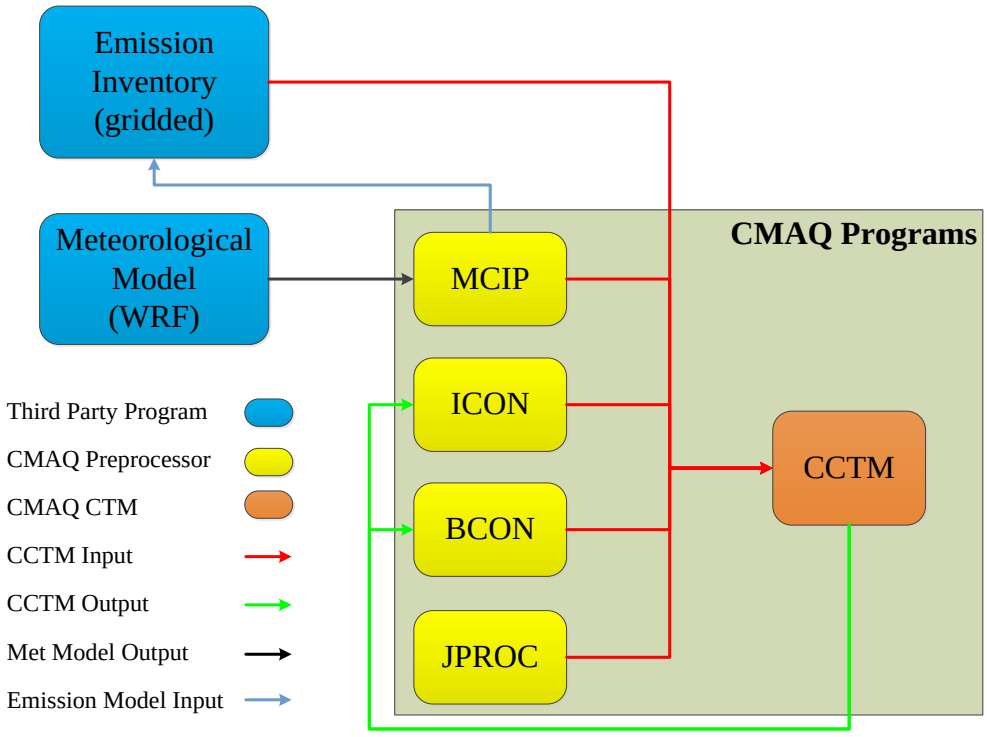

Figure 3-1 Logic of the CMAQ model

The multi-scale modeling function of this model provides adequate technical formulations to address air quality issues on multiple spatial scales from urban to hemispheric. In this study, the air quality impacts of EV penetration in two typical regions (i.e. YRD and JJJ) in China with a three-layer nested domain system are simulated.

The basic information and key parameters of the CMAQ model and WRF model used in our study are summarised in **Table 3-1**. A detailed introduction to the related modules and parameters of the two models are not presented in this report.

Table 3-1 Basic information and key parameters of the meteorology and air quality models in this study

	Meteorology	Chemical transport mechanisms
Model version	Weather research and forecasting (WRF v3.3)	Community Multiscale Air Quality (version 5.0.1) model enhanced by the two-dimensional volatility basis set (2D-VBS)
Domains (Nx, Ny, Nz, Horizontal. resolution)	Domain 1: 170, 103, 14, 36×36 km^2 Domain 2: 142, 220, 14, 12×12 km^2 Domain 3: 142, 166, 14, 4×4 km^2	Domain 1: 164, 97, 14, 36×36 km^2 Domain 2: 136, 214, 14, 12×12 km^2 Domain 3: 136, 160, 14, 4×4 km^2
Parameters	Planetary boundary layer: Mellor-Yamada-Janjic TKE Microphysics: WSM3 Cumulus scheme: Grell-Devenyi ensemble Land surface layer: Noah Long wave radiation: RRTM Short wave radiation: RRTM	Gas-phase chemistry scheme: SAPRC99 Aerosol module: AERO6 SOA module: 2D-VBS Horizontal advection scheme: Hyamo Vertical advection scheme: Vwrf Horizontal diffusion scheme: Eddy diffusivity theory Vertical diffusion scheme: Acm2 Dry deposition velocity: M3dry

3.2 Enhancements for the air quality model

The conventional CMAQ model is limited in simulating the formation of secondary organic aerosol (SOA). Researchers from Tsinghua University have made significant improvements to the simulation performance of SOA formation over the conventional CMAQ model by adding an extra module for simulating the ageing of primary organic aerosol (POA) and the multi-stage oxidation of SOA. This is called the Two-Dimension Volatile Basis Set (2D-VBS) module. The CMAQ/2D-VBS model system enhances the conventional CMAQ model. The differences between and improvements to the CMAQ/2D-VBS model system over the conventional CMAQ model are:

1) Definition of species. The SOA species of the conventional CMAQ must be switched with the 2D-VBS species. A three-layer 2D-VBS model was used to simulate the ageing of SOAs from anthropogenic sources, natural sources, and the multistage oxidation processes of POA/ Intermediate-Volatility Organic Compound (IVOC), respectively. To reduce the simulation costs of time and space, the parameters of the 2D-VBS model (not introduced in this report in detail because it's not within the scope of this study) were simplified. The simplification doesn't significantly affect the simulation results of organic aerosol (OA) and the ratio of oxygen and carbon (O:C), as shown in **Figure 3-2**.

2) Emission inventory. POA and IVOC emissions must be distributed into the inputs to the 2D-VBS model based on certain coefficients.

3) Mechanism of gaseous chemistry. This is the core work of the enhancement to the conventional CMAQ model in our study, including adding the first stage oxidation reactions of the conventional precursors, and the oxidation reactions in the three-layer 2D-VBS model. As shown in **Table 3-1**, the SAPRC99 gaseous chemical mechanism has been selected. The major precursors of SOA include a benzene series with a single substituted group (ARO1), a benzene series with a multiple substituted group (ARO2), alkanes with relatively more carbon atoms (ALK5), benzene (BENZ), isoprene (ISOP), monoterpene (TERP), sesquiterpene (SESQ). It should be noted that these species are all "alternative species" that represent a type of species.

4) Mechanism of aerosol chemistry. This study uses a gas-phase/particle-phase absorption and distribution model to iteratively calculate the distribution coefficients between the gas and particle

phases for all types of species. This assumes that the products of heterogeneous reactions are the same as those of gaseous reactions, while the only difference is the reaction rates.

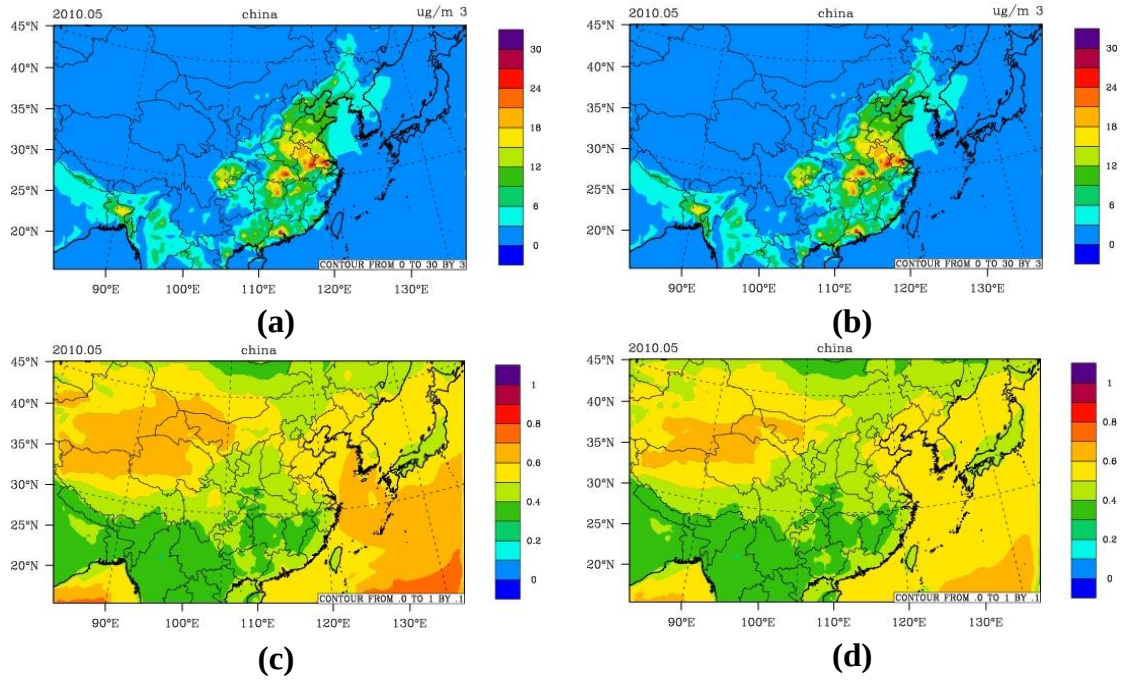

Figure 3-2 Comparison of simulation results of CMAQ/2D-VBS and conventional CMAQ. (a) OA before simplification; (b) OA after simplification; (c) O:C before simplification; (d) O:C after simplification

With these enhancements to the conventional CMAQ model, this study has significantly improved the simulation performance of SOA and OA. As shown in **Figure 3-3** and **Figure 3-4**, in both January (i.e. winter) and August (i.e. summer) 2010, the OA and SOA concentrations simulated by CMAQ/2D-VBS model were generally significantly higher than those simulated by the conventional CMAQ model from the perspective of spatial distribution.

The average OA concentrations for the entire East China area, simulated by the CMAQ/2D-VBS model in January and August, are higher by 30% and 56%, respectively, than those simulated by the conventional CMAQ model. This is caused by ample illumination and high temperatures in the summertime which are beneficial to photo oxidation reactions, leading to significant multi-stage OA oxidation processes. In addition, the spatial distribution of OA concentrations simulated by CMAQ/2D-VBS is more even than that simulated by the conventional CMAQ model. This is because the POA is a major contributor to the OA in the simulation results of the conventional CMAQ model,

which makes the OA concentrate on emission sources related to weak chemical and physical conversions. SOA is a major contributor to the OA for the CMAQ/2D-VBS model, making its spatial distribution more even. As shown in **Figure 3-4**, the SOA concentrations simulated by the CMAQ/2D-VBS model are generally much higher than those simulated in the conventional CMAQ model.

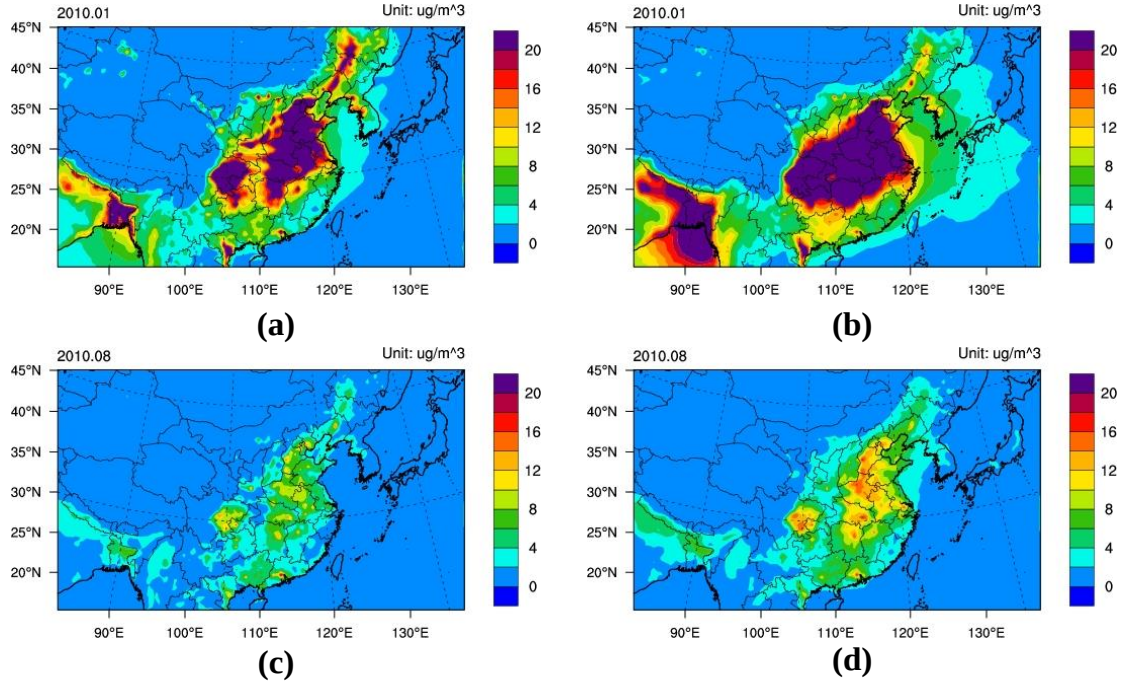

Figure 3-3 Spatial distribution of simulation results of OA concentration in China in 2010. (a) CMAQ in January; (b) CMAQ/2D-VBS in January; (c) CMAQ in August; (d) CMAQ/2D-VBS in August

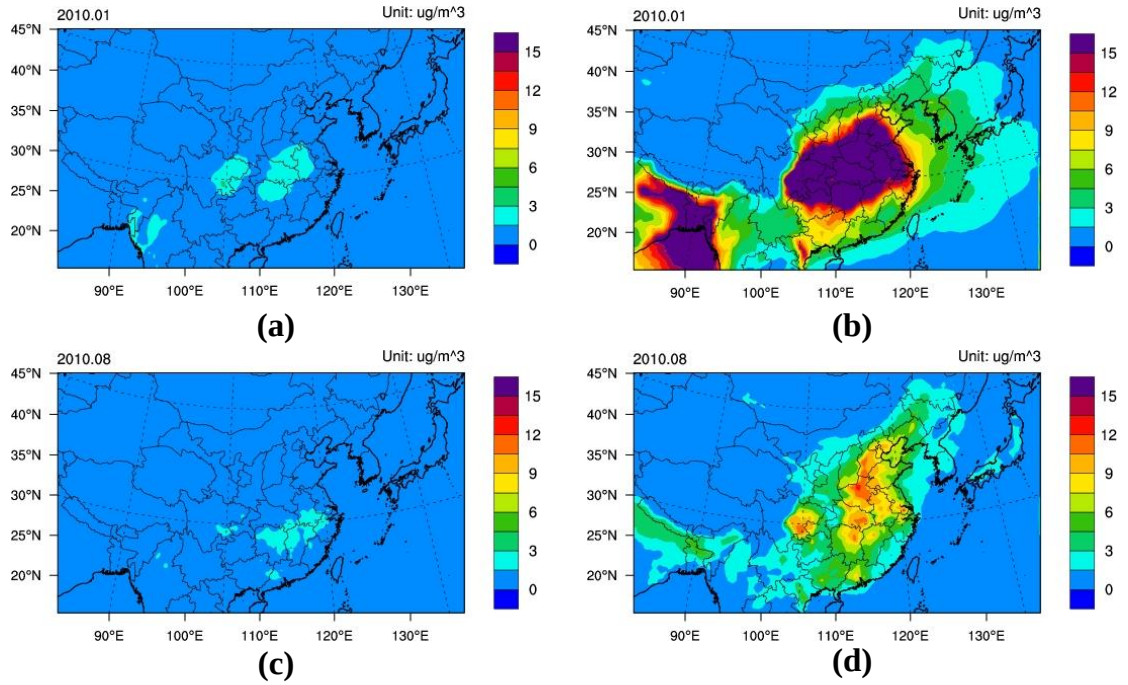

Figure 3-4 Spatial distribution of simulation results of SOA concentration in China in 2010. (a) CMAQ in January; (b) CMAQ/2D-VBS in January; (c) CMAQ in August; (d) CMAQ/2D-VBS in August

3.3 Modeling domains

As illustrated above, this study focuses on the air quality impacts from EV penetration in the YRD and JJJ regions. Therefore, in order to obtain high-resolution air quality simulation results for the two targeted regions, a three-layer nested modeling system was set up based on the WRF and CMAQ model to simulate the air quality from the wider nationwide level to the finest regional level (see **Figure 3-5**).

As mentioned in **Chapter 2**, the nationwide and regional emission inventories have been adopted as inputs to the coarse-grid and finest-grid simulations, respectively. Nesting refers to fitting a finer-resolution grid (i.e. the YRD JJJ regions in **Figure 3-5**) over part of a coarser-resolution grid (the domain with the orange frame). The finer-resolution grid receives information (such as boundary conditions) from the coarser-grid simulation.

As shown in **Figure 3-5**, the coarse domain covers most areas of East Asia, which is divided into 15,908 square cells (164×97) with a side length of 36 km in the CMAQ model. The first nested domain covers most areas of Eastern China, which is divided into 29,104 square cells (136×214) with a side length of 12 km. In addition, the two 'finest' domains cover the two regions of interest in this study - namely the YRD and the JJJ regions. For the YRD, the finest simulation domain covers Shanghai, most areas of

Jiangsu and Zhejiang, and partial areas of Anhui and Jiangxi, and is divided into 21,760 square cells (136×160) with a side length of 4 km. For the JJJ region, another 'finest' domain covers Beijing, Tianjin, Hebei, most areas of Shandong, and partial areas of Liaoning, Inner Mongolia, Shanxi, and Henan, and is divided into 30,600 square cells (150×204) with a side length of 4 km.

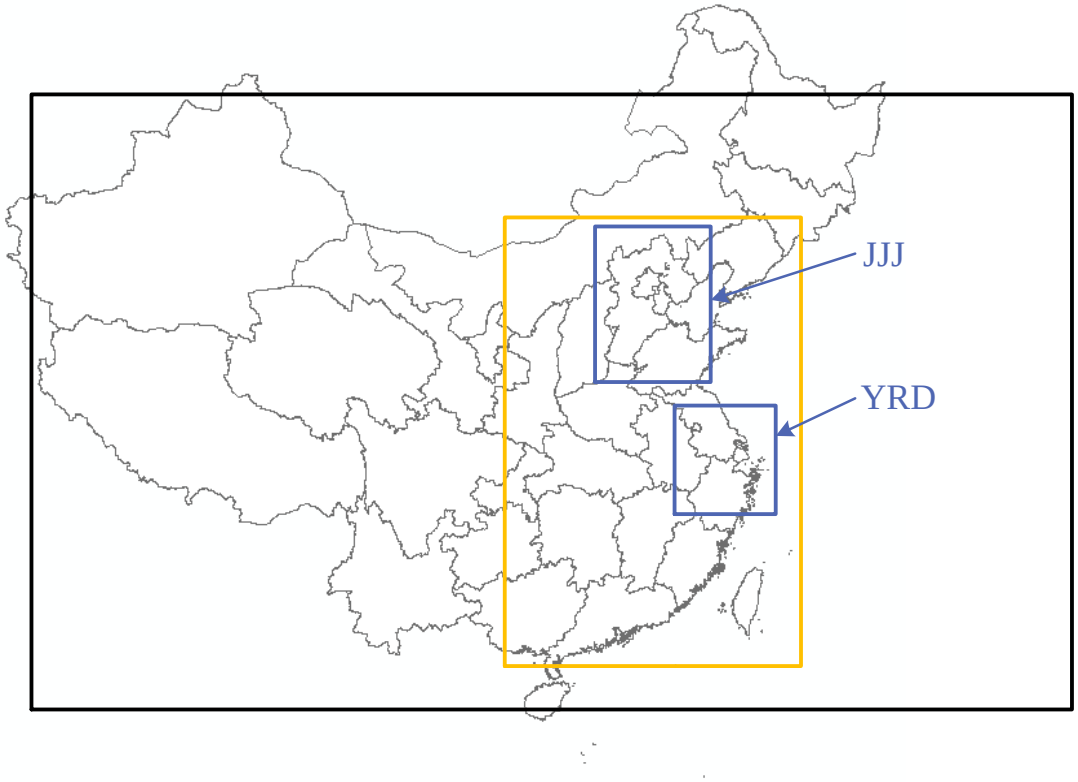

Figure 3-5 Three-layer nested grid simulation of the CMAQ model

Chapter 4 Vehicle electrification scenarios

The air quality impacts of vehicle fleet electrification are directly associated with the EV development scenarios. China has been promoting new energy vehicles nationwide, especially EVs, since 2009. In the past several years, many pilot cities have participated in national EV penetration demonstration plans with different targets, such as the famous <*Ten Cities & a Thousand Units*> [3] plan launched in 2009. The Chinese government introduced a more ambitious plan (<*The industrial development plan for energy saving and new energy vehicles in China (2012-2020)*> [4]) for developing its EV industry in 2012, setting a goal of accumulated EV production and sales of up to 5 million by 2020. Later, the central and local governments began launching a series of incentive policies to promote EVs. Based on the development status and the existing penetration targets set by Chinese central and local governments, various development scenarios for EVs have been developed to estimate the air quality impacts of vehicle electrification in MY 2030.

As mentioned in **Section 1.1**, vehicle electrification mainly refers to passenger vehicles, LDPVs, MDPVs, HDPVs, taxis and buses. Note that trucks are currently excluded in this study because no significant penetration into the EV vehicle market is expected in the next 10 to 15 years in China. In this section, vehicle electrification scenarios projections for China in MY 2030 are separately introduced by vehicle category (i.e. public and private fleets).

4.1 Public fleets

The electrification scenarios for HDPVs, MDPVs, taxis and buses were projected mainly through government plans (with specific penetration targets) and policies. In May 2015, the Ministry of Industry and Information Technology (MIIT) of China released a notice (<*Improving the subsidy policy for product oil price of city buses, accelerating the promotion of new energy vehicles*> [5]) adjusting the price subsidy for the fuels of city buses from 2015 to 2019. The notice stated that the financial subsidy for an increase in fuel pricing would depend on the penetration rate of new energy buses. Moreover, the penetration targets are different between provinces. As shown in **Figure 4-1**, the provinces are grouped into three regions, for which the penetration targets are shown in **Table 4-1**. According to the notice, an assumption was made that the electrification rates of city buses in each province in 2030 would be equal to their penetration

targets in 2019. This was used as the "reference scenario": 80% electrification rate for the key regions for air pollution control (i.e. Beijing, Shanghai, Tianjin, Hebei, Shanxi, Jiangsu, Zhejiang, Shandong, Guangdong, and Hainan), 65% for the central provinces (i.e. Anhui, Jiangxi, Henan, Hubei, and Hunan) and Fujian Province and 30% for other provinces. In addition, two supplementary scenarios considering the upper and lower changes of the reference scenario were developed, namely the High and Low scenarios, of which the penetration targets are presented in **Table 4-1**. However, there are still no officially released penetration targets for HDPVs, MDPVs and taxis in China; therefore, the penetration targets and development scenarios for these vehicle categories are assumed to be equal to those of buses in 2030, considering they are public fleets as well.

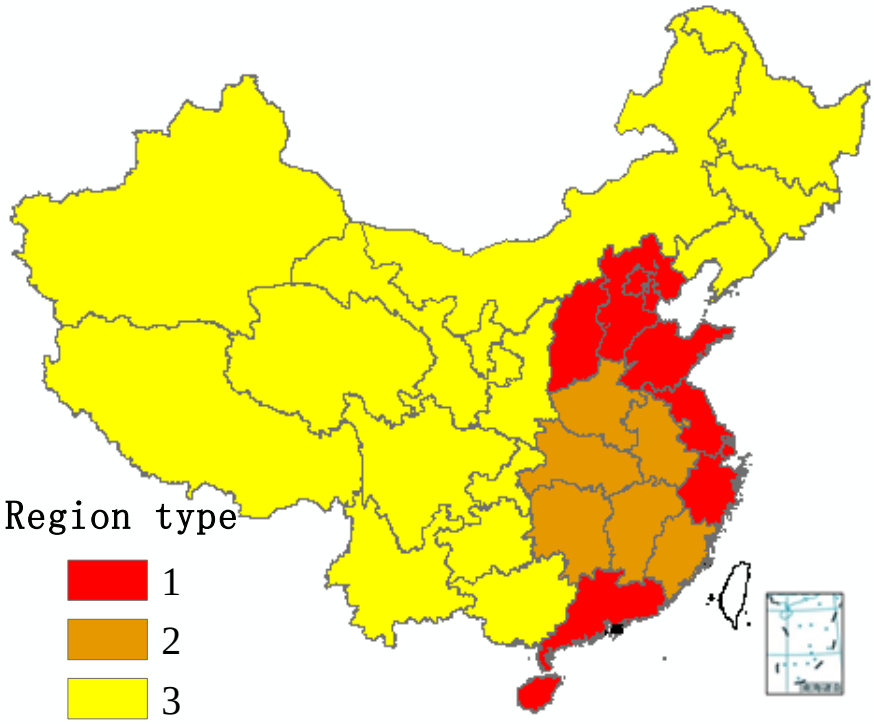

Figure 4-1 Regions with differential penetration targets of new energy buses

Table 4-1 Targets of penetration rates of new energy buses, 2015-2019

Region	Description	2015	2016	2017	2018	2019
1	Key regions for air pollution control	40%	50%	60%	70%	80%
2	Central provinces and Fujian	25%	35%	45%	55%	65%
3	Other regions	10%	15%	20%	25%	30%

4.2 Private LDPVs

Although the penetration of electric vehicles always starts from public fleets due to effective and easy control by governments, considering their huge population, LDPVs should be the primary market for electric vehicle penetration in the future. MIIT released the penetration achievements [7] from 2013 to September 2014 and targets by 2015 for new energy vehicles in the demonstration cities in China. As shown in **Figure 4-2**, the penetration targets of new energy vehicles in different provinces by 2015 are almost proportional to their LDPV stock in 2013. Therefore, it can be assumed that the electrification rates of LDPVs are not different between the provinces in China. This is different from the projections for public fleets.

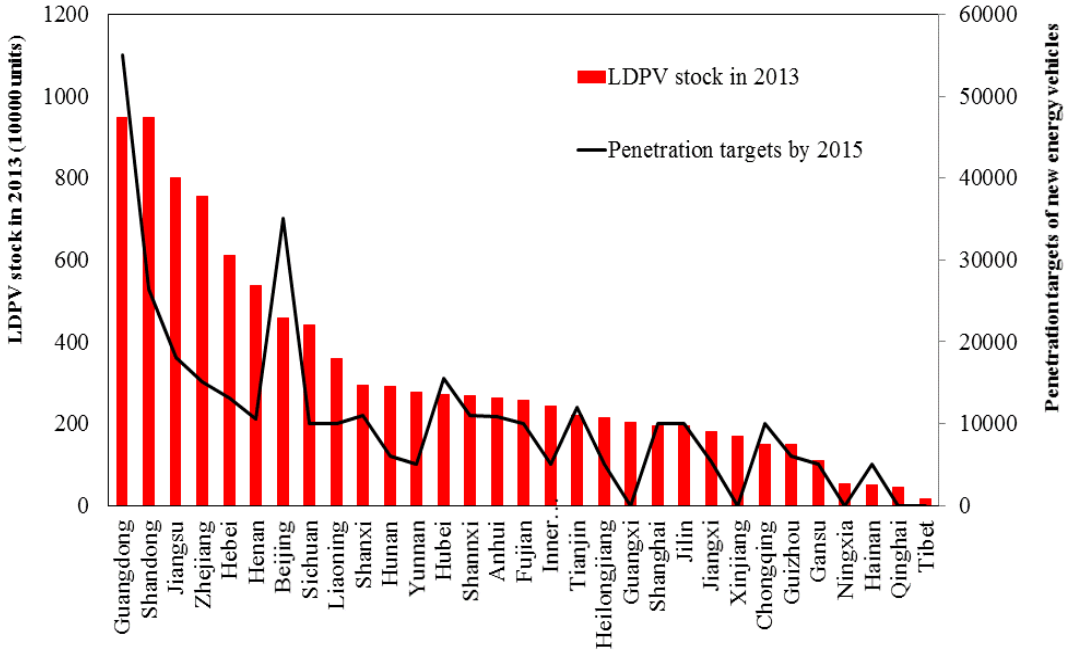

Figure 4-2 Penetration targets of new energy vehicles in China by 2015

However, it is quite difficult to predict the specific penetration rate for LDPVs in the future. As a result, three different scenarios have been developed for the vehicle electrification rates of LDPVs in China in MY 2030 based on different reference sources which correspond to the three development scenarios of public fleets.

1) Low scenario: 5%

The Bass Model is used to forecast the future sales of EVs in China from 2015 to 2030. The Bass Model

is widely used to forecast the market penetration of new products, especially under the circumstances of lacking of or even without historical sales data. The equation below is used to calculate the penetration rates of electric vehicles in the target years from 2015 to 2030 in this study:

$$f(t+1) = p \times [1 - F(t)] + q \times F(t) \times [1 - F(t)]$$

Where 'f(t)' is the penetration rate of a given product in the target year 't'; 'F(t)' is the cumulative penetration rate in the target year 't'; the coefficient 'p' is often called the coefficient of innovation; 'q' is called the coefficient of imitation.

Typical values of the coefficients 'p' and 'q' are obtained from a literature review [7]: the value of 'p' has been found to range from 0.01 to 0.03, and the value of 'q' typically ranges between 0.3 and 0.7, but hardly more than 0.5. In this study, relatively high values of the coefficients 'p' and 'q' have been adopted, considering the powerful push of electric vehicle penetration by Chinese central and local governments. Therefore, the value of 'p' linearly increases from 0.02 in 2015 to 0.03 in 2030, and similarly the value of 'q' increases from 0.4 in 2015 to 0.7 in 2030.

As **Figure 4-3** shows, the total sales of electric vehicles in China could reach the official penetration target of 5 million in 2022, a little later than the target year of 2020. Therefore, this projection was selected as the low scenario, which will be nearly 15 million electric vehicles in total, and accounting for about 5% of the total LDPV fleet in 2030 (about 300 million LDPVs in total by 2030 are projected by other studies).

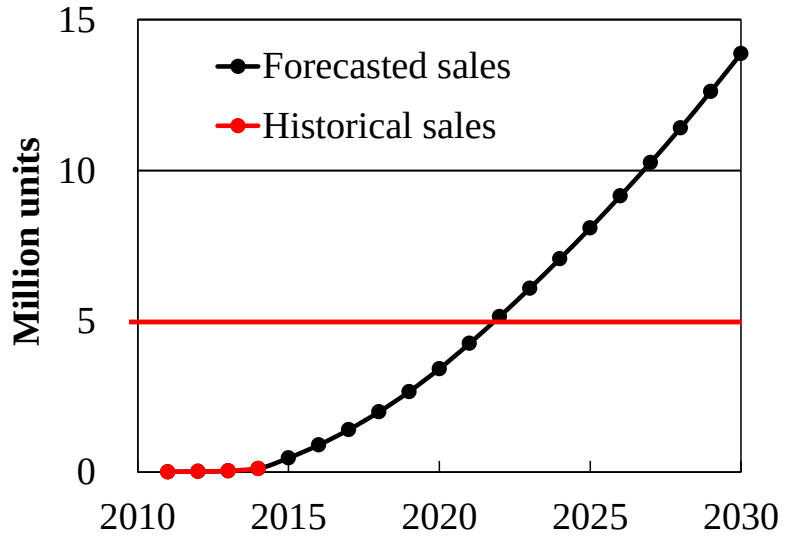

Figure 4-3 Predicted sales of electric vehicles in China using the Bass Model

2) Reference scenario: 20%

The population of conventional LDPVs in China has been increasing over the past decade, from 13 million in 2003 to 103 million in 2013, and is shown in **Figure 4-4**. There is a general prediction that the population of light-duty electric passenger vehicles in China will rapidly increase from 2020 to 2030, after a market preparation period lasting from 2010 to 2020. Therefore, the annual average increasing rate of light-duty electric passenger vehicles is assumed to remain constant at 25% from 2020 to 2030, which is close to the annual average increasing rate of conventional LDPVs from 2004 to 2013 (~23%). Therefore, the total sales of light-duty electric passenger vehicles will be about 50 million, which will be about 20% of the total LDPV fleet stock by 2030 (if the total sales of electric vehicles meet the official penetration targets of 5 million by 2020). Thus, 20% is the reference scenario for the penetration rate of electric LDPVs in China by 2030.

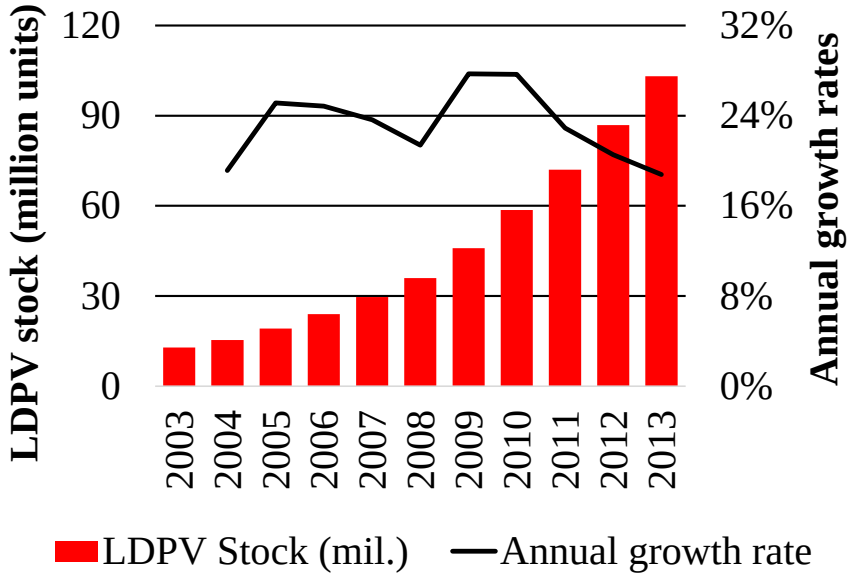

Figure 4-4 Annual stock of LDPVs in China from 2003 to 2013

3) High scenario: 35%

The <*Technology Roadmap: Electric and Plug-in Hybrid Electric Vehicles (EV/PHEV)*> [8] released by the International Energy Agency (IEA) in 2009 predicted that the total sales of plug-in electric vehicles (i.e. PHEVs and BEVs) would be 8.4 million by 2030, which is an unconvincingly low number. However, in 2012, the IEA substantially raised the expectation for electric vehicle sales in China in <*Energy Technology*

Perspectives 2012 – Pathways to a Clean Energy System> [9]. The report projected the annual sales of electric vehicles in China would be about 15 million by 2030, accounting for nearly half of the annual global sales (shown in **Figure 4-5)**. According to this projection, by 2030, sales of electric LDPVs will total about 100 million, which is about 35% of the projected total fleet stock of LDPVs in China. Therefore, 35% is the High scenario for the penetration rate of electric LDPVs in China by 2030.

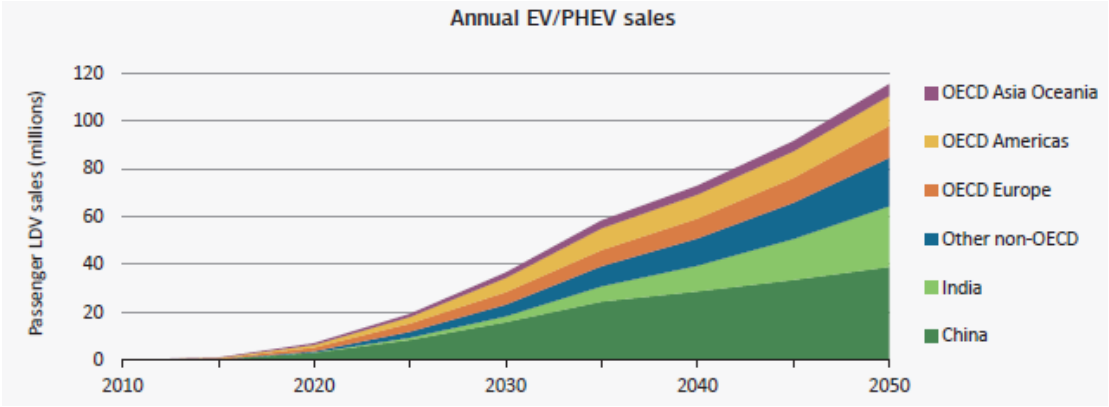

Figure 4-5 Annual EV/PHEV sales of passenger LDVs projected by IEA

(screenshot from the *"Energy Technology Perspectives 2012"*)

As mentioned above, three development scenarios (i.e. Low, Reference, and High) for those vehicle categories involved in electrification scenarios in MY 2030 have been projected. These are summarised in **Table 4-2**. In addition, an ideal scenario has been developed to represent the highest level of vehicle electrification (i.e. scenario boundary), namely, 100% electrification for all vehicle categories (the "Extreme scenario").

Table 4-2 Vehicle electrification rates for different vehicle categories

Vehicle electrification scenario	Light-duty passenger vehicles	HDPV, MDPV, Bus and taxi		
		Region1	Region2	Region3
Extreme	100%	100%	100%	100%
High	35%	90%	80%	65%
Reference	20%	80%	65%	30%
Low	5%	65%	30%	20%

Note: Region 1-3 refers to **Figure 4-1**.

4.3 Simulated scenarios

To explore the air quality impacts on the targeted regions (i.e. YRD and JJJ) in this study, three fleet electrification scenarios have been designed for 2030 (see **Table 4-3**):

(1) *Scenario w/o EVs*: which assumes that no EVs are deployed in the fleet of the research area;

(2) *Scenario EV1*: which assumes that the "Reference Scenario" (see **Table 4-2**) is deployed in the fleets of the research areas (*Scenario EV1* is seen as a most plausible plan for the medium-term future);

(3) *Scenario EV2:* which assumes that the "Extreme Scenario" (see **Table 4-2**) is deployed in the targeted regions (i.e. JJJ and YRD) and the "Reference Scenario" is deployed in the other areas. It is intended to be used to examine the maximum air quality benefit; however, this scenario may not become reality within the next fifteen years.

Both electrification scenarios consider only BEVs for simplicity because BEVs are responsible for 75% of total EV sales in China, and PHEVs can be methodologically seen as partial BEVs with adequately electrified mileage splits.

Table 4-3 Simulated scenarios for regional air quality impacts of EV penetration

Simulated scenario	EV development scenarios (refer to **Table 4-2**)	
	YRD	Other areas
w/o EVs	No	No
EV1	Reference	Reference
EV2	Extreme	Reference

Chapter 5 Air quality impact assessments

In this chapter, the air quality modeling results of various vehicle electrification scenarios in the two typical regions in China are presented. The first section of this chapter provides the results in the YRD region and the second section is for the JJJ region. Note that the air quality assessments of each vehicle electrification scenario are nested simulations, although only the results of the finest domain (i.e. the YRD and JJJ domain shown in **Figure 3-5**) are presented in this report.

5.1 Case study in JJJ

5.1.1 Emission changes for different EV scenarios

Under fleet electrifications in the JJJ region, certain trends in reduced NMVOC and NO_X emissions and increased SO_2 emissions occur, but slight changes will be realised for $PM_{2.5}$ emissions due to the significant emission distinctions between on-road vehicles and power plants. For example, *Scenarios EV1* and *EV2* could lead to reductions of 4.4% and 17%, respectively, for the total NMVOC emissions in the JJJ region, accompanied by reductions of 6.6% and 8.8% in total NO_X emissions, respectively, even though the power sector is also an important source of NO_X (21%).

5.1.2 Air quality impacts

1. Results of *Scenario w/o EVs*

Figure 5-1 presents the spatial distribution of NO_2, $PM_{2.5}$, and SO_2 concentrations under the *Scenario w/o EVs* in the JJJ region in 2030. The mean $PM_{2.5}$ concentrations in January and August in the urban areas in the JJJ region are estimated to be 45 $\mu g/m^{-3}$ (note: all results stated hereinafter in this section are intended for simulated grids covering the urban areas of 13 cities in the JJJ region). It is higher by 28% than the limit of the new national ambient air quality standards (NAAQS) [10] (35 $\mu g\ m^{-3}$) in China, which was published in 2012 and implemented in January 2016. From the perspective of different seasons, the average $PM_{2.5}$ concentrations in January (58 $\mu g\ m^{-3}$) should significantly exceed that standard limit, while the average value in August (31 $\mu g\ m^{-3}$) is estimated to be much lower than that in January. This seasonal variation of $PM_{2.5}$ concentrations is due to different meteorological conditions and chemical mechanisms in January and August. In addition, the mean NO_2 and SO_2 for January and August in the urban areas of

the JJJ region are estimated to be 42 and 47 μg m^{-3}, respectively, which is close to and lower than the new NAAQS limits (i.e. 40 and 60 μg m^{-3} for NO_2 and SO_2, respectively).

As a region with a high population, heavy industry and traffic density, the JJJ region is considered to be the last region to reach the NAAQS among the three economic power houses in China (i.e. JJJ, YRD, and Pearl River Delta (PRD)). However, recent studies have argued that the air quality in urban areas of JJJ should reach the new NAAQS limits by the end of 2030. Specifically, the annual average $PM_{2.5}$ concentrations in JJJ should be reduced by ~40% to 64 μg m^{-3} by the end of 2020 compared to the value in 2013 (106 μg m^{-3}), and reduced by 67% to reach the NAAQS limit by the end of 2030. In addition, according to data published by China's Ministry of Environmental Protection (MEP) [11], the 13 cities monitored in the JJJ region reported that air quality met national standards on 52.4% of days in 2015, a year-on-year increase of 9.6%. It is obvious that Chinese central and local governments are accelerating air pollution controls. Thus, the projections for the air pollutant concentrations (i.e. $PM_{2.5}$, NO_2, and SO_2) in JJJ in *Scenario w/o EVs* in this study might be overestimated, considering statements from recent updated studies and new findings from the latest air quality monitoring. In further studies, it should be adjusted to be in accordance with both the targets and recent trends of regional air quality improvements.

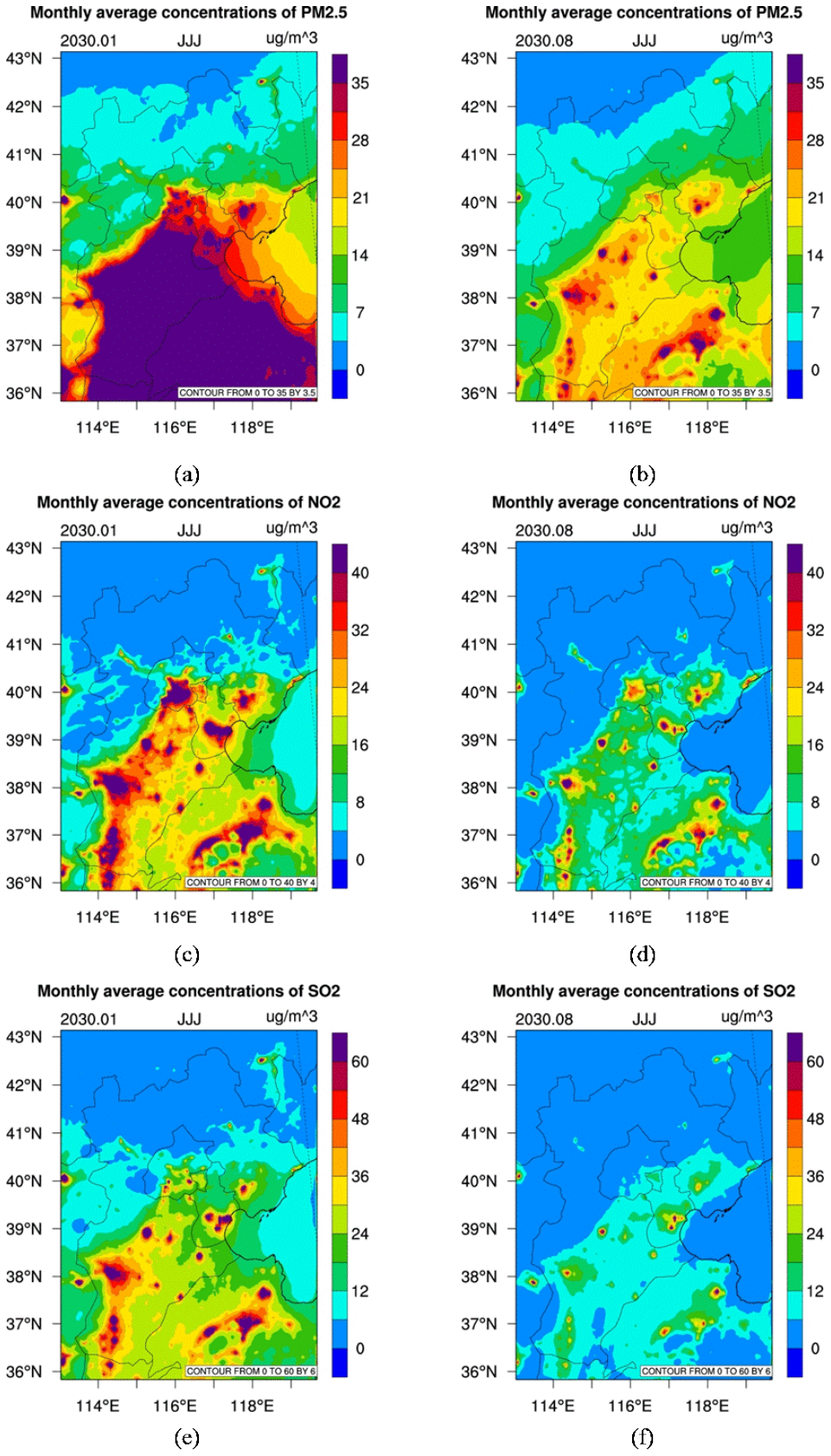

Figure 5-1 Air pollutant concentrations under *Scenario w/o EVs* in JJJ in 2030. (a) $PM_{2.5}$ in January; (b) $PM_{2.5}$ in August; (c) NO_2 in January; (d) NO_2 in August; (e) SO_2 in January; (f) SO_2 in August.

2. $PM_{2.5}$ concentration changes in EV scenarios

Figure 5-2 presents the spatial changes of simulated monthly average $PM_{2.5}$ concentrations under EV scenarios relative to *Scenario w/o EVs* for the JJJ region in MY 2030. Relative to *Scenario w/o EVs*, *Scenario EV1* in 2030 is an estimated reduction of $PM_{2.5}$ concentrations by 0.6±1.4 μg m^{-3} (note: mean value and standard deviation) in January and 0.3±0.3 μg m^{-3} in August. The reduction effects on $PM_{2.5}$ concentrations differ from region to region. For example, the reduction effects are intended to achieve more in urban areas with dense traffic but less in areas with abundant power plants.

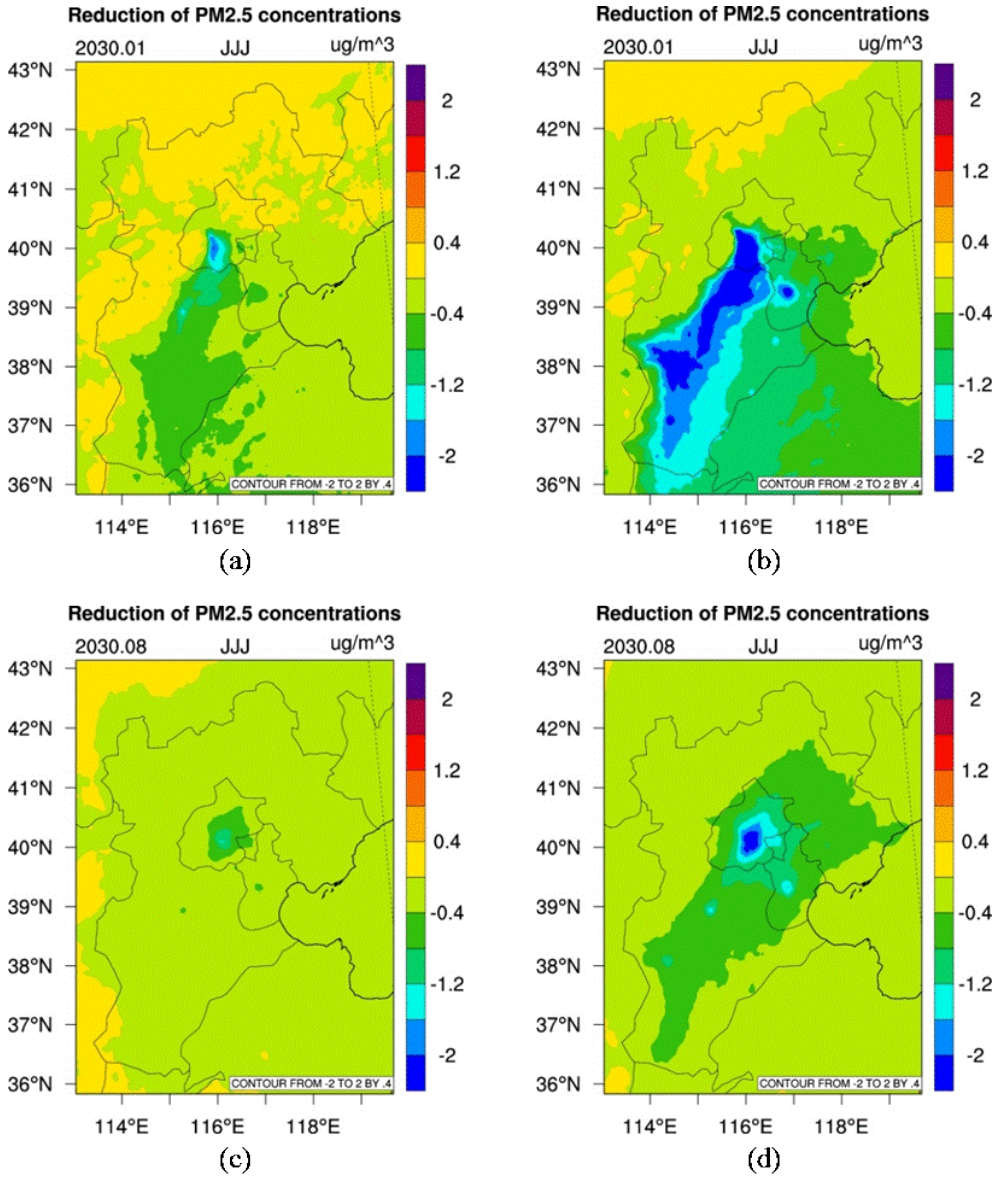

Figure 5-2 Changes of monthly mean $PM_{2.5}$ concentrations from EV scenarios relative to *Scenario w/o EVs* in JJJ in 2030. (a) *Scenario EV1* in January; (b) *Scenario EV2* in January; (c) *Scenario EV1* in August; (d) *Scenario EV2* in August

During January, the greatest $PM_{2.5}$ reductions were simulated to occur in cells within the urban areas of Beijing (1.6±3.7 μg m^{-3}) under *Scenario EV1* compared with *Scenario w/o EVs*. In August, the area with the greatest $PM_{2.5}$ concentration reduction would still occur in Beijing (0.9±0.5 μg m^{-3}). Furthermore, fleet electrification can readily deliver air quality benefits for urban $PM_{2.5}$ concentration mitigation in the urban areas of all cities. Nevertheless, the spatial patterns of $PM_{2.5}$ concentration changes in January and August (see **Figure 5-2**) are not identical to those of emission changes (e.g. hotspots of emission reductions within urban areas), which could be attributed to two aspects. First, the contribution from primary vehicular emissions to ambient $PM_{2.5}$ concentration would be minor due to stringent tailpipe emission controls in the future. Second, the reaction and transport time framework of secondary aerosol formation from gaseous precursors (e.g. NO_X and VOCs) would weaken the spatial relationship between emission mitigation and concentration reductions. The aggressive *Scenario EV2* can achieve greater reductions in $PM_{2.5}$ concentration by 1.7±2.8 and 0.9±0.8 μg m^{-3}, in January and August, respectively, according to the simulation results compared with those under *Scenario w/o EVs*. Furthermore, the areas with the greatest air quality benefits from the fleet electrification spatially resemble those under *Scenario EV1*, where the $PM_{2.5}$ concentration reductions under *Scenario EV2* would be enhanced to over 3.0 μg m^{-3} in January (cells in urban areas of Beijing and Baoding) and 2.0 μg m^{-3} in August (urban areas of Beijing) (see **Figure 5-2**).

When examining key aerosol components (see **Figure 5-3**), nitrate and SOA are the two most important contributors to the reductions in $PM_{2.5}$ concentrations. This could be attributed to the emission reductions of NO_X and NMVOC from EV deployment. The seasonal distinctions of air quality impacts from the vehicle fleet electrification are also identified. During January, under *Scenario EV1*, nitrate reduction (0.4±1.0 μg m^{-3}) is estimated to play a major role in mitigating $PM_{2.5}$ rather than under *the Scenario w/o EVs*. The large nitrate reduction could also contribute to lower concentrations of ammonium aerosol in the particle phase. In August, the reduction of SOA (0.2±0.2 μg m^{-3}) is responsible for 55% of the total $PM_{2.5}$ reduction on average under *Scenario EV1*. Meanwhile, nitrate reduction decreases to 0.1±0.1 μg m^{-3}. In January, low temperatures and poor dispersion conditions favor nitrate formation. In contrast, in August, high temperatures and high ambient oxidant concentrations would favorably lead to high SOA concentrations, which would significantly favour

nitrate evaporation. Thus, reducing NO_X emissions has more significant reduction benefits to nitrate concentrations in January than those in August; but reducing NMVOC emissions has the opposite effect on SOA concentrations. *Scenario EV2* shows similar impact patterns for aerosol components as in *Scenario EV1*. In August, the SOA reduction would be more significant than nitrate reduction and become a major contributor of total $PM_{2.5}$ reduction under *Scenario EV2*. The concentration changes of element carbon (EC) aerosol are estimated to be minor in both January and August because high-efficiency particle filters and collectors will be largely used to reduce EC emissions for both vehicles and power plants. The electrification would increase SO_2 emissions; thus, the simulations indicate that increased sulfate concentrations are an insignificant matter compared to the benefits of other aerosol components.

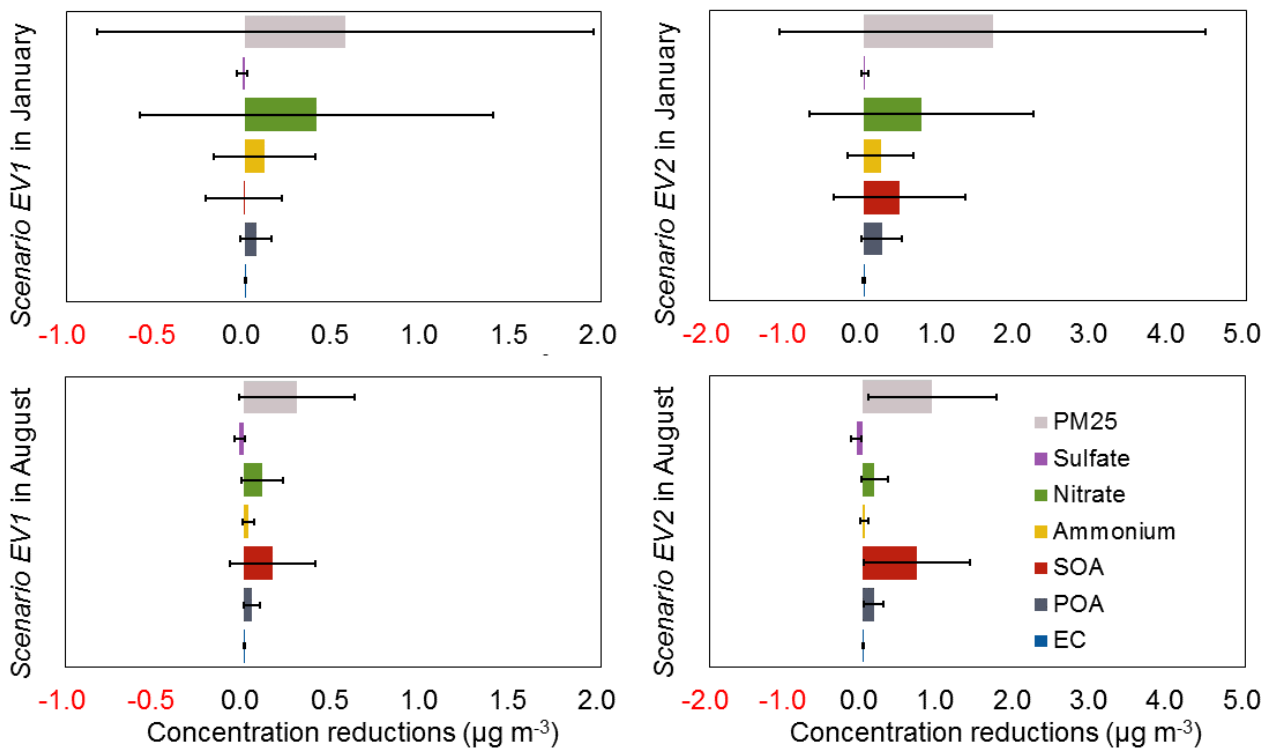

Figure 5-3 Monthly-average concentration changes of $PM_{2.5}$ and major aerosol components in the urban areas of the JJJ region under *Scenarios EV1* (left) and *EV2* (right) relative to *Scenario w/o EVs*, during January (top) and August (bottom) 2030

3. NO_2 concentration changes of EV scenarios

Figure 5-4 shows the spatial distributions of average daily NO_2 concentration differences between EV

scenarios and the base case scenario in January and August in MY 2030. Different from $PM_{2.5}$, the reductions of NO_2 concentrations are more spatially uneven in the entire JJJ region. It is because the chemical mechanisms of $PM_{2.5}$ formations are more complex than NO_2 formations. In other words, the spatial distribution of NO_2 reductions concentrates on the areas with high traffic density, and are almost identical to the spatial distribution of NO_X emissions reduction from on-road vehicles. The largest NO_2 reductions occur in the urban areas of Beijing, Tianjin, and Shijiazhuang, all of which are major cities in the JJJ region.

Compared to *Scenario w/o EVs*, *Scenario EV1* can reduce NO_2 concentrations by 2.9±3.6 μg m^{-3} in January and 2.8±2.6 μg m^3 in August, presenting a reduction of 6-8% over the urban areas of the core cities in the JJJ region. Furthermore, *Scenario EV2* has a slightly greater reducing effect on NO_2 concentrations (with a total reduction of 10-13%) than *Scenario w/o EVs*. Therefore, combined with previous conclusions, the most significant marginal effect of *Scenario EV2* compared to *Scenario EV1* is the mitigation of SOA concentrations rather than nitrate aerosol or NO_2 concentrations.

Nevertheless, the simulation results under *Scenario w/o EVs* show that NO_2 exceedance is highly likely to occur in certain hotspots in traffic-populated metropolitan areas, such as the urban areas of Beijing, Tianjin, Shijiazhuang and Baoding (see **Figure 5-1**), which has been seen in many traffic-populated cities in Europe. In the JJJ region, taking Beijing for example, the annual average NO_2 concentration was 50 μg m^{-3} during 2015, exceeding the limit of National Ambient Air Quality Standards (NAAQS). This clearly indicated that mitigating NO_2 concentrations is also a great challenge. **Figure 5-4** illustrates that a greater reduction of NO_2 concentrations from EV penetration will occur in traffic-populated urban areas (e.g. Beijing, Tianjin, and Shijiazhuang), which suggests that vehicle fleet electrification would result in adequate air quality benefits where the NO_2 exceedance risk is high. For example, the largest reductions in NO_2 concentrations under *Scenario EV1* would be up to 12 μg m^{-3} in January and 8 μg m^{-3} in August, which are simulated to both occur in the urban area of Beijing, where the baseline NO_2 concentrations under *Scenario w/o EVs* are estimated to be 47±22 μg m^{-3} in January and 27±6 μg m^{-3} in August. The NO_2 concentration reductions are shown to be 25% in January and 30% in August. The simulated monthly average NO_2 concentration of the urban area of Beijing during January (47 μg m^{-3}) exceeds the annual NAAQS limit (40 μg m^{-3}), and *Scenario EV1* is critical in order to greatly reduce the exceedance

risk. Thus, vehicle fleet electrification can effectively help in mitigating NO_2 in traffic-populated cities.

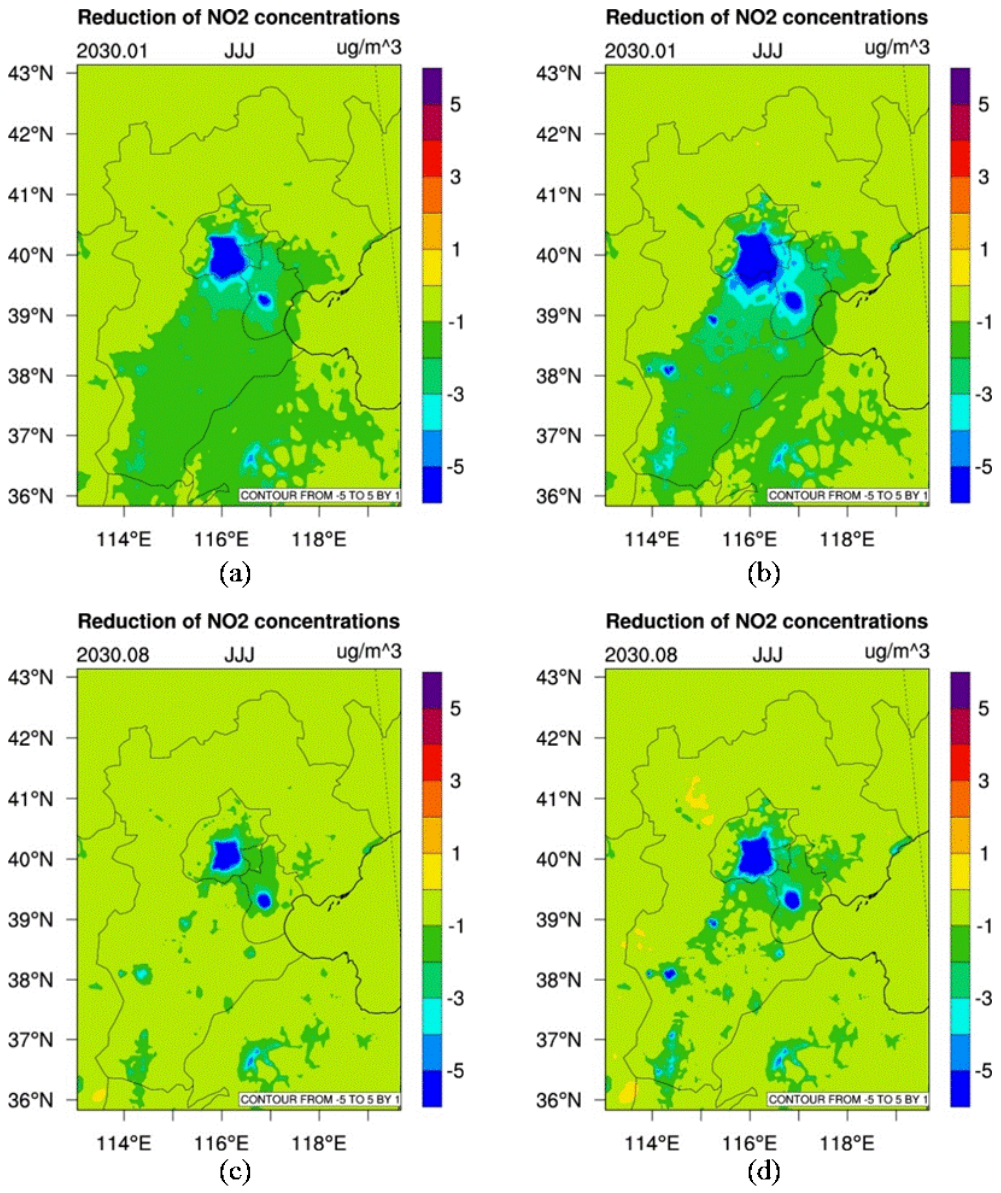

Figure 5-4 Changes of monthly mean NO_2 concentrations from EV scenarios relative to *Scenario w/o EVs* in JJJ. (a) *Scenario EV1* in January; (b) *Scenario EV2* in January; (c) *Scenario EV1* in August; (d) *Scenario EV2* in August

4. SO_2 concentration changes of EV scenarios

Figure 5-5 shows the spatial distributions of monthly average SO_2 concentration changes between EV scenarios and *Scenario w/o EVs* in January and August 2030. Different from $PM_{2.5}$ and NO_X, simulated SO_2 concentrations under EV scenarios are slightly higher than *Scenario w/o EVs* in JJJ, due to the

increases in SO_2 emissions from power plants (resulting from the marginal generation of power for the charging of BEVs). The increases are almost negligible under *Scenario EV1*. Under *Scenario EV2*, the increases are more significant (> 0.3 μg m^{-3}) in the areas in which thermal power plants are abundant (south of Hebei province). However, as noted, SO_2 concentrations in JJJ are estimated to be much lower

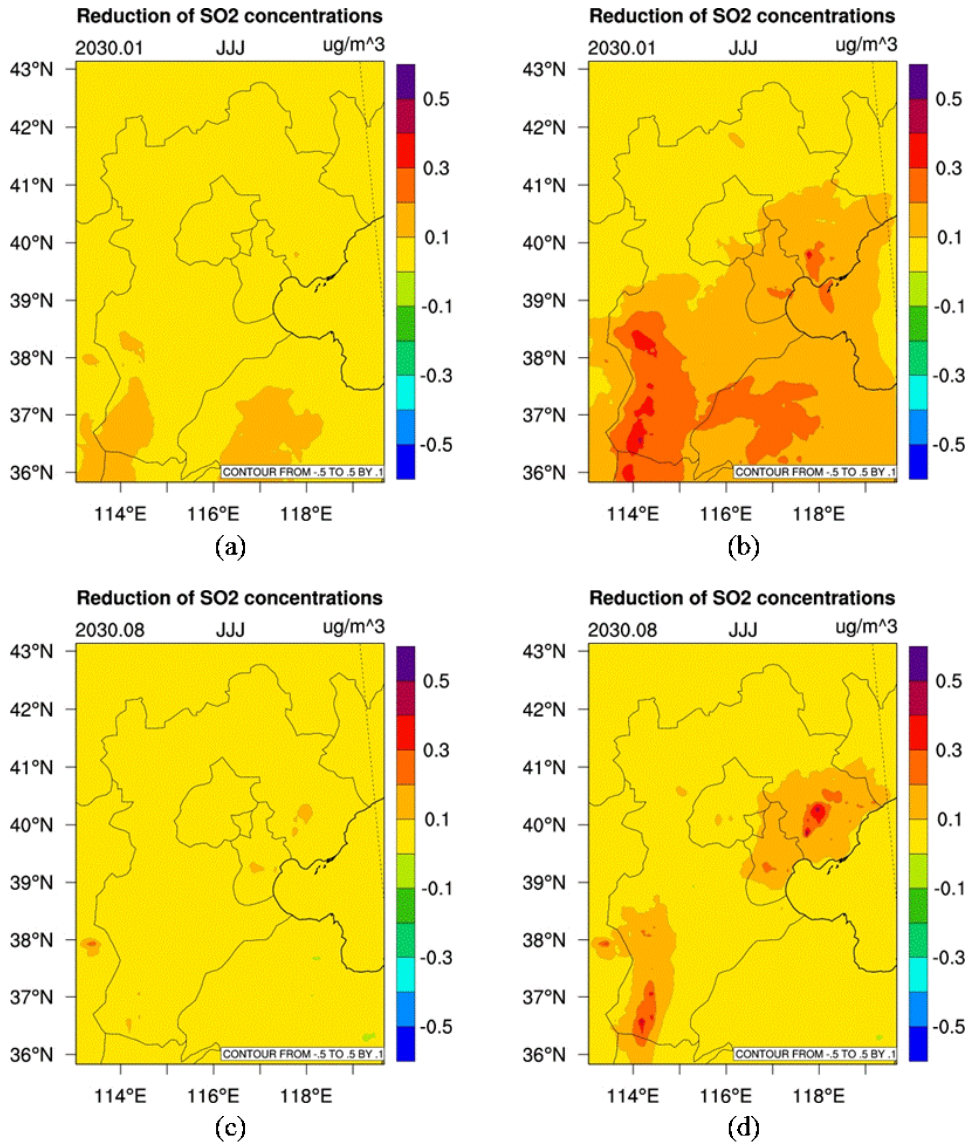

than standard limits in *Scenario w/o EVs*. Therefore, the adversely increased SO_2 concentration from fleet electrification is insignificant and acceptable for the JJJ region in MY 2030.

5.2 Case study in YRD

5.2.1 Emission changes for different EV scenarios

After fleet electrification in the YRD region, certain trends in reduced NMVOC and NO_X emissions and increased SO_2 emissions will occur, but only slight changes will be realised for $PM_{2.5}$ emissions due to the significant emission distinctions between on-road vehicles and power plants. For example, *Scenarios EV1* and *EV2* could lead to reductions of 2.2% and 7.8% in total NMVOC emissions in the YRD region, respectively, accompanied with reductions of 8.1% and 10% in total NO_X emissions, respectively, even though the power sector is also an important source of NO_X (29%). Unlike previous estimates indicating that BEVs would have higher WTW NO_X emissions than gasoline cars around 2010, the updated results (see Part 2 of this report) of this study using the up-to-date data and outlook in terms of future energy efficiency and emission end-of-pipe controls, suggest that light-duty BEVs will have comparable WTW NO_X emissions to their conventional counterparts in the YRD region by 2030. For heavy-duty buses that are important contributors to NO_X emissions in urban areas, conventional vehicles are driven by diesel fuel and dependent on selective catalytic reduction (SCR) devices to control NO_X emissions. However, low-speed urban conditions could be a significant hurdle for SCR to realise reasonable efficiency. The electric buses, although they increase electricity demand, with the high performance rate of SCR installed by thermal power units, can still reduce WTW NO_X emissions of electric buses by 75% compared with diesel buses in the YRD region by 2030 (see the report on the phase I project).

5.2.2 Air quality impacts

1. Results of *Scenario w/o EVs*

Figure 5-7 presents the spatial distribution of NO_2, $PM_{2.5}$, and SO_2 concentrations under the *Scenario w/o EVs* in the YRD region during 2030. The results indicate that the mean urban $PM_{2.5}$ concentration in the YRD region in January and August 2030 under the *Scenario w/o EVs* is simulated as 35 μg m^{-3} (note: all results stated in this section are intended for simulated grids covering the urban areas of 16 core cities in the YRD region). It meets the annual-average limit of the NAAQS (35 μg m^{-3}), which was published in 2012 and implemented in January 2016. From the perspective of different seasons, the average $PM_{2.5}$ concentrations in January (50 μg m^{-3}) should significantly exceed that standard's limit, but

the average value in August is estimated to be much lower (20 μg m^{-3}). This seasonal variation of $PM_{2.5}$ concentrations is due to different meteorological conditions and chemical mechanisms in January and August. In addition, the mean NO_2 and SO_2 concentrations for January and August in the urban areas in the YRD region are estimated to be 23 and 21 μg m^{-3}, respectively, both of which are substantially lower than the new NAAQS limits (i.e. 40 and 60 μg m^{-3} for NO_2 and SO_2, respectively). However, the NO_2 concentrations in some urban areas (e.g. Shanghai and Nanjing) with a high density of population and traffic would exceed the standard limit, especially in January. Therefore, more strategies and measures such as vehicle electrification should be considered to potentially further improve the air quality in the YRD region in the future. The YRD region is normally considered to have reached the concentration limits of $PM_{2.5}$ in the new NAAQS before 2030, as the minimum requirement from government planning targets. Thus, the *Scenario w/o EVs* seems to be a proper projection to the energy consumption and end-of-pipe emission control policies for China in the mid-term future, considering the fulfillment of regional air quality improvements targets.

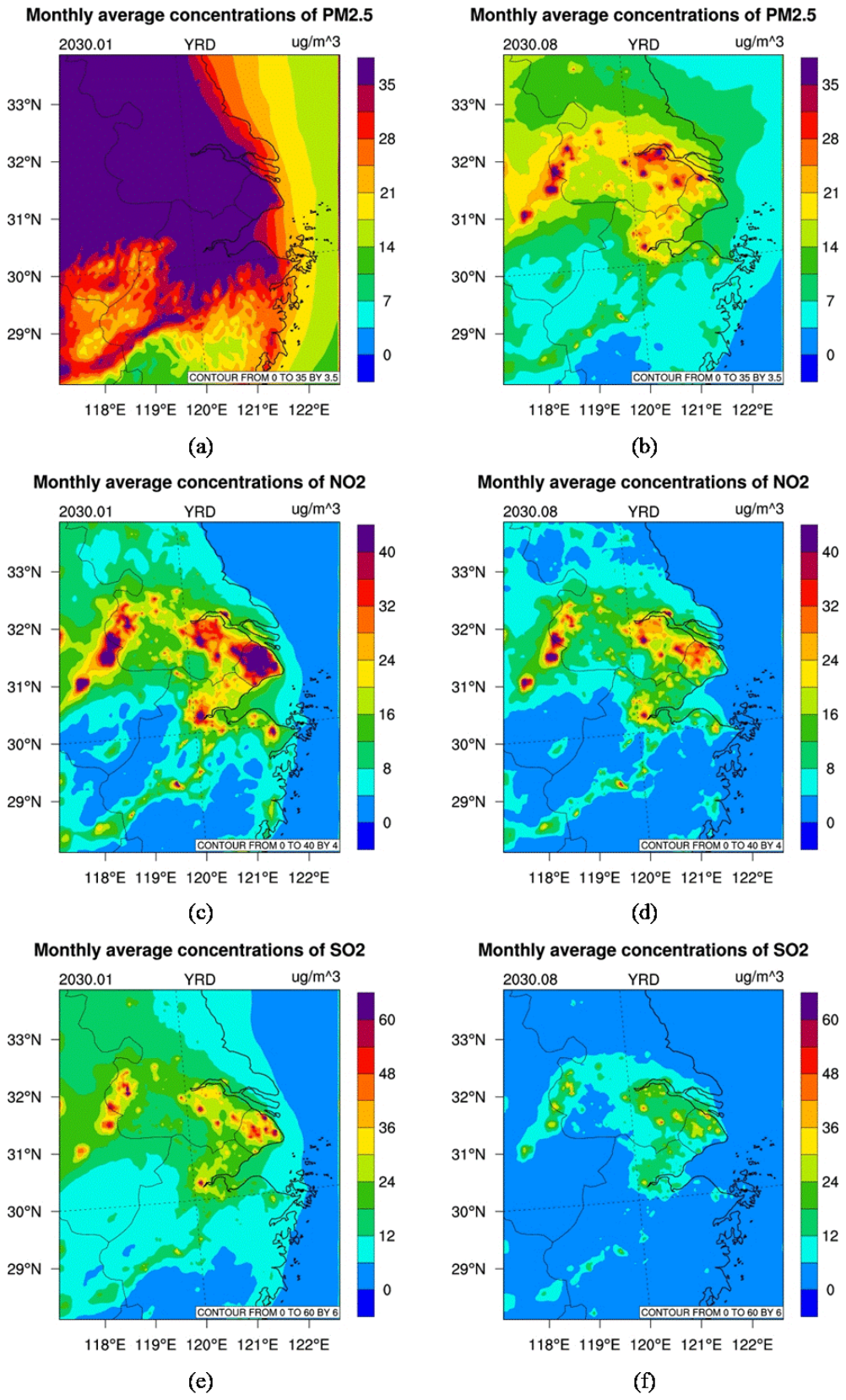

Figure 5-6 Air pollutant concentrations under *Scenario w/o EVs* in YRD in 2030. (a) $PM_{2.5}$ in January; (b) $PM_{2.5}$ in August; (c) NO_2 in January; (d) NO_2 in August; (e) SO_2 in January; (f) SO_2 in August

2. $PM_{2.5}$ concentration changes of EV scenarios

Figure 5-8 presents the spatial changes of simulated monthly average $PM_{2.5}$ concentrations under EV scenarios relative to the *Scenario w/o EVs* for the YRD region in MY 2030. Relative to the *Scenario w/o EVs*, *Scenario EV1* is estimated to reduce $PM_{2.5}$ concentrations by 0.8±0.6 μg m^{-3} in January and 0.4±0.5 μg m^{-3} in August, presenting reductions of approximately 2% in both periods.

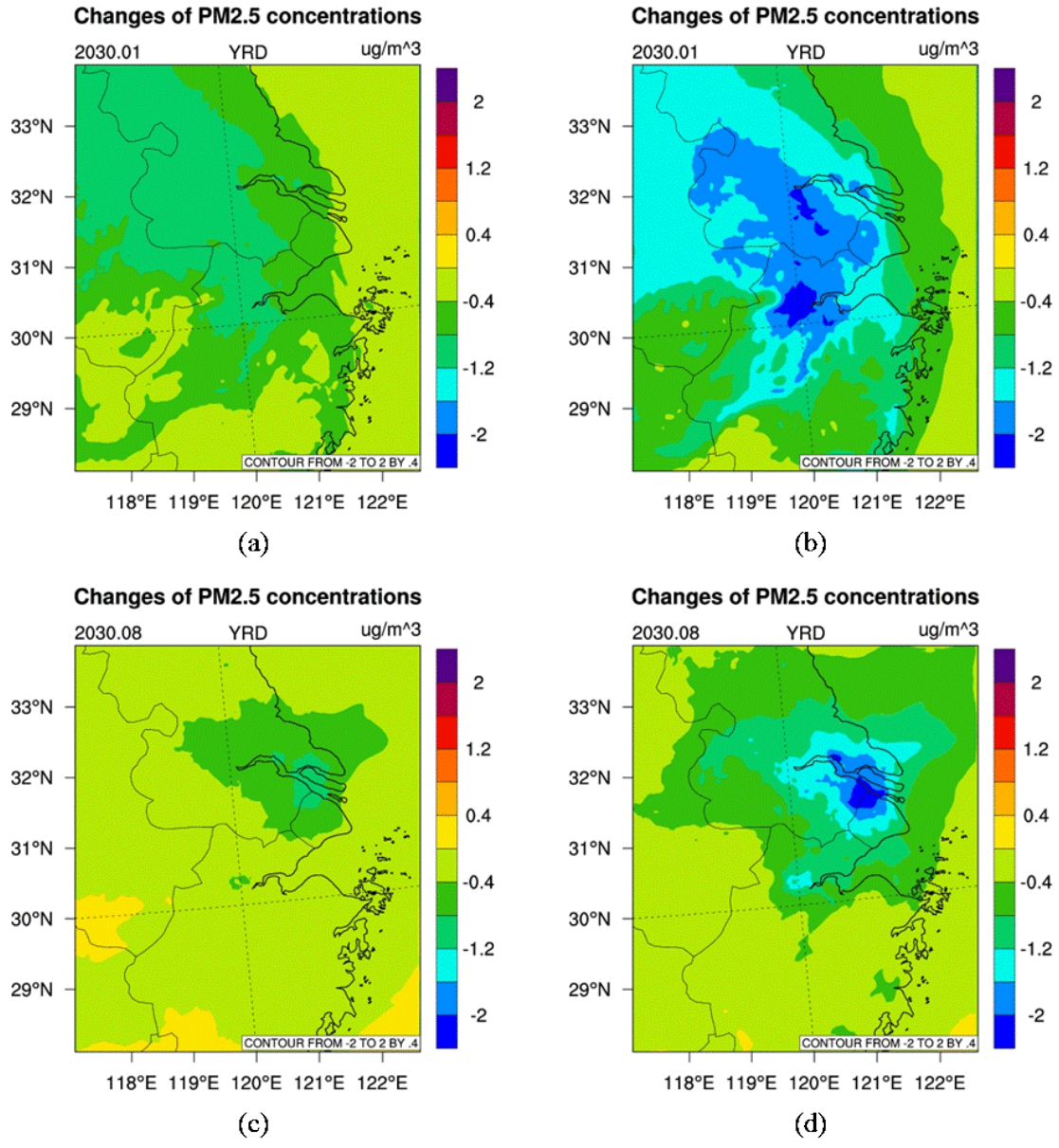

Figure 5-7 Changes of monthly mean $PM_{2.5}$ concentrations from EV scenarios relative to *Scenario w/o EVs*. (a) *Scenario EV1* in January; (b) *Scenario EV2* in January; (c) *Scenario EV1* in August; (d) *Scenario EV2* in August

During January, the greatest $PM_{2.5}$ reductions are simulated to occur in cells within the urban areas of Hangzhou and Wuxi (0.9±0.6 μg m^{-3}) under *Scenario EV1* compared with the *Scenario w/o EVs*, whereas in August, the area with the greatest $PM_{2.5}$ concentration reduction would occur in Shanghai (1.0±1.1 μg m^{-3}). Furthermore, fleet electrification can readily deliver air quality benefits for urban $PM_{2.5}$ concentration mitigation in all cities. Nevertheless, the spatial patterns of $PM_{2.5}$ concentration changes in January and August (see **Figure 5-8**) are not identical to those of emission changes (e.g. hotspots of emission reductions within urban areas), which could be attributed to two aspects. First, the contribution from primary vehicular emissions to ambient $PM_{2.5}$ concentration would be minor due to stringent tailpipe emission controls in the future. Second, the reaction and transport time framework of secondary aerosol formation from gaseous precursors (e.g. NO_X and VOCs) would weaken the spatial relationship between emission mitigation and concentration reductions. The aggressive *Scenario EV2* can achieve greater reductions in $PM_{2.5}$ concentration by 1.7±1.2 and 1.0±1.0 μg m^{-3}, respectively, in January and August, according to the simulation results compared with those under the *Scenario w/o EVs*. Furthermore, the areas with the greatest air quality benefits from the fleet electrification spatially resembles those under *Scenario EV1*, where the $PM_{2.5}$ concentration reductions under *Scenario EV2* would be enhanced to over 2.0 μg m^{-3} in January (cells in Hangzhou and Wuxi) and 2.3 μg m^{-3} in August (north Shanghai) (see **Figure 5-8**).

When examining key aerosol components (see **Figure 5-9**), nitrates and SOAs are the two most important contributors to the reductions in $PM_{2.5}$ concentrations, and could be attributed to the emission reductions of NO_X and NMVOC from EV deployment. The seasonal distinctions of air quality impacts from vehicle fleet electrification are also identified and are similar to the findings in the JJJ region. During January, under *Scenario EV1*, nitrate reduction (0.7±0.4 μg m^{-3}) is estimated to play a major role in mitigating $PM_{2.5}$ than that under *the Scenario w/o EVs*. The large nitrate reduction could also contribute to lower concentrations of ammonium aerosol in the particle phase. However, the concentrations of SOA in January will be increased by 0.1±0.2 μg m^{-3}, which could be attributed to oxidant increases (e.g. Hydroxid (OH) and Ozone (O_3)). In August, the reduction of SOA (0.2±0.2 μg m^{-3}) is responsible for 48% of the total $PM_{2.5}$ reduction on average in *Scenario EV1*. Meanwhile, nitrate reduction decreases to 0.2±0.3 μg m^{-3}. Such a seasonal difference is primarily attributed to the

meteorological conditions and atmospheric chemistry mechanisms that differ between the two periods and is consistent with seasonal patterns observed in situ in the YRD region. In January, low temperatures and poor dispersion conditions favor nitrate formation. In contrast, in August, high temperatures and high ambient oxidant concentrations would favourably lead to high SOA concentrations, which will significantly favour nitrate evaporation. Therefore, reducing NO_X emissions has more significant reduction benefits to nitrate concentrations in January than it does in August, but reducing NMVOC emissions has the opposite effect on SOA concentrations. *Scenario EV2* shows similar impact patterns for aerosol components as in *Scenario EV1*, except for the positive effect of reducing SOA levels in January (0.5 ± 0.6 μg m^{-3}). These results occur because the greater reduction in NMVOC emissions under *Scenario EV2* would play a more significant role in lowering SOA levels than the increased effects of oxidants. Furthermore, in August, the SOA reduction would be more significant than nitrate reduction and become a major contributor of total $PM_{2.5}$ reduction under *Scenario EV2*. The concentration changes of EC aerosol are estimated to be minor in both January and August because high-efficiency particle filters and collectors will be largely used to reduce EC emissions for both vehicles and power plants. Since electrification would increase SO_2 emissions, the simulations indicate that increased sulfate concentrations are an insignificant matter compared to the benefits of other aerosol components. These findings are important when evaluating the health and climate impacts of EV penetration, specifically concerning atmospheric aerosols, as health impacts and radiative forcing also differ greatly among various aerosol components.

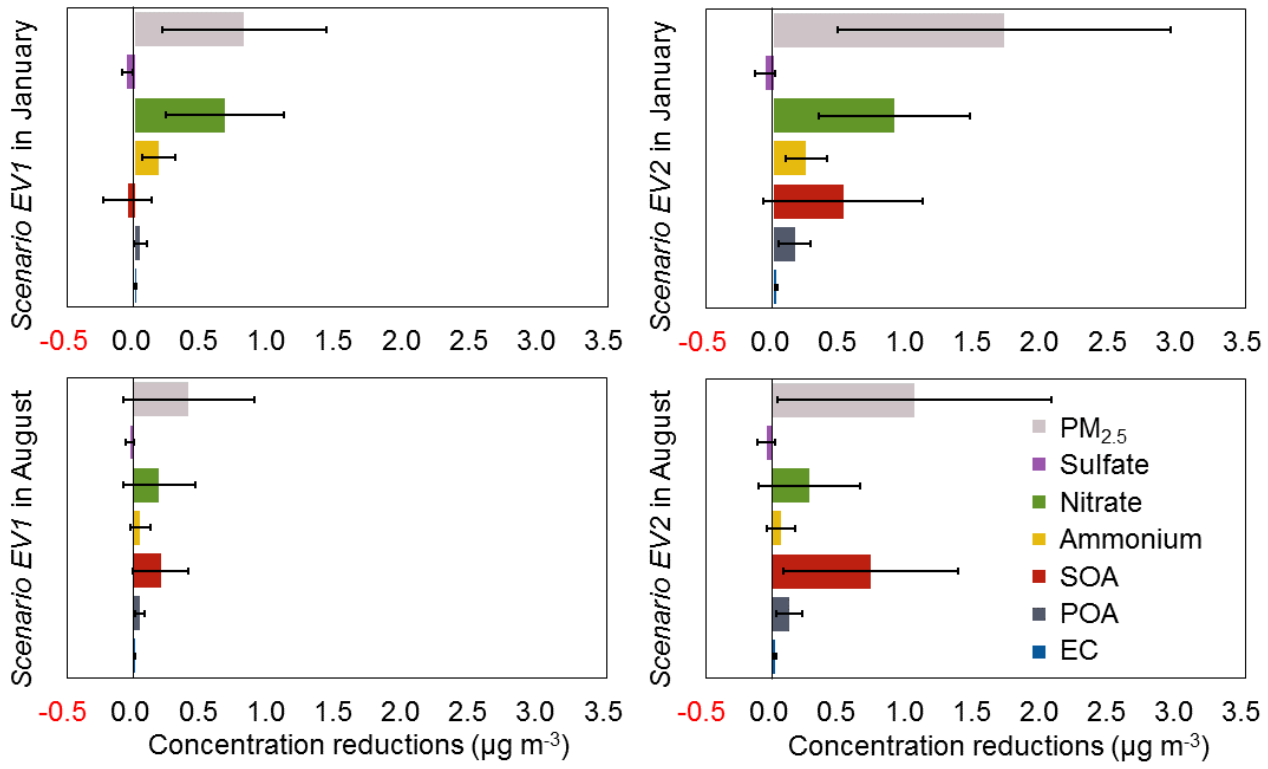

Figure 5-8 Monthly-average concentration changes of $PM_{2.5}$ and major aerosol components in the urban areas of the YRD region under *Scenarios EV1* (left) and *EV2* (right) relative to *the Scenario w/o EVs*, during January (top) and August (bottom) 2030

3. NO_2 concentration changes of EV scenarios

The simulations suggest that the mean NO_2 concentrations (23 μg m^{-3}) during January and August are able to meet the annual limits required by the NAAQS (i.e. 40 μg m^{-3}) in the YRD region in 2030. Compared to *the Scenario w/o EVs*, *Scenario EV1* can reduce NO_2 concentrations by 2.6±1.5 μg m^{-3} in January and 1.9±1.3 μg m^{-3} in August, presenting an overall average reduction of approximately 10% in the urban areas of the core cities in the YRD region. Furthermore, *Scenario EV2* has a slightly greater reducing effect on NO_2 concentrations (with a total reduction of approximately 13%) than the *Scenario w/o EVs*. Thus, combined with previous conclusions, the most significant marginal effect of *Scenario EV2* compared to *Scenario EV1* is the mitigation of SOA concentrations rather than nitrate aerosol or NO_2 concentrations.

Nevertheless, the simulation results under *the Scenario w/o EVs* show that NO_2 exceedance is highly likely to occur in certain hotspots in traffic-populated metropolitan areas, such as the urban areas of Shanghai,

Nanjing and Hangzhou (see **Figure 5-7**), and has been seen in many traffic-populated cities around the world. In the YRD region, using Shanghai as an example, the annual average NO_2 concentration was 46 μg m^{-3} during 2015, exceeding the limit of NAAQS and posing a lower reduction than other pollutants (e.g. SO_2, PM_{10}). This clearly indicated that mitigating NO_2 concentrations is also a great challenge. **Figure 5-10** illustrates that a greater reduction of NO_2 concentrations from EV penetration will occur in traffic-populated urban areas (e.g. Shanghai, Hangzhou, Suzhou, and Wuxi), which suggests that vehicle fleet electrification would result in adequate air quality benefits where the NO_2 exceedance risk is high. For example, the largest reductions in NO_2 concentrations under *Scenario EV1* would be up to 4.8 μg m^{-3} in January and 4.2 μg m^{-3} in August, which are simulated to both occur in the urban area of Shanghai, where the baseline NO_2 concentrations under the *Scenario w/o EVs* are estimated to be 45±18 μg m^{-3} in January and 27±13 μg m^{-3} in August. The NO_2 concentration reductions are shown to be 10% in January and 16% in August. The simulated monthly average NO_2 concentration of the urban area of Shanghai during January (45 μg m^{-3}) exceeds the annual NAAQS limit (40 μg m^{-3}), and *Scenario EV1* is critical to greatly reducing the exceedance risk. Thus, vehicle fleet electrification can effectively help in mitigating NO_2 in traffic-populated cities.

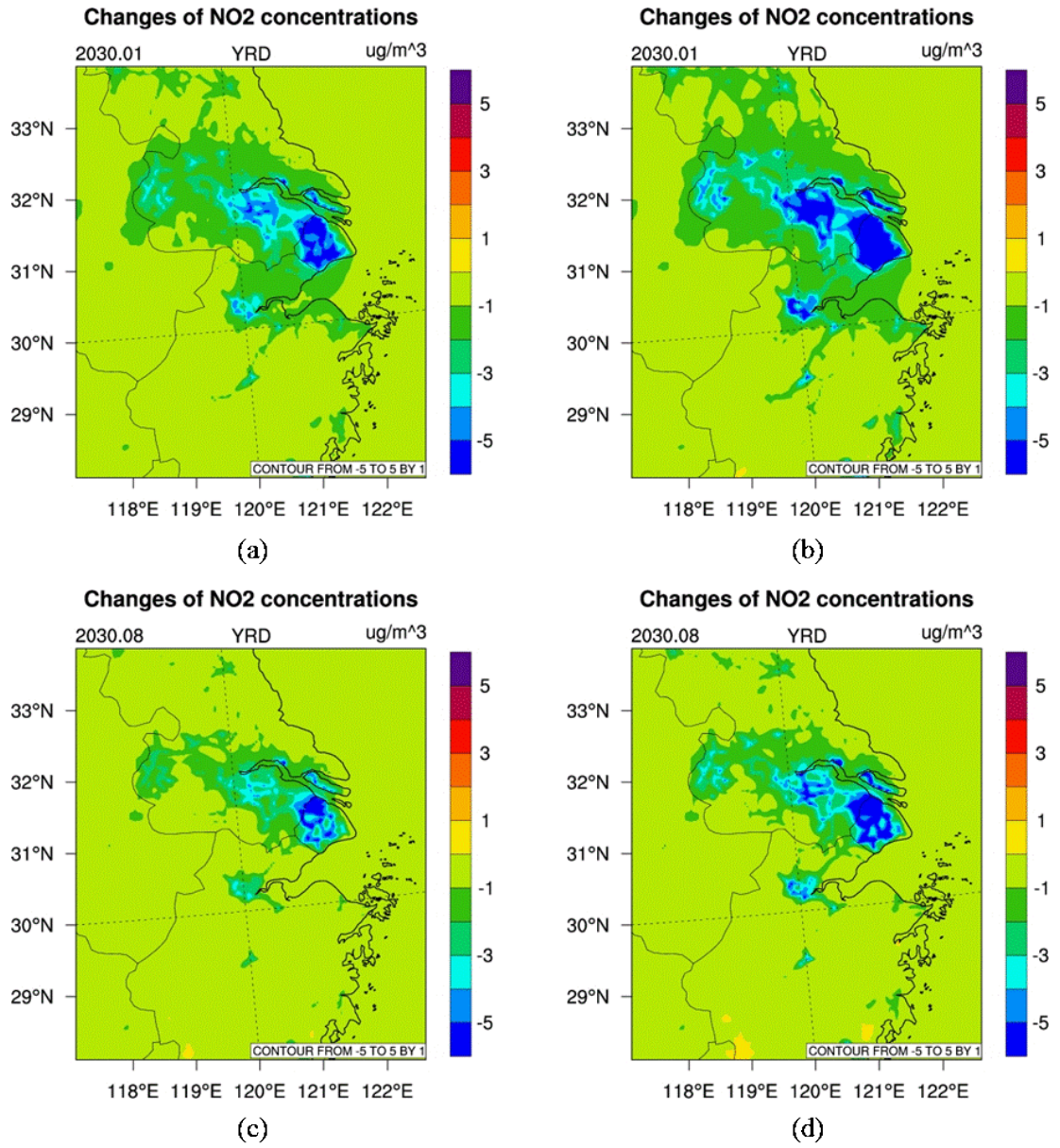

Figure 5-9 Changes of monthly mean NO_2 concentrations from EV scenarios relative to *Scenario w/o EVs*. (a) *Scenario EV1* in January; (b) *Scenario EV2* in January; (c) *Scenario EV1* in August; (d) *Scenario EV2* in August

4. SO_2 concentration changes in EV scenarios

Figure 5-11 shows the spatial distributions of monthly average SO_2 concentration changes between EV scenarios and the *Scenario w/o EVs* in January and August 2030. Different from $PM_{2.5}$ and NO_X, simulated SO_2 concentrations in EV scenarios are slightly higher than the *Scenario w/o EVs* in the YRD region. This is due to the increase of SO_2 emissions from power plants resulting from marginal

generation of power for the charging of BEVs. The increases are almost negligible under *Scenario EV1*. Under *Scenario EV2*, the increases are more significant (> 0.6 μg m^{-3}) in the areas in which thermal power plants are abundant (to the west of Shanghai). However, as noted, SO_2 concentrations in the YRD region are estimated to be much lower than standard limits in the *Scenario w/o EVs*. Therefore, the adversely increased SO_2 concentrations from fleet electrification are insignificant and acceptable for the YRD region in MY 2030.

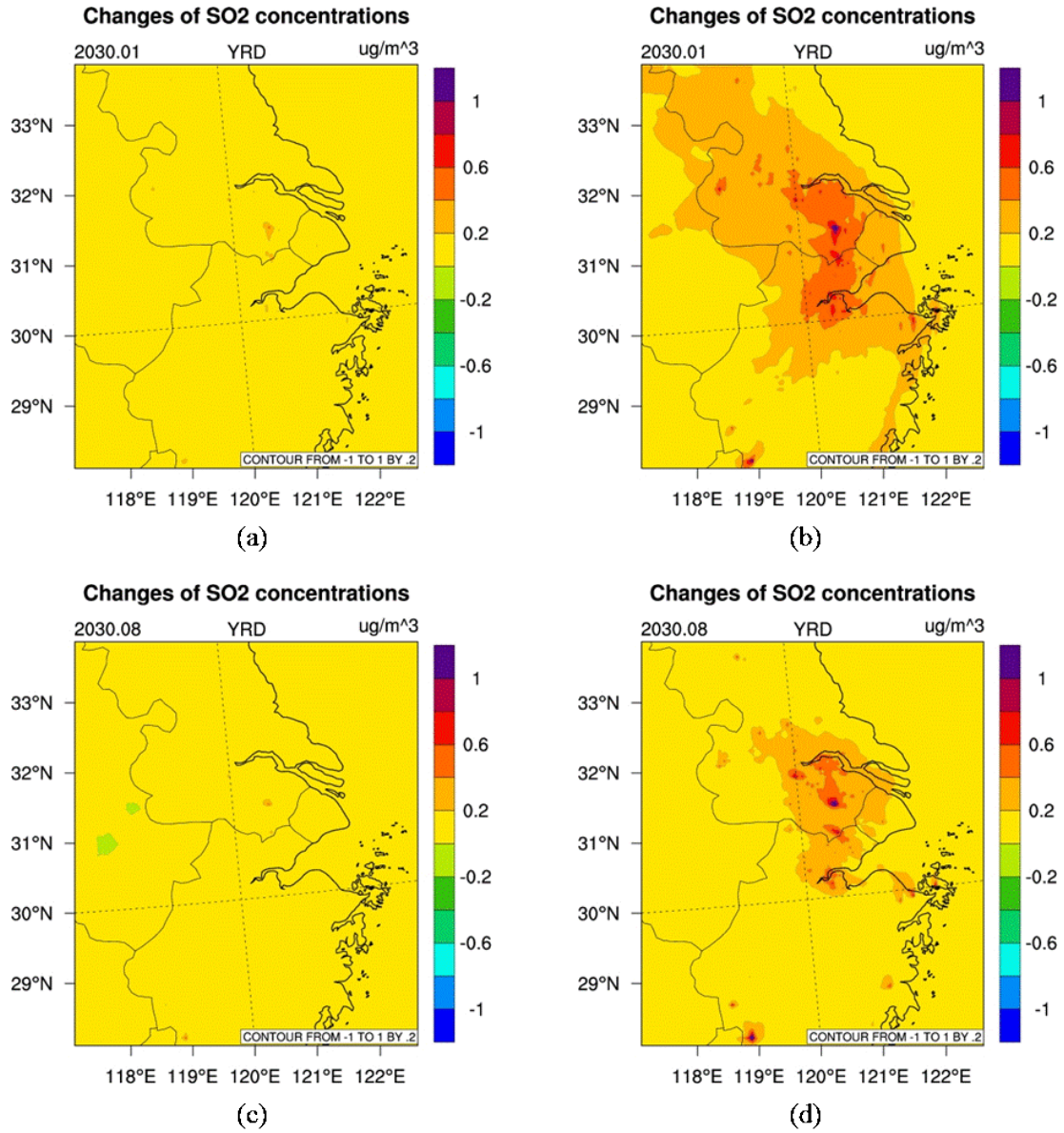

Figure 5-10 Changes of monthly mean SO_2 concentrations from EV scenarios relative to the *Scenario w/o EVs*. (a) *Scenario EV1* in January; (b) *Scenario EV2* in January; (c) *Scenario EV1* in August; (d) *Scenario EV2* in August

Part II: Climate Impact Assessment of Electro-Mobility in 2050

As illustrated in the report on the previous phase project, promoting EVs could significantly reduce fossil energy use, CO_2 and air pollutant emissions at the operation stage relative to conventional ICEVs. In the meantime, however, it could result in marginal emissions in the upstream Well-To-Tank (WTT) stages (e.g. electricity generation), especially for air pollutants such as NO_X and $PM_{2.5}$ that mainly come from power plants. Life cycle assessment tools have been employed to analyse these types of impacts and evaluate the real resources and climate benefits from the transfer of gasoline to electricity, from both a single vehicle and vehicle fleet perspective.

Currently, the forecasts of EV penetration and their climate impacts mainly focus on the near term future, such as the years 2020 to 2030. It is expected that EVs will experience early stages of intense market growth, which means that, in the next decades after 2030, large-scale electrification will happen and deeply affect energy structure and the environment. Therefore, the life cycle assessment of EV penetration with a long-term timeframe to 2050 is necessary to guide the next stage development roadmap and policy making.

In the second part of this report, the climate impacts of electric vehicle promotion up to 2050 have been evaluated by a comprehensive China-based life cycle assessment model. Two scenarios, namely *Baseline* and *Low Carbon*, are designed to describe different pathways of EV under different constraints in China. The *Baseline* scenario represents technology and cost maturity. The *Low Carbon* scenario takes a more stringent CO_2 emission control target into consideration.

Part II consists of three chapters: Chapter 6 presents the methodologies and key database, such as the electricity generation sector, on-road fuel economy and emission factor sector, and the development of a vehicle fleet and electrification roadmap; Chapter 7 presents the life cycle (WTW) fossil energy use, CO_2 and air pollutants emissions of ICEVs, PHEVs and BEVs under different implementation scenarios; Chapter 8 further presents the fleet-based total energy and environmental impacts on the road to 2050 and evaluates the benefits of the large scale promotion of EVs.

Chapter 6

6.1 Research framework

The temporal model to assess the climate impacts of EVs in 2050 includes three levels: on-road fuel economy and emissions, life cycle assessments, and vehicle stock projections. The total fossil fuel use, CO_2, and air pollutant emissions from vehicle fleets were split into these levels and an analysis was made of the changing trends of key parameters in these levels. Finally, the total changing trends are highly related to the changes of each level. From a micro point of view, the detailed fuel economy and emissions data for each vehicle technology should be adequately collected. The revised GREET-China model is used to conduct the life cycle assessment, which considers fossil fuel use and emissions from the upstream fuel producing processes. Key parameters, such as coal-fired power share and efficiency, significantly affect the life cycle energy saving and emission reduction benefits. In addition, a vehicle fleet projecting model was developed to calculate the new sales and stock situations of LDPVs. Based on this, the market share of EVs is projected in order to assess the vehicle fleet electrification impacts on energy saving and CO_2 emission control targets. **Figure 6-1** shows the framework to simulate the annual EV projection.

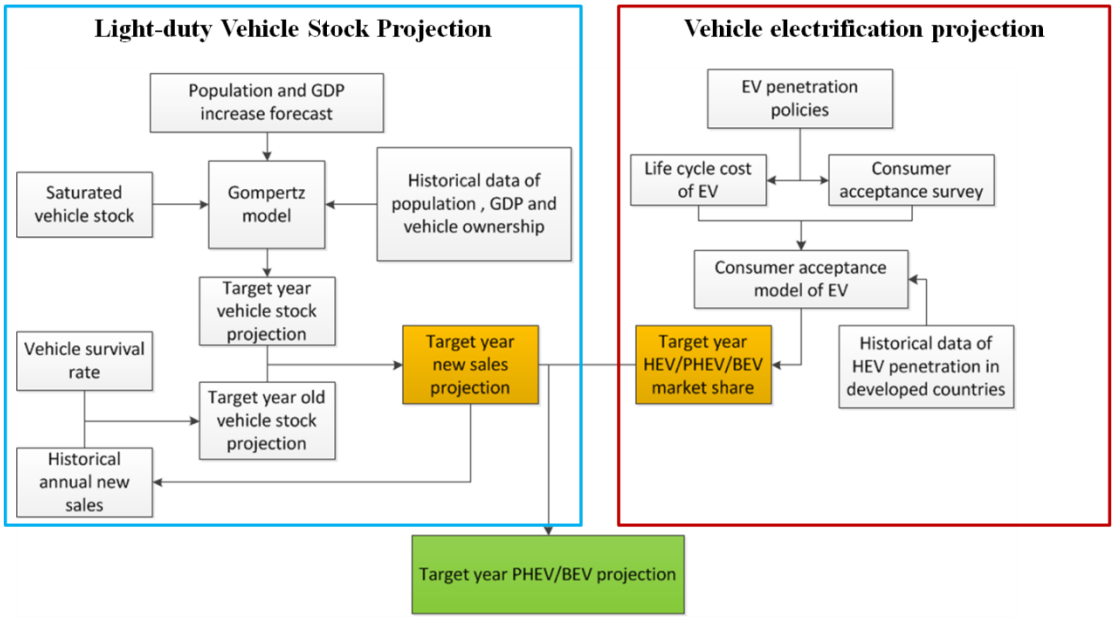

Figure 6-1 Research framework of electric vehicle fleet projection

Two EV scenarios up to 2050 are designed to explore climate impacts of different EV penetration strategies, as seen in **Figure 6-2**. The *Baseline* scenario follows the historical trends and represents conservative technical improvement and relatively poor vehicle emission control strategies. The *Low Carbon* scenario links to the two degree control (2DC) constraint, in which the key parameters could achieve a sharp CO_2 reduction. The following research mainly focuses on the comparison between the two scenarios. The parameters listed in **Figure 6-2** will be introduced in detail below. MY 2030 is used as the reference to evaluate the improvement up to 2050. For example, the coal-fired power share would fall to 50-60% and the coal-fired power efficiency would rise to 42-44%.

	Baseline	**Low carbon（2DC）**
Coal power ratio	44%	17%
Coal power efficiency	44%	50%
Fuel consumption rate	Advanced ICE techs.	High hybrid scenario
Saturated LDV population	350/1000 people	250/1000 people
VKT in 2050	10000 km/year	8000 km/year
Electrification	Moderate	2 degree constraint

Figure 6-2 List of key parameters under the two scenarios (2050)

6.2 Electricity generation database

Generation mix, power efficiency and emission factors are key parameters for analysing life cycle energy consumption, CO_2 and air pollutants emissions from electric vehicles.

Based on the <*China Electric Power Yearbook*> [12] and the projections of electricity generation mixes by other researchers, this section has developed the projections of generation mix and coal-fired efficiency on a national level.

6.2.1 Average generation mix

With rapid economic growth and massive urbanisation in China, electricity demand has been increasing in recent years. According to statistics, nationwide power generation has increased from 4207 TWh in 2010 to 5605 TWh in 2015, and the average annual growth rate is approximately 7% [13]. Not until the

late 20th century did the whole country realise the necessity of developing clean and renewable energy that could result in a clean and low-carbon energy structure to address the challenges of climate change and environmental pollution. China, a country whose economy is flourishing, has become the world's largest energy consumer, accounting for a significant amount of current global emissions. In order to address issues related to energy security and the growth of greenhouse gas and air pollutant emissions in China, it is vital and obligatory to further cut down on the use of fossil fuels and to develop clean energy such as wind energy, solar energy, hydropower, nuclear energy, etc. as Premier Li has promised in his report on government work in 2015 [14]. China's electrical power generation in 2014 is shown in **Figure 6-3**. However, in spite of developments in clean energy, fossil fuels are still dominant in the nationwide electricity generation mix.

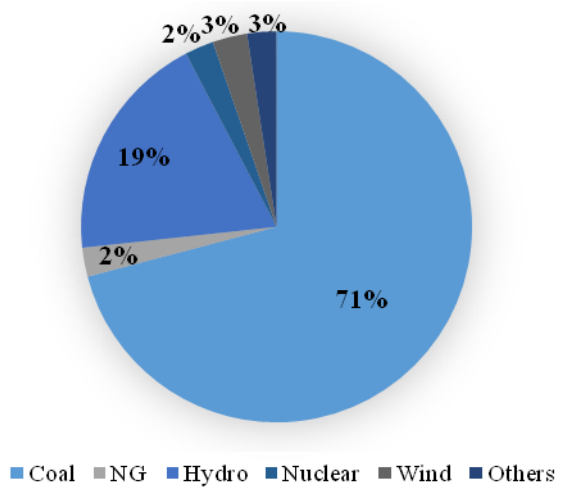

Figure 6-3 Electrical power generation in China, 2014

As reflected in China's policymaking, China will further reduce the use of fossil fuels and develop clean and renewable energy in the following decades. The official issue of <*National Nuclear Long-and-medium Term Development Planning (2005-2020)*> [15] marked the beginning of the rapid development of nuclear power in China. According to this plan, the installed capacity of nuclear generators will approach 0.7, 1.6, 4 TW by 2020, 2030 and 2050, respectively. <*Wind Power Development Roadmap of China to 2050*> [16] has proposed that the goal for the installed capacity of wind power should be to reach 1.0 TW by 2050, and should meet the target of 17% of the generation demand. The National Development and Reform Commission's Energy Research Institute considered high renewable energy penetration in 2050. The

International Energy Agency forecasted the long-term (up to 2050) energy mix for power generation in China under a 2DC scenario (2DS) in <*Energy Technology Perspective 2015*> [17]. The 2DS, which sets the target for the cutting of energy- and process-related CO_2 emissions by almost 60% by 2050 (compared to 2012), lays out the pathway to deploy an energy system and emissions trajectory that is consistent with what recent climate science research indicates would give at least a 50% chance of limiting the average global temperature increase to 2℃. Moreover, there are many papers that predict the electricity generation mix in 2050, taking into account several critical factors, such as government policies, power demand, total cost, CO_2 and other emissions targets. As shown in **Table 6-1**, there are significant distinctions among various predictions. According to their attitudes towards renewable and clean energy penetration, researchers can be divided into two categories - aggressive and conservative. Conservative researchers maintain the opinion that renewable and clean energy will occupy an equally important position with fossil fuels in 2050, while aggressive researchers believe that, by 2050, clean and renewable energies will account for 70%~90% of China's total electricity generation.

Table 6-1 Prediction of electricity generation mix of China in 2050

Literature	Fossil fuels				Non-fossil fuels						
	total	Coal	NG	Oil	total	Nuclear	renewable fuels				Others
							Hydro	Wind	Solar	Biomass	
Jiang et al.,2009 [18]	49%	/	/	/	51%	27%	15%	6%	1%	2%	0%
	42%	/	/	/	58%	29%	16%	9%	1%	2%	0%
Chen and Chen,2011 [19]	30%	/	/	/	70%	20%	15%	11%	10%	/	/
	30%	/	/	/	70%	28%	15%	11%	10%	/	/
Rout et al.,2011 [20]	69%	56%	1%	12%	31%	14%	14%	/	/	1%	2%
Wu et al., 2011 [21]	44%	39%	5%	0%	56%	33%	12%	7%	4%	0%	0%
Zhang et al.,2012 [22]	25%	25%	0%	0%	75%	44%	10%	9%	10%	2%	0%
Wu,2013 [23]	50%	43%	7%	/	51%	18%	13%	12%	7%	/	1%
Luo et al., 2014 [24]	45%	37%	8%	0%	56%	30%	11%	9%	6%	0%	0%
Cheng et al., 2015 [25]	23%	23%	0%	0%	77%	43%	13%	4%	10%	7%	0%
ERI/NDRC,2015 [26]	10%	7%	3%	0%	89%	14%	4%	35%	28%		8%
IEA, 2015 [17]	19%	11%	7%	1%	81%	19%	16%	21%	18%	6%	1%
Dai et al. 2016 [27]	/	45%	6%	/	/	9%	13%	13%	28%	7%	0%

In light of literature reviews, two scenarios have been developed. The conservative scenario assumes that renewable energy will develop at a moderate pace. The aggressive scenario envisions a high penetration

of renewable energy by 2050. As **Figure 6-4(a)** demonstrates, the proportion of coal-fired power generation shows a decrease from 71% in 2014 to 44% in 2050 with an average annual rate of decrease of approximately 0.9%, while the share of renewable and clean energy generation will increase from 27% in 2014 to 51% in 2050. **Figure 6-4(b)** shows a sharper annual growth trend of about 1.8%, making the share of non-fossil energy in the generation mix over 70% in 2050.

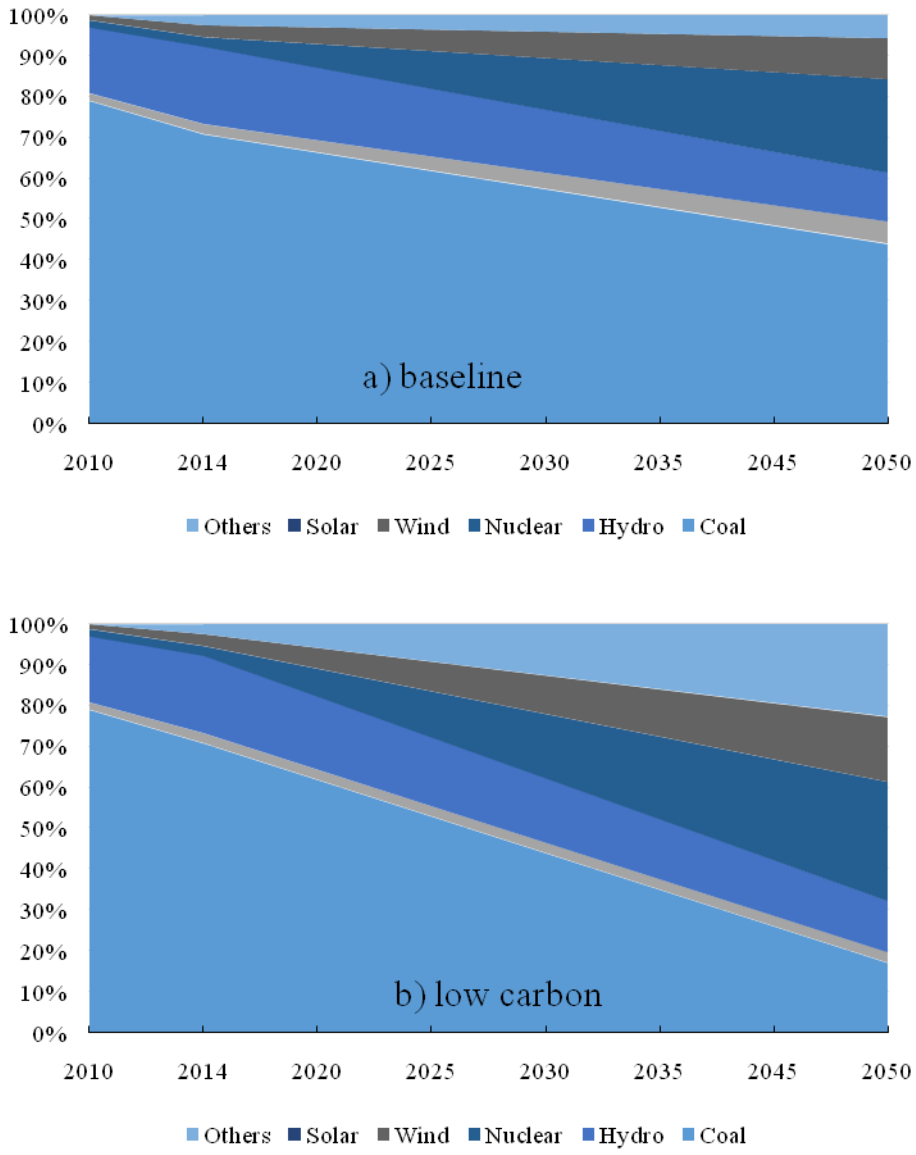

Figure 6-4 Prediction of generation mix from 2010 to 2050 under two scenarios

6.2.2 Electricity generation efficiency

Electricity generation efficiency can significantly affect the energy consumption and CO_2 emissions of

thermal power plants. This section concentrates on the generation efficiency of coal-fired power plants in China, which can be calculated using equation 6-1:

$$\omega = \frac{P \times m}{T \times n} \times 100\% \quad (6\text{-}1)$$

ω = the energy efficiency of coal in units of %;

P = the coal-fired electricity generation in units of kWh;

M = the conversion factor from electricity to heat in J kWh^{-1};

T = the total consumption of coal used for electricity generating in unit of kg coal-equivalent;

n = the average low calorific value of standard coal in unit of J kg^{-1}.

There is much room for the improvement of electricity generation efficiency in China. Both the <*Middle and Long Term Program of Energy Saving*> [28] (NDRC, 2004) and the <*National Policy for Energy Saving Technology*> (NDRC, 2007) explicitly propose the direction for development and technology selection of future electricity generation technology in China: i.e. gradually shut down the electricity generation units with medium and small generation capacity, vigorously develop supercritical (SC) and ultra-supercritical (USC) units with a capacity of more than 300 megawatts (MW), and promote high-efficiency, clean coal-fired units and large combined cycle units such as the Integrated Gasification Combined Cycle (IGCC). IEA reported that the generating efficiency of SC/USC could reach 42%. At the same time, the projections of some domestic Chinese researchers indicate that other high-efficiency technologies could achieve 54% (IGCC) - 63% (IGCC integrated with fuel cells). With the continuous development of the power industry and generating technology in China, SC and USC units will dominate the electricity generating technology market. Referring to the IEA report, that study forecasts that electricity generation from SC/USC would account for 45% of total coal power in 2050, while the IGCC and IGCC integrated with fuel cells account for 35% and 20% respectively.

Thus, the average generation efficiency of China's coal-fired power plants in 2050 is 50% based on the projections of generation share and efficiency of each generating technology, which is a remarkable improvement when compared to the current 34% average efficiency. This study forecasted the generating efficiency for the years between 2010 and 2050 using the linear interpolation method. For

regional generating efficiency, the study assumed they were equal to the national average level without considering regional discrepancies.

6.3 Vehicle operation database

In this section, the key parameters for LDPVs at the vehicle operation stage (i.e. TTW stage), including fuel economy and vehicle emissions factors are presented.

6.3.1 Fuel economy of LDPVs

Wang et al. (2010) [29] demonstrated that the average fuel economy of light duty passenger cars in China is 8.1 L/100km^{-1} in 2006, which was lower by 12% than that of 2002 [29]. In the assessment report for the implementation of the <*National Fuel Consumption Standard for Light Duty Passenger Cars*> [30], the average fuel economy for 2002 and 2006 was 9.1 L/100km^{-1} and 8.1 L/100km^{-1}, respectively, which was calculated using the corporate-average fuel consumption (CAFC) from 34 manufacturers and their corresponding sales numbers. Some other studies (Wagner et al., 2009; Huo et al., 2011) pointed out that the fuel economy of LDPVs improved to 7.8-7.9 L/100km^{-1} in 2009 [31-32]. The research report on CAFC [33] development by Chinese passenger car manufacturers showed the fuel economy was 7.8 L/100km^{-1} in 2009, which was almost identical to the other studies.

In December 2012, the Chinese Phase Ⅲ fuel consumption standard for new passenger vehicles was implemented and is more stringent than the former standards. The target limit for the average fuel economy of conventional LDPVs is 6.9 L/100km^{-1} in < *The industrial development plan for energy saving and new energy vehicles in China (2012-2020)*> [4], which was issued by the State Council of China. Moreover, the Phase IV standard set a target of 5.0 L/100 km^{-1} in 2020 and 4.0 L/100 km^{-1} in 2025, including the zero fuel use of EVs.

The fuel consumption values mentioned above are all based on laboratory testing under specific driving cycles, which are remarkably lower than real-world driving fuel consumption. Huo et al. [34] illustrated that the fuel economy under real-world conditions is lower by about 15% than that under laboratory testing conditions.

However, there is new evidence to illustrate that the discrepancy of fuel consumption rates for passenger vehicles between laboratory measurements and real-world testing is much greater than ~15%. The Innovation Center for Energy and Transportation (iCET) published a report studying the fuel

consumption divergences of passenger vehicles between type-approval values released by official institutions and real-world values reported by drivers [35]. The results show that the overall average divergence of fuel consumption rates of passenger vehicles in China in the model year 2014 between type-approval and real-world values is about 27%, based on an analysis on over 210,000 samples.

Additionally, the International Council on Clean Transportation (ICCT) has been studying the gap between type-approval and real-world fuel consumption of passenger vehicles in Europe for years. The latest results, released in September 2015, show that the gap between real-world and official CO_2 emissions increased from about 8% in 2001 to 40% in 2014, based on an investigation of almost 600,000 vehicles from six countries in Europe [36]. It reveals a clear trend that the gap between the real-world and type-approval fuel economy of passenger vehicles is growing larger and larger.

Based on global research, in 2050, the fuel economy of traditional ICEVs worldwide would be stabilised. **Table 6-2** shows the possible vehicle fuel saving and emission control technologies. Vehicles equipped by single internal combustion engine (ICEs) could achieve 3.5-5.0 L/100 km^{-1}, cutting 30-50% from that of 2010-2015. Moreover, hybrid power technology could save another 10-15% over ICEs to reach 2.5-3.0 L/100 km^{-1} under type-approval testing. When adding the real-world correction, the fuel economy of ICEVs and HEVs will improve to 4.5-7.0 L/100 km^{-1} and 3.5-4.2 L/100 km^{-1} in 2050. Hybrid technology, as one of the efficient energy-saving technologies, would be widely applied after 2030, so in the chart below the ICEVs and HEVs have been merged together and ICEVs have been used to represent them. PHEVs owning off-board charging functions combines the performance of the new defined ICEVs and BEVs.

Table 6-2 Energy-saving effects and penetration targets of energy-saving technologies of passenger cars

Main technologies		Energy saving effects	Current situation	Targets in 2020
Advanced engine technologies	Turbocharger gasoline engine	1.8% ~ 4.8%	7%	40%
	Gasoline direct injection	10% ~ 20%	7%	40%
	Variable valve timing	2% ~ 3%	25%	100%
	Variable valve lifts	1% ~ 3%	25%	100%
	Lower engine friction loss	2% ~ 5%	Quite low	50%
	Idle stops	5% ~ 8%	Quite low	100%
	Cylinder fuel-cut technologies	3.9% ~ 5.5%	0%	2%
Advanced transmission technologies	Lifting component performances	3% ~ 5%	Quite low	50%
	Multiple gears	1.4% ~ 3.4%	6MT: 1% 6/7/8AT: 12%	100%
	DCT	2.7% ~ 7.5%	2%	25%
Other advanced technologies	Continuously variable transmissions	0.7% ~ 2.0%	4%	5%
	Lightweight	2% ~ 8%	Quite low	Average weight lighted: 15%
	Hybridisation (excluding idle stops)	10% ~ 40%	Quite low	20%
	Electric power steering	1% ~ 2%	Quite low	100%
	Monitoring systems to lower air resistance	2% ~ 3%	Quite low	75%
	Low rolling-resistance tires	1% ~ 2%	Quite low	100%
Small displacement passenger vehicles		20%	65%	1.6L and even lower: 80%
Diesel vehicles		20%	0.80%	20%
Green driving/green maintenance		15%	5%	75%
Smart transport		15%		

BEV fuel economy is expressed by the relative improvement rate compared to conventional vehicles

based on the fuel equivalent low heat value transformation. As shown in **Figure 6-5**, the conservative scenario determined the improvement rate is 225% based on comparisons between BEVs and the corresponding ICEVs of three brands. Taking the uncertainty of future policies into account, the improvement rate has been fixed at 250%.

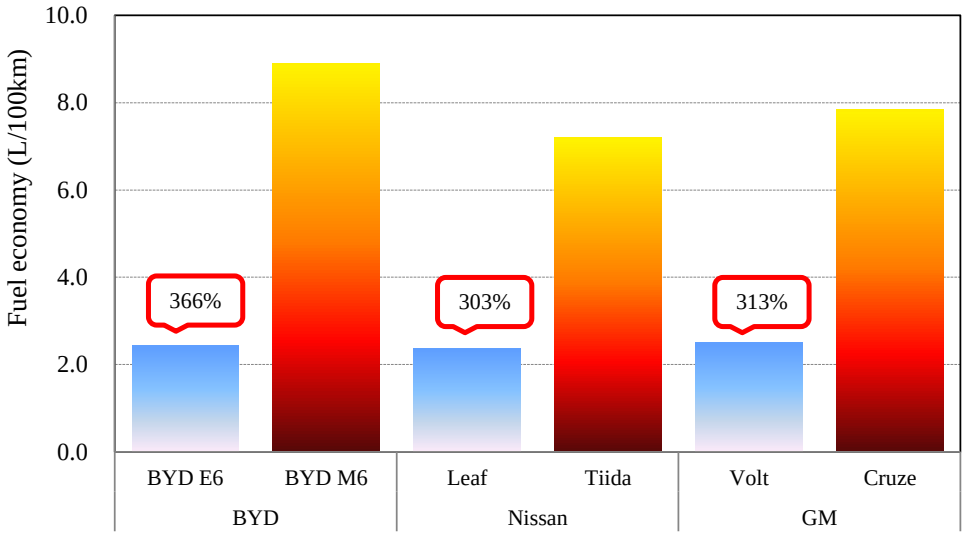

Figure 6-5 Comparisons of fuel economy between EVs and the corresponding ICEVs (2010)

The fuel economy of PHEVs is strongly related to the ratio of its all-electric range (AER) and total travel range, called the utility factor. The higher the AER, the longer electricity-driving distance and less consumption of oil fuels. In addition, daily travel mileage also significantly affects the fuel economy of PHEVs. Shorter daily travel means more distances can be covered by electricity-driving patterns, leading to better combined fuel economy. After investigating the PHEV50 (AER=50 km) driving patterns in several cities in China, the utility factor (VKT split under CD mode, UF) is 68% and the annual VKT averages out at 44.5 km. When the state of charge (SOC) is high, the PHEVs will be driven in charge-depleting (CD) mode. In this case, the electricity from batteries is the primary energy for propulsion and oil fuel is used as a complement for fast accelerations. If the SOC is relatively low, PHEVs will be driven on charge-sustaining (CS) mode. In this case, the internal combustion engine will primarily be used to drive the vehicles, like HEVs.

Two scenarios were projected in **Figure 6-6**. In 2050, ICEVs could reach 4.1 and 3.4 L/100 km^{-1} in *Baseline* and *Low Carbon* scenarios including the real world correction, The *Low Carbon* scenario requires

86% hybridisation and the *Baseline* scenario only requires 36%. In this case, BEV's average fuel economy falls from 15 kWh/100 km^{-1} (2030) to 11 kWh/100 km^{-1}.

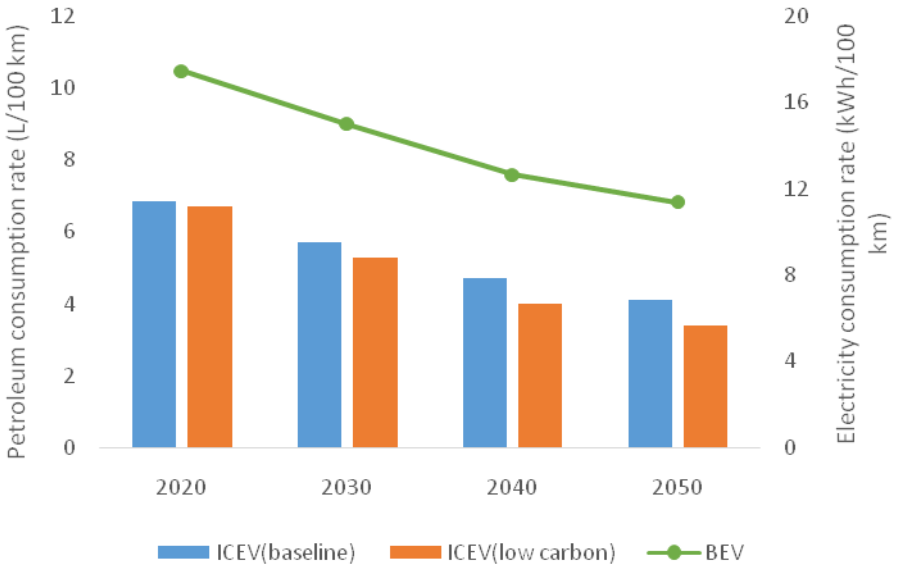

Figure 6-6 Projection of fuel economy of light duty passenger vehicles in China

6.3.2 Air pollutant emission of LDPVs

The emission level of conventional vehicles in this study is presented by tailpipe emission factors in unit of gram per kilometer, while the emission levels of new energy vehicles are presented by the ratio to that of conventional vehicles.

The estimation of the emission factors of conventional light duty gasoline vehicles was based on long-term and large-scale collections of laboratory and real-world testing data, including certified testing data on about 1,500 new vehicles, dynamometer testing data on 200 in-use vehicles, emissions testing data under different driving conditions on 400 vehicle-times, and real-world emission testing data on 50 vehicle-times.

At first, the zero-mile emission factors obtained from the certified data of new vehicles and testing data on in-use vehicles were combined to obtain the impacts of vehicle miles traveled on vehicle emissions. Then we analysed and estimated the modification factor for vehicle degradation to obtain the basic emission factors. Based on the analysis of testing emissions data under different driving speeds, a speed-correcting curve for emission factors could be established. In addition, the emissions of light duty

vehicles can be affected by other factors such as fuel quality, environmental temperature, proportion of high emission vehicles, and use pattern of air conditioning. These influential factors correspond to different correcting modules to the basic emission factors, among which some correcting factors referred to the results of previous domestic and foreign research on urban vehicle emission factor models, such as MOBILE, COPERT and MOVES.

The equations for the calculation of light duty vehicle emission factors are:

$$EF_{total} = EF_{run} + EF_{cold\ start} + EF_{eva} \quad (6\text{-}2)$$

$$EF_{run} = (ZML_{NEDC} + DR \cdot M)\ C_S \cdot C_A \quad (6\text{-}3)$$

Equation 6-2 refers to the integrated emission factor, which is the sum of operation emissions, cold start emissions and volatile emissions.

Equation 6-3 refers to the operation emission factor, where ZML_{NEDC} is the zero-mile emission level, DR is the degradation rate of vehicle emissions, M is the cumulative travel distance, C_S is the correcting factor of average speed, and C_A is the integrated correcting factor including use of air conditioning, fuel quality, environment temperature, and the proportion of high emission vehicles.

China launched the China V emission standard and implements China VI by 2020 and China VI b (equivalent to the California Tier III) by 2023. After that, the emission standard tends to stabilise. **Figure 6-7** shows the integrated emission factors of LDPVs on the road to 2050. In the target year 2050, the emission factors of Volatile Organic Compounds (VOC), CO, NO_x and $PM_{2.5}$ could fall to 0.54, 0.28, 0.009 and 0.002 g km^{-1} respectively. For convenient comparison, the average speed of all LDPVs has been set at 25-26 km/h^{-1}, with vehicle emission control levels consistent with their fuel quality standards.

The tests conducted in Macau showed a remarkable reduction in HEV emissions compared to conventional gasoline cars under the China IV standard. The reduction rates for VOC, CO, NO_X, and $PM_{2.5}$ are all between 60% and 80% in the aggressive scenario for the emission reduction of HEVs. For PHEVs, the CD mode is similar to that of BEVs, which have no emissions in the operation stage; while the emission reduction rate of the CS mode is equal to that of HEVs. For BEVs, there are no emissions

during the vehicle driving stage.

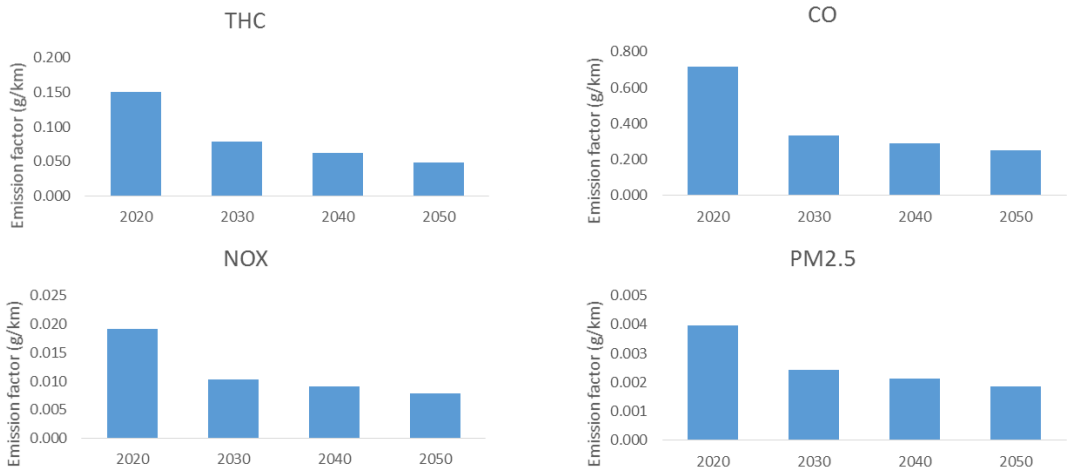

Figure 6-7 Emission factors for driving stages of light duty gasoline vehicles

6.4 Projection of LDPV fleet growth to 2050

Previous studies have performed forecast studies on China's vehicle stock using different methods. Among these studies, the approach using the Gompertz curve is considered the preferred solution to project the mid- and long-term trends in China's vehicle stock. Huo and Wang reviewed the historical Chinese vehicle stock data with three functions: the Gompertz function, the logistic function and the Richards function [37]. The Gompertz function fit the original data better than the other two. The Gompertz curve is an S-shaped curve, representing three periods of vehicle growth. In the beginning, when the income levels are relatively low, the vehicle stock grows slowly. In the second period (also called the boom period), the vehicle stock grows swiftly along with the rapid development of the economy. In the third period, the vehicle growth slows and approaches a saturation level. The Gompertz function (see Equation 6-4 below) was applied to relate per-capita LDPV ownership to per-capita GDP.

$$VS_i = VS_S \times e^{\alpha e^{\beta EI_i}} \quad (6\text{-}4)$$

VS_i represents the per-capita LDPVs in the target year i; VS_s represents the saturation level of LDPV ownership; EI_i represents an economic indicator, which is the GDP per capita in this study; α and β are two parameters, which were obtained during the fitting process of this S-shaped curve with

the historical data.

Different research indicated that the population will reach the top by 2030, as seen in **Table 6-3**. In this research the population will go down after the peak year, 2030, and the top population will not exceed 1.5 billion.

GDP is another key parameter that can be applied in the Gompertz model, as seen in **Table 6-4**. China will become a middle income country by 2050, and the growth rate of GDP will slow down to 1.7-3.2%.

Table 6-3 Different forecasts of population growth in China

Population (Billion)	NDRC	UN	This study
2010	1.34		1.34
2015		1.38	1.38
2020	1.44		1.44
2025			1.46
2030	1.47	1.42	1.47
2035			1.48
2040	1.47		1.47
2045			1.44
2050	1.46	1.35	1.42

Table 6-4 Different forecasts of GDP growth in China

GDP growth (%)	DRC	WB	This study
2011-2015	7.9	8.6	7.3-8.6
2016-2020	7.0	7.0	6.4-6.9
2021-2025	6.6	5.9	5.7-6.2
2026-2030	5.9	5.0	5.2-5.6
2030-2040			3.4-5.1
2040-2050			1.7-3.2
2050 Middle income countries	15,000 USD per capita	4,13-12,75 USD per capita	23,500 USD per capita (ER=6.35)

Different saturation levels for the two scenarios were developed. For the *Baseline* scenario, an assumption that 350 LDPVs per 1,000 people (as the high provincial saturation level) was made, which is also similar to that for metropolitan areas in Britain and Japan. However, a further assumption that a

low level of 250 to take into account factors such as strict purchase restrictions was made.

Figure 6-8 shows the vehicle growth of each province under the same saturated number of 350. The Gompertz model forecast varies by province due to the economy and population levels: Zhejiang will reach saturation in 2030 but Xinjiang hardly gets to saturation before 2050. Furthermore, due to the current "license control" policy, the estimated trend for Beijing is different from other regions. The quota, in place since 2011 is 20,000 for each month.

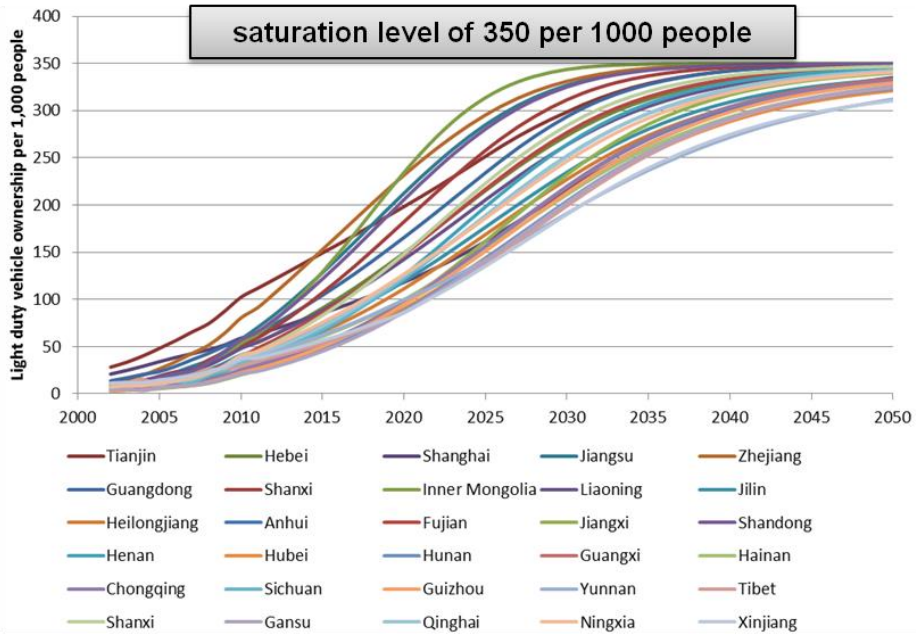

Figure 6-8 Ownership of LDPVs in different provinces

The average vehicle age for LDPVs in the registered population and real traffic flows was 5.4 and 4.6 years, respectively.

Summing up all provincial results, the national vehicle fleet growth trends are shown in **Figure 6-9**. Rapid increases occur in 2020-2030 and the total ownership ranges from 360 to 490 million by 2050. This indicates that the vehicle boom period (i.e. high growth rate) in the S-shaped curve will not end sooner than 2020 for all of the regions in China. Strict purchase control to fulfill CO_2 emission control targets could reduce up to 130 million of the top fleet amount.

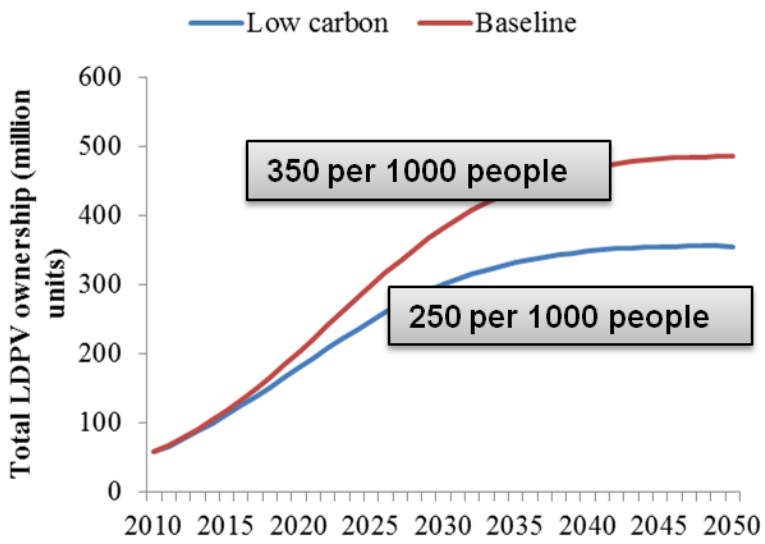

Figure 6-9 Ownership trends of LDPVs under different saturation scenarios

6.5 Penetration of EVs into the new LDPV market

6.5.1 Current Status of EV penetration in China

As shown in **Figure 6-10**, most countries are now in an early stage of EV development and many studies envision a rapid growth of EVs in the next decade. Northern European countries are leading in the market share of EVs (e.g. Norway and Sweden). In saturated markets with large populations (e.g. the U.S. and Japan), EVs account for ~1% at the early stage. China has a large growth rate of EVs and jumped to the world's top EV market in 2015. EV development has been accelerated since 2013. The total sales worldwide in 2014 were 0.3 million, which will rise to 6 million in 2020 according to the IEA's forecast (**Figure 6-11**). China's annual sales would increase to 1.5 million and total stock will rise to 5 million in 2020, meeting the official targets set by the central government.

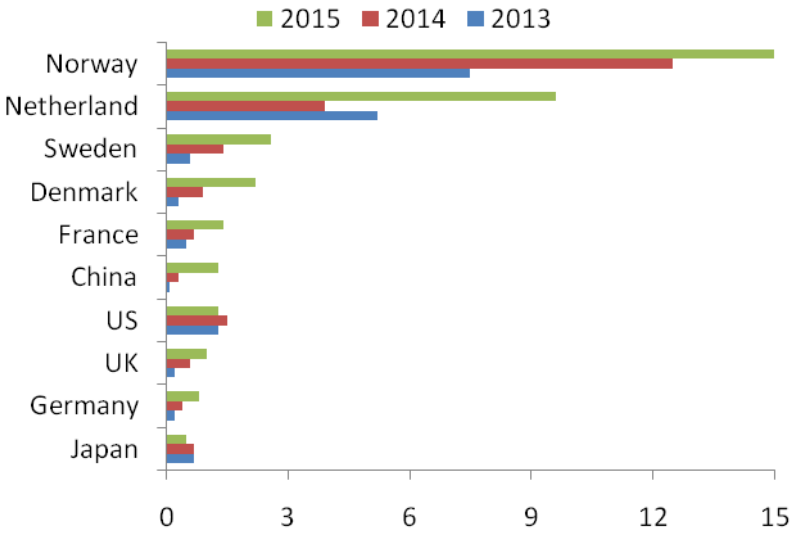

Figure 6-10 Market share of sales of EVs in major countries

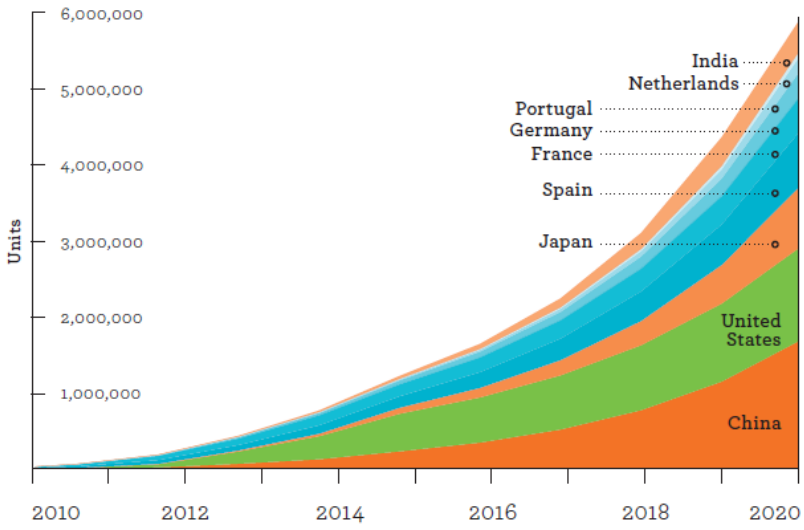

Figure 6-11 Forecast of world EV penetration (IEA, 2013)

The growth of EVs in China has been accelerated since 2014 due to national and local supportive policies. In 2014, China accounted for 12% of the global EV population. In the first half of 2015, EV sales reached 72,711 units - 3.4 times that of the same period in 2014. China has now become the world's largest EV market. The market share of EV sales rose from 0.3% in 2014 to 1.3% in 2015. LDPVs dominate the market and BEVs are more popular than PHEVs. LDPVs were responsible for 70% of newly sold vehicles. By 2020, the market share of EVs will probably rise to 5-6%, this would be below the target set by the State Council of China.

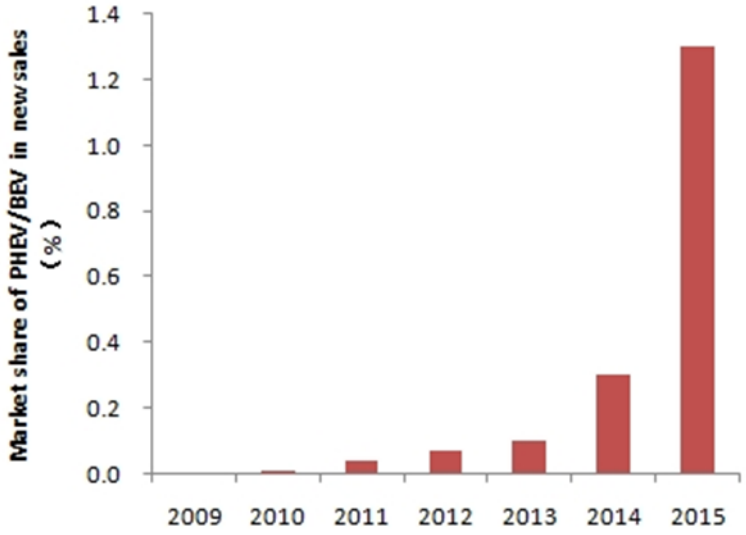

Figure 6-12 Annual sales of EV in China

6.5.2 Penetration of EVs by 2050

HEVs, PHEVs and EVs are widely discussed and are considered promising vehicle technologies to provide near-term and long-term energy savings and carbon and tailpipe emission reduction. Since these three vehicle technologies partly or exclusively rely on electricity (either produced from an internal combustion engine or charged from the grid), the commercialisation of these three technologies has been named a 'process of vehicle electrification'.

HEVs can significantly improve fuel economy because the engine used in the HEV operates close to constant speed and is a highly efficient power source independent of road conditions. Regenerative braking technology results in a higher overall energy efficiency of the system. The battery or capacitor size in the HEV determines the power management strategy. The HEV is already a commercially available technology, best exhibited by the Toyota Prius. Another advantage of the HEV is that no additional charging infrastructure is needed; therefore, the HEV is usually considered more competitive than PHEVs and EVs in the near-term future.

BEVs only use power from batteries to drive the vehicle through an electric motor, demanding a large energy storage capacity. BEVs consume electricity generated by power plants while maintaining high energy conversion efficiency during vehicle operation. PHEVs combine the characteristics of HEVs and BEVs and are capable of using power from electricity when depleting its electric charge, or operating like

an HEV when the state of charge (SOC) is low. Currently, battery technology is the bottleneck for the development of EVs, especially for BEVs. Battery energy density, battery lifetimes, safety and cost are the limiting factors. Another disadvantage is the extensive charging infrastructure network necessary. This is especially true for BEVs since it exclusively relies on charging electricity.

In general, there are two views that estimate the future of these three technologies which bracket many of the growth predictions. One view is represented by the US Energy Information Agency (EIA). In reference to oil price scenarios, EIA's published <*Annual Energy Outlook (2009)*> [38] projected HEVs, PHEVs and BEVs together will account 40% of total new LDPV sales in the U.S. by 2030, and could range from 38-45% depending on the fluctuation of oil prices. However, such a market share is dominated by HEVs. PHEVs were assumed to have a small share of only 2% of total new sales and, for BEVs, the share is negligible. However, a more optimistic opinion for PHEVs is held by others, such as the Electric Power Research Institute (EPRI), Rocky Mountain Institute (RMI), and Ou, et al. They assume that, by 2020, PHEVs could reach 30% of total new LDPV sales in the U.S., and by 2030 such a market share could even climb to 50-70%. Ou expects BEVs to reach 64% in 2050.

The Chinese government is also actively pursuing the process of vehicle electrification. In 2009, the State Council released its <*Automotive Industry Restructuring and Revitalization Plan*> [39]. The plan aggressively concludes that HEVs, PHEVs and EVs together would account for 5% of the total passenger car sales by 2012. Further, as noted earlier, MIIT released a draft of < *The industrial development plan for energy saving and new energy vehicles in China (2012-2020)*> [4] in 2010. It expects the stock for PHEVs and EVs in China to reach 500,000 by 2015, and the total stock for energy-saving and new energy vehicles to exceed 5 million by 2020. Meanwhile, the new vehicle fuel economy limit of Chinese OEM's will be reduced to 4.0 L/100 km^{-1}. As discussed before, it is difficult to fulfil this target through ICEV improvement alone. Therefore EV implementation could benefit the quotas for OEMs.

Figure 6-13 and **Figure 6-14** show the EV new sales share under different scenarios. In the *Baseline* scenario, the EV development basically relies on the market, technology and cost. Before 2030 production capacity, cost and infrastructure restrict the increasing demand of EVs. EVs will account for 2% of market share in 2020 – the same as the current level of the U.S. BEVs will be widely accepted after 2030 and account for 28% by 2050. But, in the *Low Carbon* scenario, the GHG control target is set

the top priority. Any boost in EV sales would occur after 2020 in order to meet the 2DC target- 65% of new sales in 2050 would be comprised of EVs. The CO_2 emissions in 2050 should be reduced by 80% compared to those of 2010.

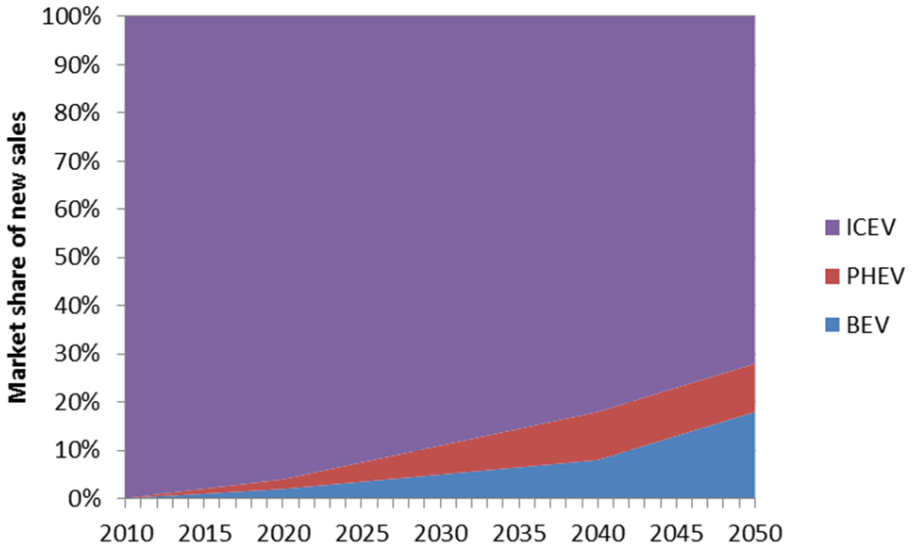

Figure 6-13 Share of different power train technologies to the total LDPV sales market in the *Baseline* scenario

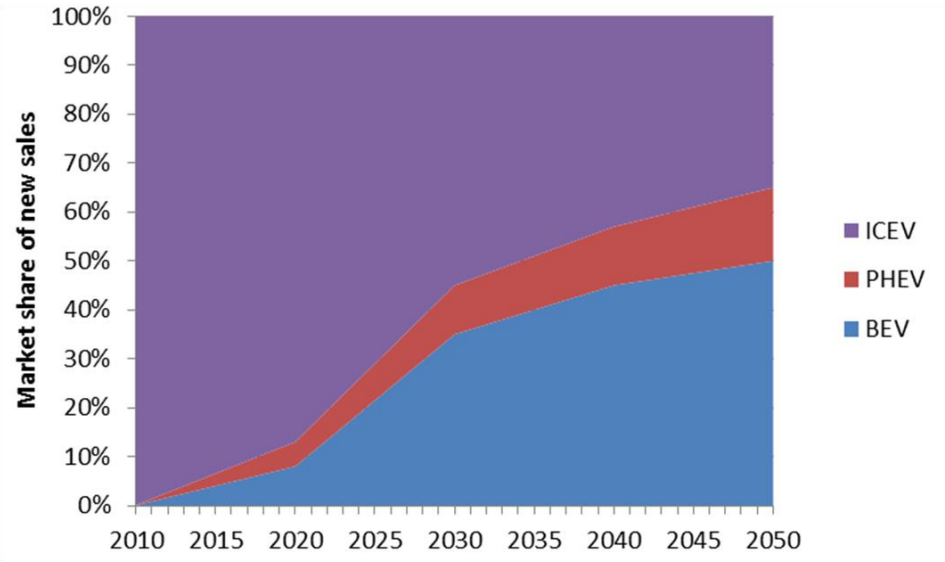

Figure 6-14 Share of different power train technologies to the total LDPV sales market in the *Low Carbon* scenario

Chapter 7 WTW energy use and emissions

7.1 Fossil energy use

Traditional fossil fuels include petroleum, natural gas and coal. **Figure 7-1** presents the distance-based WTW fossil energy consumption for PHEVs and BEVs relative to their ICEVs (including hybrid vehicle) counterpart under two scenarios for the periods from 2020 to 2050.

WTW fossil energy consumption for all vehicle types will decrease continuously. In the *Baseline* scenario, BEVs have higher energy efficiency than ICEVs in the TTW stage (i.e. vehicle operation). For example, in 2020, the specific fossil use of BEVs will only be 23% of that of the ICEVs. But the WTW fossil energy consumption of PHEVs and BEVs decreases by 51% and 54% compared to ICEVs in 2020. Such a reduction in the TTW stage is partly offset by a significant increase in fossil energy consumption in the WTT stages (e.g. power generation) and the EV benefit will increase due to improvements in clean energy power share and coal-fired generation efficiency. For example, ICEV fossil energy use in 2050 could be reduced by 54% relative to 2020, while that of BEVs could be reduced by 63%. Looking at each stage, BEV's WTT stage accounts for 58% of the total WTW result in 2020. This is mainly attributed to an overwhelming share of coal-based electricity nationwide. But, in 2050, the WTT results of BEVs falls to 43%, pushing the BEVs to achieve a higher benefit over ICEVs.

In the *Low Carbon* scenario, ICEV fleets accelerate their hybridisation, leading to 50% and 81% reduction in 2030 and 2050, respectively, over those of 2020. 86% of newly sold ICEVs in 2050 will be equipped with hybrid powertrain systems, while there were only 31% in the *Baseline* scenario. But BEVs in the same situation will experience an 84% reduction over 2020 owed to only a 17% of coal-fired generation share and over 50% of generation efficiency. And, by 2050, BEVs will have reduced up to 60% of WTW fossil energy consumption over ICEVs in the same period. PHEVs achieve similar energy-savings benefits to the *Baseline* scenario.

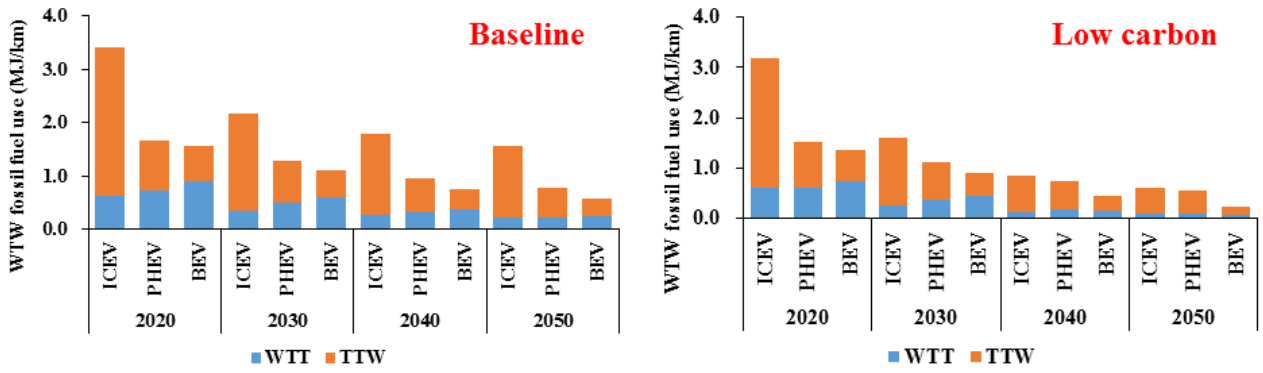

Figure 7-1 WTW fossil energy consumption of LDPV technologies in China, 2020-2050

7.2 CO_2 emissions

Figure 7-2 presents the distance-based WTW CO_2 emissions for PHEVs and BEVs relative to their ICEV counterparts from 2020 to 2050. CO_2 emissions are directly related to the consumption of fossil energy which will continuously decrease over the next four decades due to the improvement of the upstream generation efficiency and the downstream vehicle fuel economy, as well as the increase of the clean energy generation share.

In the *Baseline* scenario, WTW CO_2 emissions of PHEVs and BEVs in 2020 are lower by 29% than those of ICEVs, which is much lower than that of fossil energy reduction. Due to the high carbon content of coal, large amounts of CO_2 would be emitted during the upstream coal-fired generation stage. In 2020, BEVs could not even gain a reducing benefit over PHEVs under the nationwide coal-fired generation share and regions with a higher coal power share. But the benefit for BEVs will increase due to improvements in the clean energy power share and coal-fired generation efficiency. For example, WTW CO_2 emissions from ICEVs will be 42% lower in 2050 relative to those in 2020; while BEVs will gain a 63% reduction. Finally, BEVs will have 55% lower WTW CO_2 emissions relative to ICEVs in 2050. Thus, the newly sold vehicles will emit 53-119 g CO_2 /km^{-1} from the fuel cycle perspective in 2050.

In the *Low Carbon* scenario, ICEV fleets accelerate their hybridisation, which leads to 23% and 51% CO_2 reductions in 2030 and 2050, respectively, over that of 2020. On the other hand, BEVs will achieve a 58% and 83% CO_2 reduction over that of 2020. This is mainly attributed to the 17% of coal-fired generation share and over 50% of generation efficiency. Those vehicles will emit 21-98 g CO_2 /km^{-1} in 2050 from a fuel cycle perspective, of which BEVs achieve higher emission-reducing potential than

ICEVs. Based on the estimations of other researchers, in order to reach the 2DC target in 2050, CO_2 emissions from vehicle fleets should be cut over 80% compared to current emission levels. Therefore, in 2050, the new vehicle market must involve large amounts of EVs to realise the constraint target.

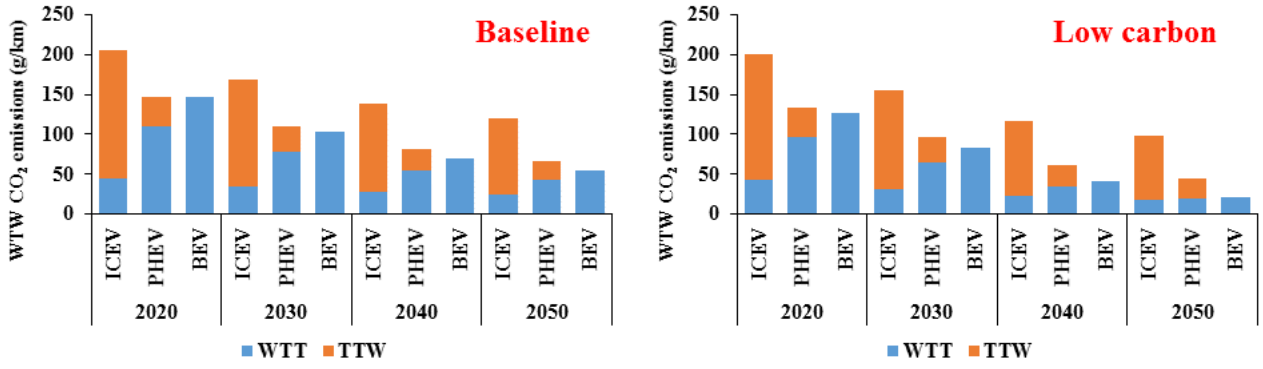

Figure 7-2 WTW CO_2 emissions of LDPV technologies in China, 2020-2050

7.3 Air pollutants emissions

1. VOC Emissions

Figure 7-3 presents the distance-based WTW VOC emissions for PHEVs and BEVs relative to their ICEV counterparts from 2020 to 2050. Emissions from the TTW operation stage dominate the WTW VOC emissions of ICEVs, while BEVs achieve zero VOC emissions and a small amount in the upstream WTT processes. Thus, even in the *Baseline* scenario, EVs could remarkably reduce WTW VOC emissions. For example, in 2020, BEVs and PHEVs would be reduced by 94% and 70%, respectively, relative to ICEVs. As time goes on, ICEV's TTW VOC emission would decrease as the vehicle emission standards become more stringent. In light of previous studies, it is assumed that there will not be more stringent VOC control standards for light-duty gasoline vehicles (LDGV) after China VI. Therefore, the TTW VOC emissions will remain unchanged, while the reduction of WTW VOC emissions will slow down after the China VI implementation in the near future. In 2050, the distance-based WTW VOC emissions of BEVs will fall to 0.05 g km^{-1}, which is 95% lower than those of ICEVs over the same period.

Figure 7-3 WTW VOC emissions of LDPV technologies in China (*Baseline*)

2. CO Emissions

Figure 7-4 presents the distance-based WTW CO emissions for PHEVs and BEVs relative to their ICEV counterparts from 2020 to 2050. Similar to VOC emissions, the TTW stage (i.e. vehicle operation) dominates the WTW CO emissions of ICEVs, while BEVs achieve zero CO emissions and emit only a small amount in the upstream WTT processes. Thus, even in the *Baseline* scenario, EVs could significantly reduce WTW CO emissions. For example, in 2020, BEVs and PHEVs could be reduced by 97% and 74%, respectively, relative to ICEVs. Compared to VOC emissions, BEVs could provide a higher benefit in reducing WTW CO emissions. As time goes on, TTW CO emissions of ICEVs will decrease as the vehicle emission standards become more stringent. An assumption was made that there would not be more stringent CO emission control standards for LDGVs after China VI. Therefore, the TTW CO emissions will remain unchanged, while the decrease of WTW CO emissions will slow down. In 2050, the distance-based WTW CO emissions of BEVs will fall to 0.05 g/km^{-1}, which is 96% lower than those of ICEVs over the same period.

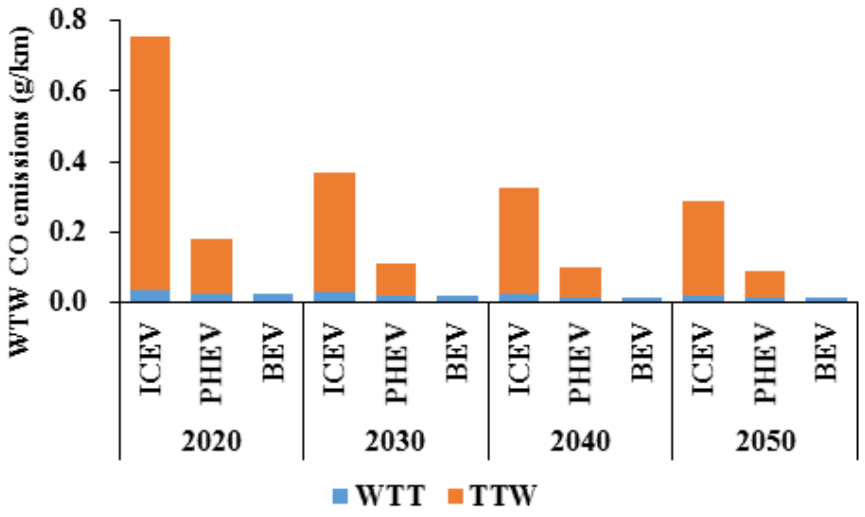

Figure 7-4 WTW CO emissions of LDPV technologies in China (*Baseline*)

3. NO_X Emissions

Figure 7-5 presents the distance-based WTW NO_X emissions for ICEVs, PHEVs and BEVs from 2020 to 2050. WTW NO_X emissions mainly come from the WTT upstream stages (e.g. fuel production), which is quite different from VOC and CO emissions.

In the *Baseline* scenario, WTT NO_X emissions from ICEVs and PHEVs account for 89% to 98% of total WTW emissions, respectively. For BEVs, all WTW NO_X emissions come from the WTT stage and are higher than those of ICEVs due to the high NO_X emission intensity in the upstream coal-fired generation process. For example, in 2020, WTW NO_X emissions from BEVs and PHEVs are 45% and 21% higher than those of ICEVs, when the coal-fired power generation share has already decreased from 79% (2010) to 70%. As the power generating efficiency and clean energy generation share increases, WTW NO_X emissions of BEVs will decrease dramatically. For example, the WTW NO_X emissions of BEVs will pass through the breakeven point over ICEVs until 2040 and start to attain a WTW NO_X emission reducing benefit.

In the *Low Carbon* scenario, BEVs could achieve more benefits in reducing WTW $PM_{2.5}$ emissions, and the breakeven point over ICEVs would occur earlier in the 2030s. The coal-fired power generation share and efficiency, as mentioned before, will reach 17% and 50%, respectively, leading to a 52% and 37% reduction for BEVs and PHEVs compared to ICEVs in 2050. BEVs, PHEVs and ICEVs will emit 34, 44 and 70 mg NO_x km^{-1} from the WTW perspective, respectively, at that time.

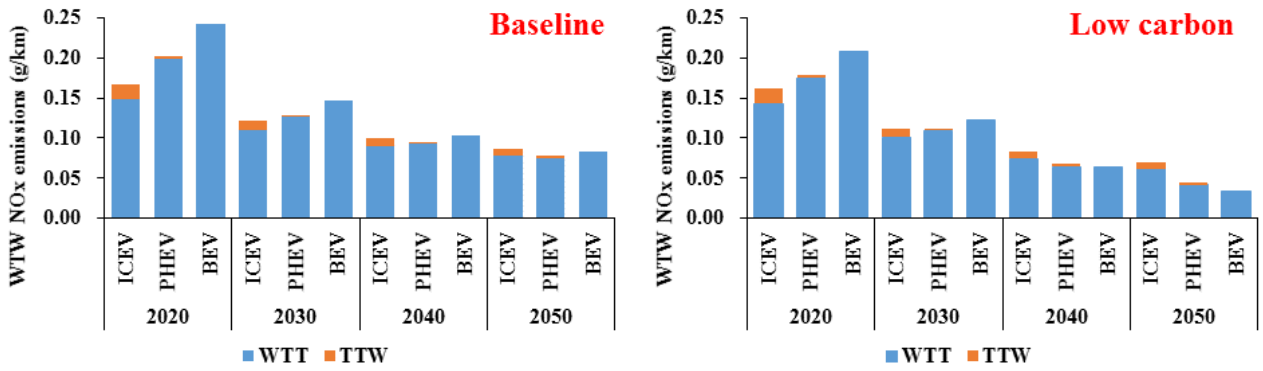

Figure 7-5 WTW NO_X emissions of LDPV technologies in China, 2020-2050

4. $PM_{2.5}$ Emissions

Figure 7-6 presents the distance-based WTW $PM_{2.5}$ emissions for ICEVs, PHEVs and BEVs from 2020 to 2050. Similar to the results of NOx, the WTW $PM_{2.5}$ emissions mainly come from the WTT upstream stages (e.g. fuel production).

In the *Baseline* scenario, WTT $PM_{2.5}$ emissions from ICEVs and PHEVs account for 78% to 97% of total WTW emissions. For BEVs, all WTW $PM_{2.5}$ emissions come from the WTT stage, which shows no emission-reducing benefit because of the high $PM_{2.5}$ emission intensity in the upstream coal-fired generation process. For example, in 2020, WTW $PM_{2.5}$ emissions from BEVs and PHEVs are 87% and 141% higher than those of ICEVs when the coal-fired power generation share has already decreased to 70%. As the power generation efficiency and clean energy generation share increase, WTW $PM_{2.5}$ emissions of BEVs decrease gradually - but not the same as for NO_x. In the *Baseline* scenario, BEVs cannot reach the breakeven point over ICEVs before 2050. For example, the distance-based WTW $PM_{2.5}$ emissions from BEVs and PHEVs are 87% and 141% higher than those of ICEVs, respectively, in 2050.

When considering the *Low Carbon* scenario, BEVs could achieve more benefits in reducing WTW $PM_{2.5}$ emissions; and the breakeven point over ICEVs would occur after 2040. The coal-fired power generation share and efficiency, as mentioned before, will reach 17% and 50%, respectively, leading to 15% and 12% reductions for BEVs and PHEVs compared to ICEVs in 2050. BEVs, PHEVs and ICEVs will emit 6.3, 6.5 and 7.3 mg $PM_{2.5}$ km^{-1} from the WTW perspective, respectively, at that time.

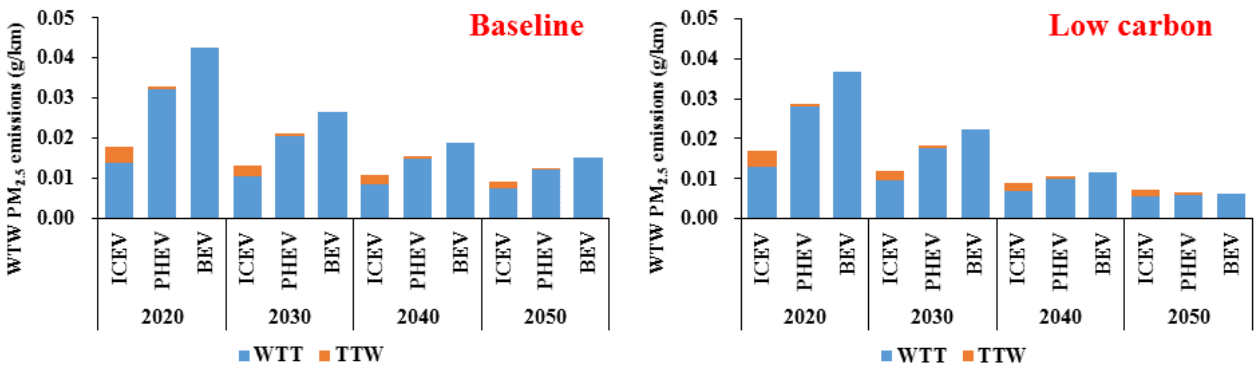

Figure 7-6 WTW $PM_{2.5}$ emissions from LDPV technologies in China, 2020-2050

Chapter 8 Reduction potential of energy use and emissions from the LDPV fleet

Combining the forecasts for LDPV fleet stock, EV deployment and vehicle fuel economy, the fleet-based fuel consumption under different scenarios could be calculated. Adding up the results at the WTT stages, this chapter evaluates the specific trends of fossil energy demand, CO_2 and major air pollutant emissions from fuel cycle perspective. The model is able to calculate the total amount of energy and environmental impacts on the road up to 2050 by putting in the vehicle kilometres travelled (VKT). **Figure 8-1** shows the variation trend of the annual VKT used in this model, which relied on our previous studies in Beijing and Guangzhou. For example, a continuous survey in Beijing indicates a daily-average VKT of 44 km, which is equal to 16,000 km per year. In 2050, the annual VKTs will fall to 10,000 and 8,000 km, respectively, in the *Baseline* and *Low Carbon* scenarios.

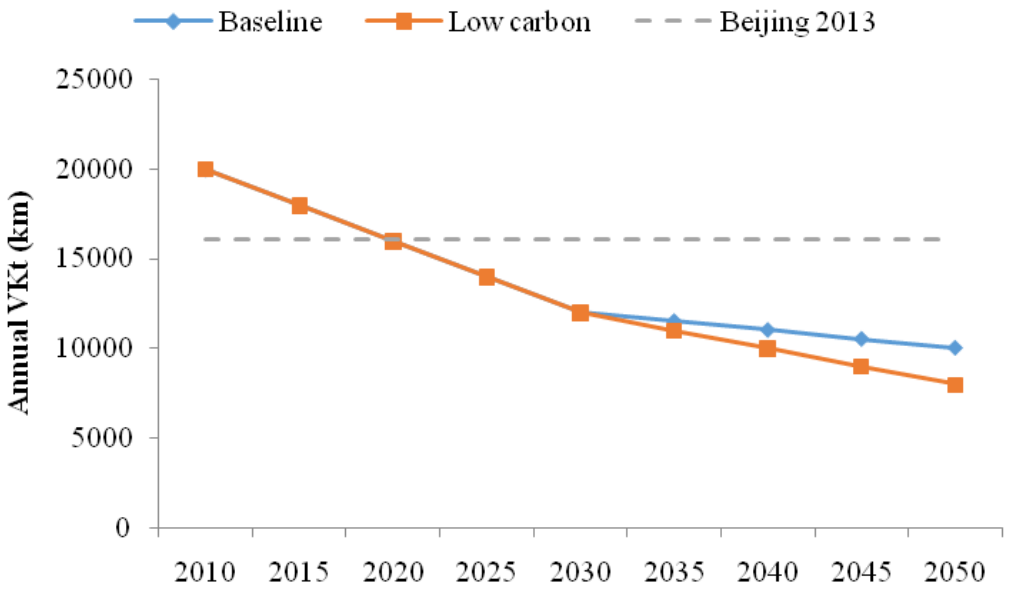

Figure 8-1 Annual VKT of LDPV in this research

8.1 Fossil energy use

Figure 8-2 shows the variation trends of total fossil energy demand under different developing scenarios. It is proven that, though the vehicle fleet continues to grow after 2030, the total amount of

annual fossil energy demand decreases significantly. For example, in the *Baseline* scenario, the fossil energy demand of vehicle fleets will fall to 7.9 billion GJ in 2050, which is a reduction of 40% of that in 2030. All vehicle technologies can reduce their energy consumption during 2020-2050. For example, the energy consumption of ICEVs will be reduced by over 50% and of BEVs by 63%. The *Baseline* scenario requires a 28% of vehicle electrification ratio by 2050, so the main contribution of the reduction of fossil energy demand can be attributed to the hybridisation of ICEVs.

While in the *Low Carbon* scenario, fossil energy demand further falls to 3.0 billion GJ in 2050, this is only 35% over that of 2030. In this scenario, EVs dominate the vehicle market (up to 65%) and also the fleet stock (around 50%), so the contribution of ICEV's fossil energy demand will drop to 60-70% by 2050. Comparing the two scenarios, the *Low Carbon* scenario could save up to 4.9 billion GJ of fossil energy demand in 2050, which is 62% lower than that of the *Baseline* scenario.

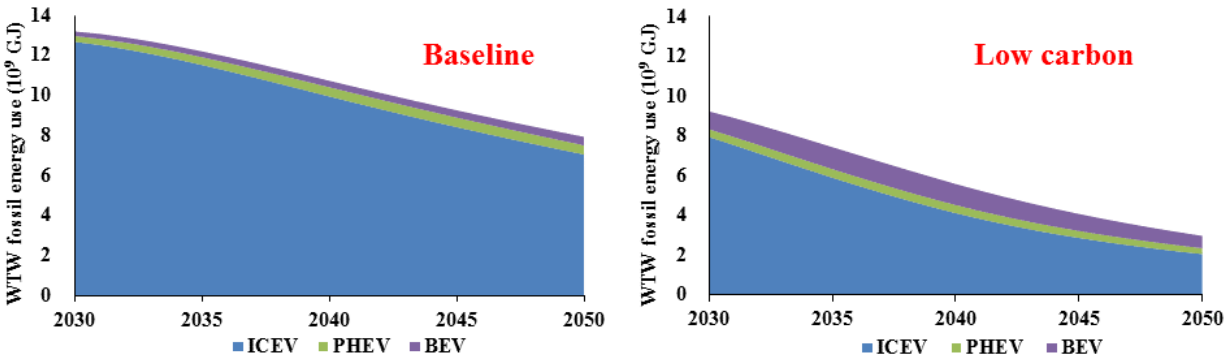

Figure 8-2 WTW fossil energy consumption of LDPV fleets in two different scenarios

8.2 CO_2 emissions

Figure 8-3 shows the variation trends of total CO_2 emissions under different developing scenarios. Because the *Low Carbon* scenario has a clear CO_2 emission control target, the time frame was extended from 2020 to 2050. It is proven that, though the vehicle fleet will continue to grow after 2020, fleet CO_2 emissions will decrease after three decades. But in the *Baseline* scenario, fleet CO_2 emissions will rise during the early period and then decline sharply. The peak is estimated to occur around 2030. The fleet CO_2 emissions in 2030 could reach 1.0 billion tons, which is 25% higher than those in 2020. During this period, the profits of fuel economy improvement and fleet electrification are offset by the rapid increase in vehicle population, assuming that China remains the leader of the global vehicle market in the next

decades. But after the year 2030, the cumulative benefits of low carbon technologies and policies will have the advantage over the fleet growth. The total emissions in 2040 will be equal to those in 2020; while the emissions in 2050 will be 22% lower than those in 2020. The *Baseline* scenario requires a 28% of vehicle electrification ratio in 2050, so the main contribution of CO_2 emission reduction can be attributed to the hybridisation of ICEVs.

While, in the *Low Carbon* scenario, the peak year occurs before 2025, the rapid penetration of EVs helps to control the peak emissions at 0.8 billion tons, which is 20% lower than that in the *Baseline* scenario. In this situation, the total emissions in 2050 would be reduced by 70-80% over the current (2005-2015) level. As **Figure 8-3** shows, the annual CO_2 emissions of LDPV fleets in 2050 drop to 0.24 billion tons (30% of that in the current condition) with a 68% EV share, 17% of the coal-fired generation ratio, 50% of the coal-fired generation efficiency and a 20% reduction in annual VKT. Under this scenario, EVs dominate both the vehicle market and fleet stock, playing a remarkable role in fulfilling the 2DC constraint target.

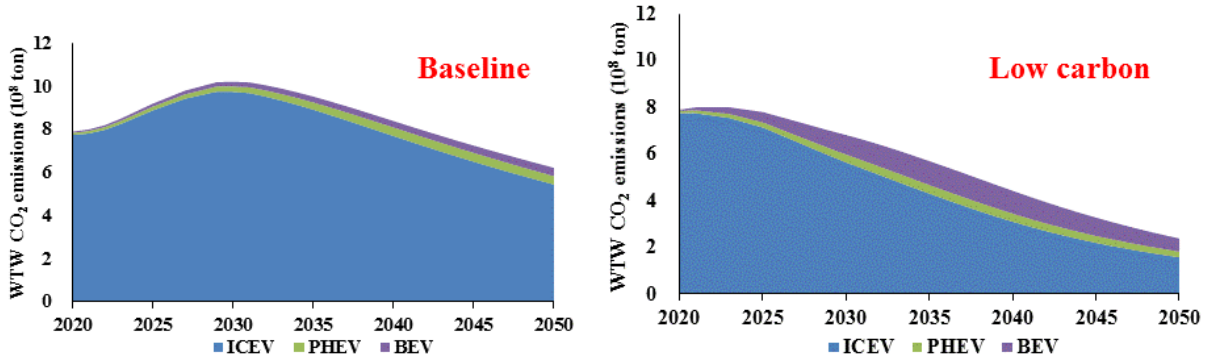

Figure 8-3 WTW CO_2 emissions of LDPV fleets in two different scenarios

8.3 Air pollutant emissions

Figure 8-4 shows the variation trends of four air pollutants from 2030 to 2050. It is proven that, although vehicle fleets continue growing after 2030, the total amount of annual emissions of all air pollutants decreases significantly.

VOC and CO, which are mainly emitted during the TTW stage, will be well controlled by strict emission control regulations and can achieve further reductions through fleet electrification in the *Low Carbon* scenario. For example, in the *Baseline* scenario, VOC and CO emissions could be reduced by 51% and

61%, respectively, in 2050 relative to those in 2020. In the *Low Carbon* scenario, more benefits could be achieved for VOC and CO emissions. In 2050, the annual emissions of VOC and CO would be limited to 0.2 and 0.5 million tons, which reflects cuts of 65% and 66%, respectively. As seen in **Figure 8-4**, the fleet-based WTW emission differences between the years 2020 and 2050 are not that significant compared to the total amount. But the fleet populations are different from each other, and the fleets in the *Low Carbon* scenario have been reduced by 15% of the fleet amount.

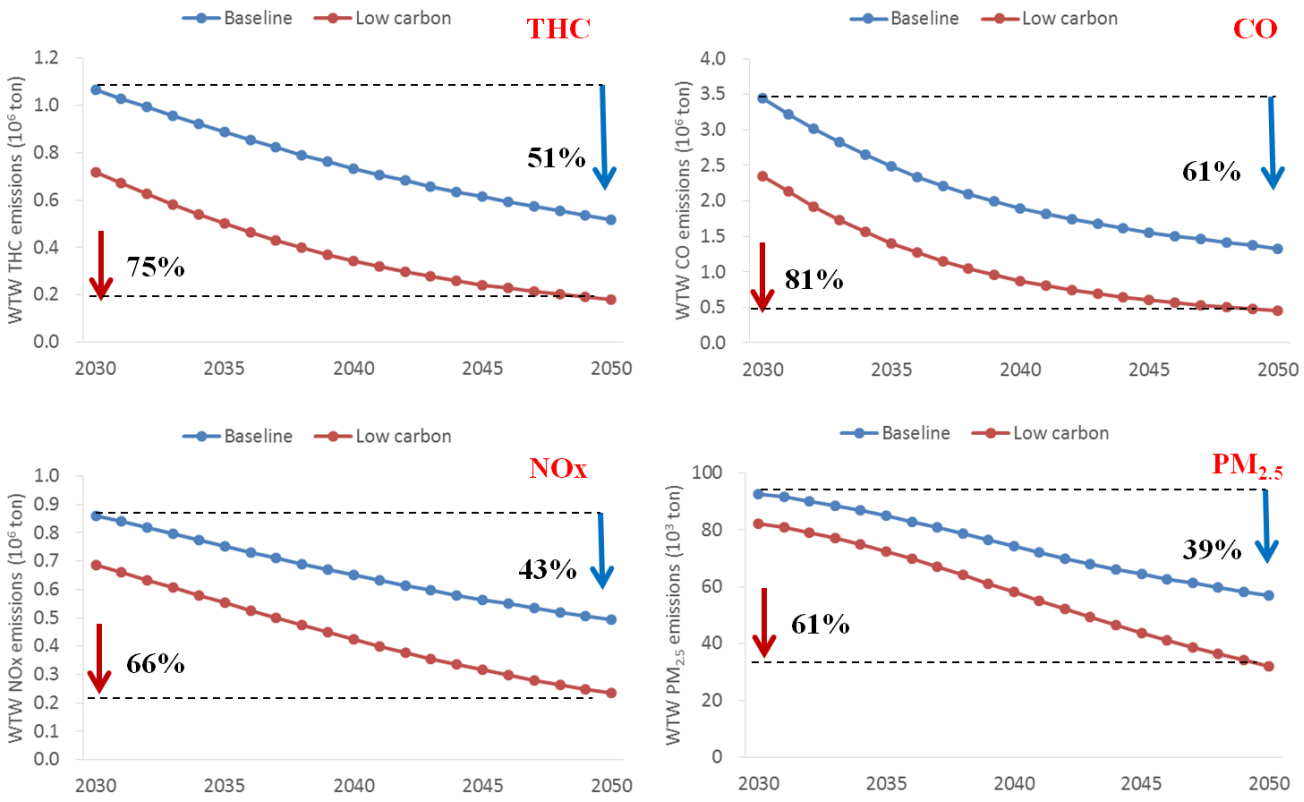

Figure 8-4 WTW air pollutant emissions of LDPV fleets in two different scenarios

Though WTW NO_x and $PM_{2.5}$ emissions of BEVs increase in the early years, the general trends of decreasing have not changed due to the low electrification ratio in the early period. After that, EV deployment increases to a significant degree, especially in the *Low Carbon* scenario, in which the WTW emission disadvantages are diminished due to clean power and high-efficiency coal-fired generation. However, WTW $PM_{2.5}$ emissions from BEVs well exceeds those of ICEVs and the emission peak only appears around 2020 while the others will have already turned into a monotonous decline before 2020. In 2020, the fleet in the *Low Carbon* scenario only reduces 12% of $PM_{2.5}$ emissions over the *Baseline*

scenario. As seen in **Figure 8-4**, the fleet NO_x and $PM_{2.5}$ emissions under the *Low Carbon* scenario are 0.49 and 0.032 million tons, respectively, in 2050, which is a reduction of 53% and 44% over the *Baseline* scenario.

In **Figure 8-5**, EV contributes 12% and 37% of total fleet emissions in the *Baseline* and *Low Carbon* scenarios in 2020. As time goes on, the EV contributions rise to 26% and 61% in the *Baseline* and *Low Carbon* scenarios, respectively, in 2050. $PM_{2.5}$ is the only air pollutant from EV's emissions to exceed ICEV emissions in 2050.

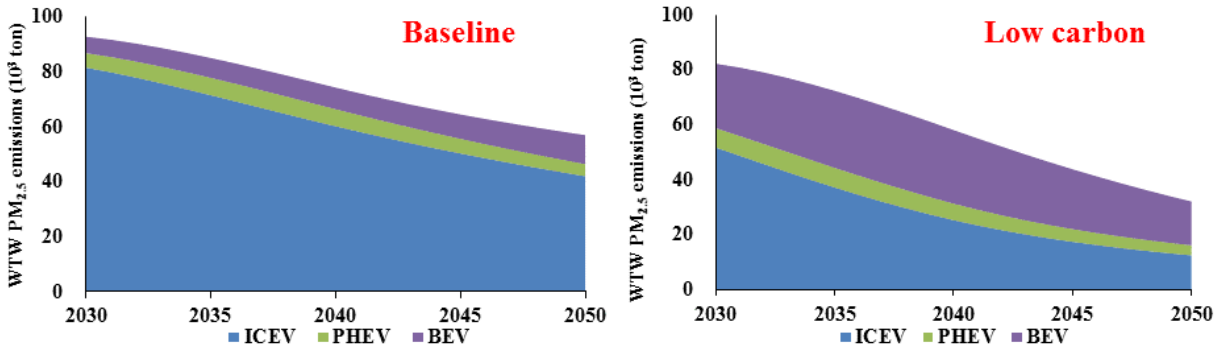

Figure 8-5 WTW $PM_{2.5}$ emissions of LDPV fleet in two different scenarios

Conclusions

Part I: Air quality impact assessment of vehicle electrification

(1) Vehicle fleet electrification could reduce $PM_{2.5}$ concentrations in the urban areas of both the JJJ and YRD regions in MY 2030. Using the YRD region as an example, the average $PM_{2.5}$ concentration in urban areas of all the cities could be reduced by 0.8 and 0.4 μg m^{-3} in January and August, respectively, under *Scenario EV1*.

(2) EVs should be promoted as aggressively as possible to obtain further air quality improvements in the future. Using the YRD region as an example, the average $PM_{2.5}$ concentration reduction is 1.7 μg m^{-3} under *Scenario EV2*, 110% higher than that of *Scenario EV1* (0.8 μg m^{-3}).

(3) The concentration changes of chemical compositions of $PM_{2.5}$ differ by season: Nitrate dominates in January, while SOA dominates in August.

(4) Vehicle fleet electrification has higher reduction benefits for NO_2 than those of $PM_{2.5}$, especially in places with a high risk of NO_2 exceedance (i.e. urban areas of megacities).

(5) In 2030, emission mitigation for many sources (e.g. residential and industry) other than on-road vehicles and power plants should be considered as an essential supplementation to vehicle electrification in order to achieve significant improvements in regional air quality.

Part II: Climate impact assessment of e-mobility

(1) The total ownership of LDPVs will range from 360 to 490 million in 2050 and EVs will account for 28-65% of annual new sales under different scenarios.

(2) In 2050, the fossil energy use of new sale fleets would be reduced by over 80%

of their life cycle demand in 2020 and BEVs could reduce up to 60-65% of fossil energy over the ICEV between the same periods due to the dramatic growth of both fuel efficiency and clean power share. The total fossil energy use under a strict climate control scenario in 2050 would be reduced by 62% compared to the *Baseline* scenario as a result of the aggressive 65% electrification ratio of newly-sold vehicles.

Under the *Low Carbon* scenario, the distance-specific fuel cycle CO_2 emissions from BEVs could be 30 g/km^{-1}. The CO_2 emission peak of LDPV fleets will occur between 2020 and 2030. The annual CO_2 emissions drop to 0.24 billion tons in 2050 (equal to 30% of that of the current level) in the *Low Carbon* scenario with an aggressive vehicle electrification projection to generally fulfill the 2DC target.

References

[1] Zhang S, He X, Wu Y, Hao J. Well-to-wheels energy consumption and emissions of electric vehicles: Mid-term implications from real-world features and air pollution control progress. Applied Energy, 2017, 188: 367-377.

[2] Zhou B, Wu Y, Zhou B, Wang R, Ke W, Zhang S, Hao J. Real-world performance of battery electric buses and their life-cycle benefits with respect to energy consumption and carbon dioxide emissions. Energy, 2016, 96: 603-613.

[3] Ministry of Finance of the People's Republic of China (PRC). Notice of working on the promotion and demonstration of energy-saving and new energy vehicles. 2009: Beijing. Available at http://www.mof.gov.cn/zhengwuxinxi/caizhengwengao/2009niancaizhengbuwengao/caizhengwengao2009dierqi/200904/t20090413_132178.html (in Chinese)

[4] The State Council of the PRC. The industrial developmeng plan for energy saving and new energy vehicles in China (2012-2020). available at http://www.gov.cn/zwgk/2012-07/09/content_2179032.htm (in Chinese)

[5] Ministry of Industry and Information Technology (MIIT) of the PRC. Improving the subsidy policy for product oil price of city buses, accelerating the promotion of new energy vehicles. Available at http://www.miit.gov.cn/n1146285/n1146352/n3054355/n3057585/n3057592/c3617190/content.html (in Chinese)

[6] MIIT of the PRC. The progress of new energy vehicle demonstration in the pilot cities of new energy vehicle promotion. Available at http://www.miit.gov.cn/n1146285/n1146352/n3054355/n3057585/n3057592/c3616843/content.html (in Chinese)

[7] Forecast of electric vehicles in China based on Bass model. Electric Power. 2013; 46(1): 36-39. (in Chinese)

[8] International Energy Agency (IEA). The Technology Roadmap: Electric and Plug-in Hybrid Electric Vehicles (EV/PHEV). 2009. Paris. Available at http://www.iea.org/publications/freepublications/publication/technology-roadmap-electric-and-plug-in-hybrid-electric-vehicles-evphev.html

[9] IEA. Energy Technology Perspectives 2012 – Pathways to a Clean Energy System. 2012. Paris. Available at http://www.iea.org/etp/publications/etp2012/

[10] Ministry of Environmental Protection (MEP) of the PRC. Ambient air quality standards. Available at http://kjs.mep.gov.cn/hjbhbz/bzwb/dqhjbh/dqhjzlbz/201203/W020120410330232398521.pdf (in Chinese)

[11] MEP of the PRC. The air quality situations of national monitoring cities of China in 2015. Available at http://www.zhb.gov.cn/gkml/hbb/qt/201602/t20160204_329886.htm (in Chinese)

[12] The editorial board of the China Electric Power Yearbook. China Electric Power Yearbook. China Electric Press. 2016.

[13] China Electricity Council. The checklist of basic statistical numbers of China's electricity generation industry in 2015. Available at http://www.cec.org.cn/guihuayutongji/tongjxinxi/niandushuju/2016-09-22/158761.html (in Chinese)

[14] China's central government work report in 2015. Available at http://news.xinhuanet.com/fortune/2016-03/05/c_128775704.htm

[15] National Development and Reform Commission. National Nuclear Long-and-medium Term Development Planning (2005-2020). Bejing, 2007. Available online at http://www.sdpc.gov.cn/gzdt/200711/t20071102_170163.html (accessed January 19, 2017) (in Chinese).

[16] Energy Research Institute of National Development and Reform Commission (ERI/NDR). Wind Power Development Roadmap of China to 2050. Beijing, 2011. Available online at http://www.fenglifadian.com/news/china/33489BB97.html (accessed January 19, 2017) (in Chinese).

[17] International Energy Agency (IEA). Energy Technology Perspectives 2015. Paris, 2015. Available online at http://www.iea.org/etp/etp2015/ (accessed January 19, 2017).

[18] Jiang K, Hu X, Zhuang X, Liu Q. China′ s low-carbon scenarios and roadmap for 2050. Sino-global Energy. 2009, 14(06):1-7 (in Chinese).

[19] Chen J, Chen X. China's long-term carbon emission reduction strategy objectives (V) - non-fossil energy demand and carbon emissions. Sino-global Energy. 2011,16(09): 1-14 (in Chinese).

[20] Rout U, Voβ A, Singh A, Fahl U, Blesl M, ó Gallachóir B. Energy and emissions forecast of China over a long-time horizon. Energy. 2011, 36(1): 1-11.

[21] Wu J, Qiu Y, Yang S, He B. Study on low - carbon development strategy of China 's electric power industry from 2010 to 2050. Beijing: China Water&Power Press. 2012 (in Chinese).

[22] Zhang D, Liu P, Ma L, Li Z, Ni W. A multi-period modelling and optimization approach to the planning of China's power sector with consideration of

carbon dioxide mitigation. Computers & Chemical Engineering. 2012, 37: 227-247.

[23] Wu J. Prospects for Electric Power Industry from 2012 to 2050. China Electric Power News. 2013, 02:1-5 (in Chinese).

[24] Luo J, He B, Xing Y. Development Forecast of China 's Electric Power Industry. Energy of China. 2014, 36(6):31-35 (in Chinese).

[25] Cheng R, Xu Z, Liu P, Wang Z, Li Z, Jones I. A multi-region optimization planning model for China's power sector. Applied Energy. 2015,137:413-426.

[26] Energy Research Institute of National Development and Reform Commission (ERI/NDR). China 2050 high renewable energy penetration scenario and roadmap study. Beijing, 2015. Available online at http://www.efchina.org/Reports-en/china-2050-high-renewable-energy-penetration-scenario-and-roadmap-study-en (accessed January 19, 2017).

[27] Dai H, Xie X, Xie Y, Liu J, Masui T. Green growth: The economic impacts of large-scale renewable energy development in China. Applied Energy. 2016,162:435-449.

[28] National Development and Reform Commission (NDRC) of the PRC. Middle and Long Term Program of Energy Saving. Available at http://zfxxgk.ndrc.gov.cn/PublicItemView.aspx?ItemID={c9d6bd55-7d7b-4f8c-bfbc-cdff53b85364}

[29] Wang Z, Jin Y, Wang M, Wu W. New fuel consumption standards for Chinese passenger vehicles and their efforts on reductions of oil use and CO2 emissions of the Chinese passenger vehicle fleet. Energy Policy: 2010, 38: 5242-5250.

[30] MIIT of the PRC. National Fuel Consumption Standard for Light Duty Passenger Cars. Available at http://chinaafc.miit.gov.cn/n2257/n2340/c79074/content.html

[31] Wagner V, An F, Wang C. Structure and impacts of fuel economy standards for passenger cars in China. Energy Policy. 2009, 37:3803-3811.

[32] Huo H, He K, Wang M, Yao Z. Vehicle technologies, fuel-economy policies, and fuel consumption rates of Chinese vehicles. Energy Policy. 2012, 43:30-36.

[33] Innovation Center for Energy and Transportation (iCET). Annual report of fuel consumption of passenger vehicles in China in 2016. 2016. Available at http://www.icet.org.cn/registration2.asp?rid=103

[34] Huo H, Yao Z, He K, Wu X. Fuel consumption rates of passenger cars in China: Labels versus real-world. Energy Policy. 2011, 39:7130-7135.

[35] Innovation Center for Energy and Transportation. General analysis on the divergence between real-world and type-approval fuel economy, Beijing; 2015 (in Chinese).

[36] Tietge U, Zacharof N, Mock P, Franco V, German J, Bandivadekar A, et al. From laboratory to road: a 2015 update. ICCT; 2015. Available at http://www.theicct.org/sites/default/files/publications/ICCT_LaboratoryToRoad_2015_Report_English.pdf.

[37] Huo H, Wang M. Modeling future vehicle sales and stock in China. Energy Policy, 2012,43:17-29.

[38] IEA. World Energy Outlook 2009. 2009. Available at http://www.iea.org/newsroom/news/2010/november/world-energy-outlook-2010.html

[39] MIIT of the PRC. Automotive Industry Restructuring and Revitalization Plan. Available at http://www.miit.gov.cn/n1146285/n1146352/n3054355/n3057585/n3057592/c3551903/content.html (in Chinese).

Deutsche Gesellschaft für

Internationale Zusammenarbeit (GIZ) GmbH

Sunflower Tower 860

Maizidian Street 37, Chaoyang District

100125 Beijing, PR China

T +86 (0) 10 8527 5589

F +86 (0) 10 8527 5591